Grant agreement no: 101097101

TERahertz ReconfigurAble METAsurfaces for ultra-high rate wireless communications

TERRAMETA

Deliverable D2.2
Network architecture and updated requirements and scenarios

Technical Manager:	George Alexandropoulos
Organization:	NKUA
Project Coordinator:	Luís Pessoa
Organization:	INESC TEC
Start date of project:	01-01-2023

Date of issue: 16-07-2024

Due date: 30-06-2024

Document Reference:

TERRAMETA Deliverable 2.2 - Network architecture and updated requirements and scenarios

Leader in charge of deliverable: Sean Ahearne, EISI

	Dissemination level	
PU	*Public*	*X*
CO	*Confidential, only for members of the consortium (including the Commission Services)*	

Table of Contents

List of Figures

Change register

Version	Date	Author	Organization	Changes
0.1	22-04-2024	Sean Ahearne	EISI	Created overall structure
0.2	13-05-2024	Sean Ahearne	EISI	Added content in section 5
0.3	15-05-2024	Evangelos Pikasis, Dimitrios Kritharidis	ICOM	Added content in section 7
0.4	17-05-2024	Antonio, Jose	CEA	Added content in section 7
0.5	21-05-2024	Bo Kum, Georg, Qi Luo	TUBS, UH	Added content in section 8
0.6	28-05-2024	Ryan Husbands	BT	Added content in section 6
0.7	05-06-2024	Panagiotis Gavriilidis, Kyriakos Stylianopoulos	NKUA	Added content in section 10,6
0.8	12-06-2024	Verónica Lain-Rubio	ACST	Added content in section 7
0.9	17-06-2024	Sean Ahearne	EISI	Revised sections 1,2,3,4, and 9
1.0	28-06-2024	Sean Ahearne	EISI	Final Version
1.1	12-07-2024	George Alexandropoulos	NKUA	Final revisions
1.2	16-07-2024	Luis Pessoa	INESC	Correction of typos and formatting

1. <u>Statement of independence</u>

The work described in this document is genuinely a result of efforts pertaining to the TERRAMETA project: any external source is properly referenced.

Confirmation by Authors:

Ryan Husbands

Sean Ahearne

Bo Kum Jung

Qi Luo

Luís Pessoa

George Alexandropoulos

Kyriakos Stylianopoulos

Panagiotis Gavriilidis

Evangelos Pikasis

Dimitrios Kritharidis

Antonio Clemente

Verónica Lain-Rubio

Jose Luis Gonzalez

2. <u>Abbreviations</u>

3GPP	Third Generation Partnership Project
5G	Fifth Generation
6G	Sixth Generation
AI	Artificial Intelligence
AiP	Antenna in Package
AoA	Angle of Arrival
AoD	Angle of Departure
AP	Access Point
ASE	Area Spectral Efficiency
BPSK	Binary Phase-Shift Keying
BS	Base Station
CSI	Channel State Information
CU	Centralised Unit
D2D	Device-to-Device
DMA	Dynamic Metasurface Antenna
DU	Distributed Unit

EIRP	Equivalent Isotropic Radiated Power
EM	Electro-Magnetic
FEC	Forward Error Correction
FDMA	Frequency Division Multiple Access
GHz	Gigahertz
gNB	gNodeB (Next Generation NodeB)
H-RIS	Hybrid Reconfigurable Intelligent Surface
HW	Hardware
IEEE	Institute of Electrical and Electronics Engineers
IoT	Internet of Things
IF	Intermediate Frequency
ISAC	Integrated Sensing and Communications
KPI	Key Performance Indicator
LB	Lower Band
LDPC	Low-Density Parity-Check
LLS	Link-Level Simulator
LoS	Line-of-Sight
MAC	Medium Access Control
MEMS	Micro-Electro-Mechanical Systems
MIMO	Multiple-Input Multiple-Output
MNO	Mobile Network Operator
NLoS	Non-Line-of-Sight
NR	New Radio
OOK	On-Off Keying
O-RAN	Open Radio Access Network
PCB	Printed Circuit Board
PHY	Physical Layer
PoC	Proof of Concept

QAM	Quadrature Amplitude Modulation
QPSK	Quadrature Phase-Shift Keying
QoS	Quality of Service
RAN	Radio Access Network
RF	Radio Frequency
RFC	Radio Frequency Chain
RCU	RIS Control Unit
RIC	RAN Intelligent Controller
RISA	RIS Actuator
RISC	RIS Controller
RISO	RIS Orchestrator
RIS	Reconfigurable Intelligent Surface
RIS-CP	RIS Control Plane
RLC	Radio Link Control
RPRS	Reflective Polarisation Rotating Surface
RU	Remote Unit
RX	Receiver
SLAM	Simultaneous Localisation and Mapping
SMO	Service Management Orchestrator
SNR	Signal-to-Noise Ratio
SoC	System on Chip
SOTA	State of the Art
ToA	Time of Arrival
TX	Transmitter
UB	Upper Band
UE	User Equipment
WLAN	Wireless Local Area Network
WP	Work Package

3. <u>Executive summary</u>

This deliverable (D2.2) focuses on the network architecture and updated requirements and scenarios necessary to achieve the project's ambitious goals.

The document outlines the integration of advanced THz communication technologies within factory and telecommunication use cases. The proposed network architecture leverages THz wireless links and Reconfigurable Intelligent Surfaces (RIS) to enable high-speed, low-latency, and reliable communications, essential for the next generation of Industry and Telco use cases and beyond. A key aspect of the project is the adaptation of IEEE and Open Radio Access Network (O-RAN) architecture standards for wireless communications and RIS control at 150 and 300 GHz, ensuring robust and efficient control and implementation of high frequency wireless links aided by RIS.

To support these advanced network requirements, the deliverable presents a comprehensive RIS control architecture. This includes the RIS Orchestrator (RISO), RIS Controller (RISC), and RIS Actuator (RISA), which collectively manage the dynamic adjustments of the RIS elements to optimise signal propagation and network performance in O-RAN based architecture deployments. In IEEE based architecture deployments, the integration of RIS functions into wireless access points (APs) is also detailed, highlighting the importance of adaptive beamforming, real-time channel state information (CSI), and energy-efficient designs.

Simulations play a crucial role in this project, providing a platform to test and validate the proposed architectures and technologies under different conditions and scenarios. The deliverable includes extensive simulation environments to evaluate the performance and feasibility of the RIS-enabled THz networks. These simulations help in identifying potential challenges and optimising system parameters to ensure robust and efficient operation in practical deployments.

The document also features a detailed section on the hardware (HW) architecture, designed to provide in-depth technical details and discuss approaches for hardware architectural integration. This section is crucial for the implementation of Work Package 6 (WP6) demos, showcasing the practical integration of sub-THz components, RF front-ends, and baseband units from various project partners. The HW architecture section elaborates on the design and integration strategies necessary for successful demonstration scenarios, including use cases in factory environments and telco front-haul applications. It outlines the specific hardware components, their configurations, and how they may interoperate to achieve the project's goals.

This deliverable also revises and discusses various new use case scenarios, demonstrating the practical applications of THz and RIS technologies in real-world environments beyond Telco and industry applications intended to be demonstrated in WP6.

Overall, the deliverable underscores the required new approaches in network architecture and technology required to meet the high demands of future communication networks. Through iterative development phases—evaluation, design, simulation, and demonstration—the TERRAMETA project aims to provide groundbreaking solutions that will pave the way for the next era of wireless communications.

4. <u>Introduction</u>

The TERRAMETA project is an ambitious initiative aimed at revolutionising wireless communications through the development and deployment of Terahertz (THz) Reconfigurable Intelligent Surfaces (RIS). The project brings together a consortium of research institutions and industry partners to explore the potential of THz frequencies for ultra-high rate communications. This deliverable focuses on the network architecture and updated requirements and scenarios necessary to achieve the project's goals.

<u>WP2 approach and relation to other WPs</u>

Work Package 2 (WP2) is pivotal to the TERRAMETA project, being responsible for defining the scenarios, use cases, and requirements that drive the developments across the project. WP2 lays the groundwork by specifying the requirements for THz-based RIS systems and detailing how these systems can be evaluated. The specifications provided by WP2 describe the artefacts to be built, enhanced, or combined within the project to achieve a practical THz communication system.

WP2's work is intricately linked with other WPs in the project. It governs the work covered in WP3, WP4, and WP5, with all technical WPs contributing to WP6. WP3 is tasked with developing new sub-THz and THz hardware solutions for the fundamental building blocks of the RIS design, while WP4 focuses on designing, synthesising, fabricating, and characterising the THz metasurfaces developed in the project. WP2 interacts closely with WP3 and WP4 to receive inputs on the design characteristics and limitations of the investigated and proposed hardware architectures for various reconfigurable metasurfaces, which is reflected in the hardware integration approaches described in section 7. WP3 will create new hardware implementations of meta-elements (e.g., MEMS, CMOS, Microfluid MEMS) that form the foundation for various types of RIS based on operation modes—Transmissive RIS (T-RIS), Reflective RIS, Receiving RIS (R-RIS), and Hybrid RIS (H-RIS). WP4 will study the scalability of the developed RIS technology and its application in various operational modes. Additionally, WP4 will design and integrate the control unit of RIS into the prototype. WP5 plays a crucial role in channel sounding and modelling activities, designing efficient algorithms for most envisioned functionalities with ultra-massive Multiple-Input Multiple-Output (MIMO) metasurface-based antenna arrays. This includes any of the available types of RIS. WP6 is the demonstration work package, focusing on showcasing the effective exploitation of THz RIS wireless links through simulations, lab-based testing, and real-world use case demonstrations.

The iterative approach of WP2—evaluation, design, simulation, and demonstration—ensures continuous enhancement of the specifications. Evaluation of the technologies and components for THz RIS, followed by their design (both physical and algorithmic), and culminating in demonstration via testbeds, enables practical assessment and refinement of the technologies.

<u>Network Architecture Approaches</u>

Network architecture is fundamental to the successful deployment of any wireless communication system, especially at the cutting-edge THz frequencies targeted by the TERRAMETA project. The importance of robust and adaptable network architectures cannot be overstated, as they form the backbone that supports the entire communication ecosystem.

The IEEE 802.11 standards are globally recognised frameworks for wireless local area networks (WLANs). These standards were initially developed to provide wireless networking capabilities within short ranges, such as within a home, office, or campus environment. The standards cover the physical (PHY) layer and medium access control (MAC) layer protocols, ensuring interoperability between devices from different manufacturers. IEEE 802.11 standards have evolved over time to support higher data rates, increased reliability, and enhanced security features. These standards are crucial for applications that require robust wireless connectivity over relatively short distances with high data throughput, such as video streaming, online gaming, and enterprise networking.

On the other hand, the 3rd Generation Partnership Project (3GPP) standards are developed for cellular networks, covering a much broader range of applications and environments. These standards support

mobile communication across vast geographic areas, providing seamless connectivity as users move between different network cells. 3GPP standards encompass various generations of mobile communication technologies, from 2G to the latest 5G and beyond, each iteration bringing significant improvements in speed, latency, and capacity. 3GPP standards are designed to handle the demands of mobile broadband, massive machine-type communications (mMTC), and ultra-reliable low-latency communications (URLLC). They ensure that mobile networks can support a wide array of services, from voice calls and text messaging to high-definition video streaming and real-time interactive applications.

THz Communications and RIS Control: A New Challenge

Both IEEE 802.11 and 3GPP standards are still in their infancy concerning THz communications and RIS control. The high-frequency THz spectrum offers immense potential for ultra-high-speed data transmission, but it also presents unique challenges. THz waves have shorter wavelengths, leading to higher path loss and susceptibility to obstacles and atmospheric absorption. This necessitates highly directional, point-to-point communication links, which differ significantly from the more omnidirectional nature of traditional wireless communications. RIS technology aims to mitigate these challenges by dynamically controlling the propagation environment. By adjusting the phase, amplitude, and polarisation of incident waves, RIS can enhance signal strength, extend coverage, and improve link reliability. However, integrating RIS into existing network standards requires significant adaptations.

This deliverable proposes extending both IEEE 802.11 and 3GPP standards to better support and prepare for THz and RIS based communications. The directional, point-to-point nature of THz links and the fine-grained, real-time nature of RIS control pose new challenges that need to be overcome. For IEEE 802.11, this means adapting the PHY and MAC layers to handle highly directional links and dynamic beamforming. For 3GPP, it involves enhancing the network's ability to manage and coordinate multiple RIS devices, ensuring seamless handovers and consistent performance.

For 3GPP standards, for instance, the extension involves integrating RIS control mechanisms into the network's control architecture. The RIS Orchestrator (RISO), RIS Controller (RISC), and RIS Actuator (RISA) modules need to be incorporated into the existing 3GPP architecture, allowing for efficient management of RIS devices. This includes defining new interfaces for communication between the RIS modules and the network, ensuring seamless coordination and synchronisation. Both standards must also address the challenges of managing highly directional THz links. This involves developing algorithms for dynamic beamforming, channel estimation, and interference management. The network needs to support real-time adjustments to RIS configurations based on feedback from user devices and environmental conditions. Additionally, security measures must be implemented to protect RIS-enabled communications from eavesdropping and malicious attacks.

The network architecture plays a critical role in the deployment and operation of THz and RIS technologies. It must be robust, flexible, and capable of adapting to the dynamic nature of THz communications. The architecture needs to support high-speed data transmission, low-latency communication, and reliable connectivity, ensuring the network can meet the demands of various applications. In industrial settings, the network architecture must support mobile robots and other autonomous devices that require high-bandwidth, low-latency connections. This includes enabling Simultaneous Localisation and Mapping (SLAM) and other advanced capabilities that enhance operational efficiency. In Telco applications, the architecture needs to support seamless handovers, efficient resource allocation, and robust performance, ensuring consistent service delivery in urban environments.

Simulation Environments

Simulations play an indispensable role in the TERRAMETA project, offering a platform to test, validate, and optimise the proposed network architectures and technologies. The deliverable includes comprehensive simulation environments designed to evaluate the performance and feasibility of the RIS-enabled THz networks under various conditions and scenarios. These simulations help identify potential challenges and provide insights into the optimal configurations and parameters for THz and RIS technologies. By simulating different use case scenarios, the project can assess the impact of

various factors such as interference, path loss, and environmental conditions on the network performance. Some initial results for this can be seen in section 8. This allows for a thorough evaluation and refinement of the network architecture before practical deployment.

The simulation environments also facilitate the development of advanced algorithms for dynamic beamforming, channel estimation, and resource allocation. By leveraging simulation results, the project can ensure that the proposed solutions are robust, efficient, and capable of meeting the high demands of future communication networks.

Hardware Integration Architecture

A critical component of the TERRAMETA project is the hardware integration architecture. This section of the deliverable provides detailed technical insights into the design and integration of various hardware components necessary for successful implementation of THz and RIS technologies. The HW integration architecture covers the sub-THz components, RF front-ends, and baseband units provided by different project partners. The HW architecture is designed to support WP6 demonstrations, showcasing practical applications and integration strategies. It outlines the specific configurations of hardware components and their interoperation to achieve high-performance THz communication links. This includes the design of metasurface-based antenna modules, up/down conversion techniques, and the possible integration strategies of RF front-end architectures with baseband units.

By providing detailed technical specifications and integration approaches, the HW architecture section ensures that the hardware components are seamlessly integrated into the overall network architecture. This is crucial for achieving the project's goals of demonstrating the practical viability and performance benefits of THz and RIS technologies in real-world scenarios.

5. Factory Use Case Network Architecture

In recent years, the manufacturing industry has been undergoing a digital transformation known as Industry 4.0. This new era of manufacturing is characterised by the integration of advanced technologies, such as IoT, AI, and automation, into traditional manufacturing processes. One of the key goals of Industry 4.0 is to create a fully mobile, software-defined factory that can be quickly and easily reconfigured to meet changing customer demands and production requirements [1]. An example of the design of a software-defined factory can be seen in Figure 5-1, which highlights a manufacturer choosing to produce a certain product. The IT and manufacturing infrastructure then autonomously reconfigures its resources in a distributed but collaborative fashion to produce this product.
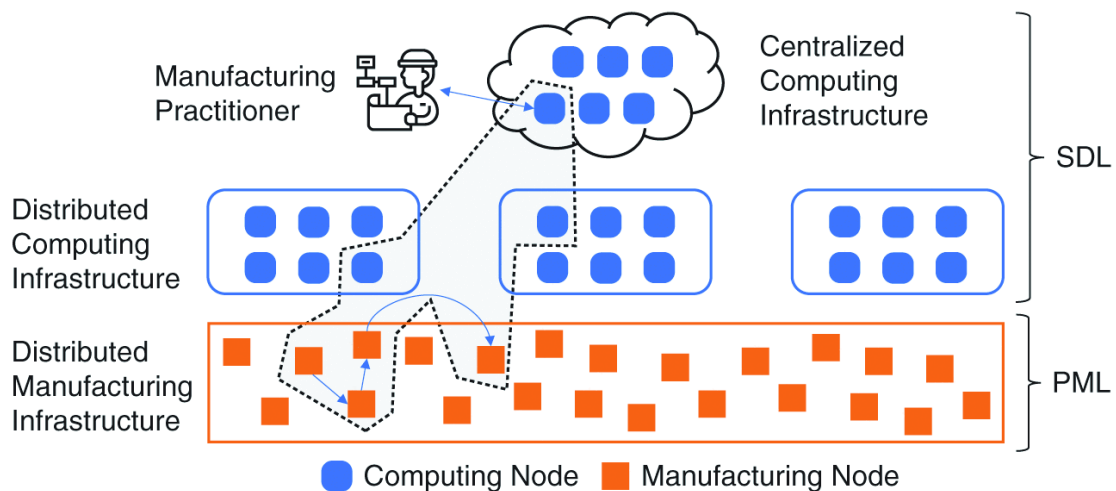
Figure 5-1: Example of a software-defined factory highlighting the division of the manufacturing ecosystem into software definition layer (SDL) and physical manufacturing layer (PML).

A software-defined factory offers several benefits over traditional manufacturing environments. One of the most significant advantages is flexibility. With a software-defined factory, the entire manufacturing process can be programmed and controlled through software, allowing for rapid reconfiguration and customisation to meet changing customer demands or production requirements. This level of agility is essential in today's fast-paced business environment, where companies must be able to quickly respond to shifting market demands and customer preferences. Another benefit of a software-defined factory is improved efficiency. Automation and machine learning algorithms can be integrated into the manufacturing process, allowing for real-time monitoring and optimisation of production processes. This not only helps to reduce waste and downtime but can also lead to increased output and quality.

However, creating a fully mobile software-defined factory also poses several challenges, particularly around mobility. Traditional factories are typically fixed in location, with machines and equipment permanently installed and connected to utilities such as electricity and copper or fibre network connections. In contrast, a software-defined factory may need to be rapidly deployed and redeployed in different locations, making it essential to ensure that all equipment and machines can be easily transported and connected to necessary utilities. To overcome these challenges, solutions such as modular designs, standardised connections, and new network architectures need to be created to create easily transportable and deployable factory units such as robotic assemblers, conveyer systems, and packaging configurations. By addressing these mobility challenges, a fully mobile, software-defined factory can be created that offers unprecedented flexibility and efficiency in the manufacturing process.

Current and future factories require a high-performance network infrastructure to operate effectively. Traditional fixed network infrastructure, such as copper wire and fibre optic cables, are not ideal for a software-defined factory due to their limited flexibility and mobility. A software-defined factory requires

a network that is flexible, scalable, and reliable to support the high volume of data traffic generated by machines, sensors, and robots. Wireless technologies such as Wi-Fi and cellular networks such as Long-Term Evolution (LTE) and 5G are currently not able to meet the demands of a software-defined factory due to a variety of limitations. These limitations include limited bandwidth, high latency, and susceptibility to interference and network congestion. Additionally, current-generation wireless technologies will struggle to provide high-bitrate connections to a large number of devices at scale, simply due to the limited wireless spectrum available and the often-used omni-directional broadcast method limiting spectrum re-utilisation.
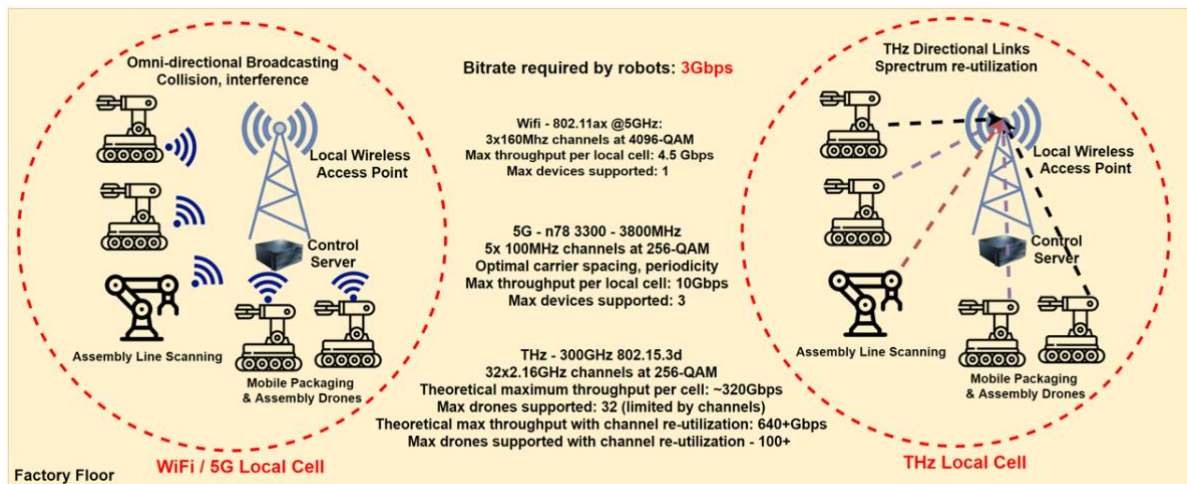
Figure 5-2: Example diagram showing the overall network throughput available per local cell for WiFi, 5G, and THz and number of high bitrate robots are supported.

To meet the network requirements of a software-defined factory, new technologies such as THz wireless links are being investigated. THz wireless links offer increased bitrates, more wireless channels, and lower latency than previous generations of wireless networks, making them well-suited for the high-volume, low-latency, and large-scale data traffic generated by a software-defined factory [2]. The use of directional antennas combined with RIS, also enables THz wireless links to re-use the same THz wireless channels more efficiently and effectively for communication between devices in the same local area. This greatly increases the total amount of throughput available for a given area and enables THz technology to provide a feasible alternative to fixed network infrastructure to meet the growing data demands of Industry 4.0 use cases. A simplified example of this advantage can be seen above in Figure 5-2.

Computer vision is an essential component of robots in Industry 4.0. It allows them to "see" and analyse their environment, which is critical for carrying out their tasks accurately and safely. Computer vision technology includes various techniques such as image processing, pattern recognition, and machine learning, which enable robots to interpret and make sense of visual information. One critical application of computer vision in robots is Simultaneous Localisation and Mapping (SLAM). SLAM is a technique that enables a robot to create a map of an unknown environment while simultaneously locating itself within that environment [3]. This technology allows robots to navigate autonomously in complex environments, which is particularly useful in manufacturing plants and warehouses.

In a software-defined factory, SLAM mapping technology is useful for creating digital twins of the manufacturing plant's physical environment. These digital twins can be used to simulate the production process, optimise the factory's layout, and improve the efficiency of material handling [4]. However, SLAM mapping technology requires high network performance to enable the robot to transmit the mapping data to other machines for processing and analysis. These high-performance requirements are due to the large amounts of data being generated by the robot's sensors and the need for real-time data transmission and feedback. As such, having a high bitrate and low latency network infrastructure is crucial for implementing SLAM mapping technology in Industry 4.0.

In addition to SLAM mapping, current trends in robotics are incorporating object detection technology to enable mobile robots to interact with machines and objects in a software-defined factory. Object detection technology uses computer vision techniques to identify and locate specific objects in an image or video feed. In a software-defined factory, object detection technology allows mobile robots to interact with machines and objects in the factory environment autonomously. For example, a mobile robot equipped with object detection technology could identify and locate a specific machine on the factory floor, then interact with that machine to carry out a particular task. This technology can be particularly useful for tasks such as material handling and logistics, where mobile robots need to locate and interact with specific objects and machines in the factory environment. By incorporating object detection technology, mobile robots can operate more efficiently and effectively, reducing the need for human intervention and improving overall factory productivity.

This use case scenario focuses on testing THz wireless links using RIS to provide a high-speed wireless connection between a mobile or semi-mobile robot and the local Edge server which will be processing its information in order to provide an overall SLAM map of the factory environment. These robots will connect to the processing server using THz wireless links and the THz RIS to provide mobility tracking and maintaining a connection in a NLoS environment. The robots and processing servers are designed to be deployed in a scalable local cell architecture design, meaning the local processing servers operate as part of a distributed software-defined architecture and collaborate to build a complete map of the factory floor and all of the objects and machines contained within it. These control servers can communicate to each other using fixed optical links (as for this use case they can be considered static), or by utilising THz MIMO as a local backhaul, to increase the available bitrate for server-server communication for SLAM map sharing. An example of this architecture and implementation can be seen in Figure 5-3.
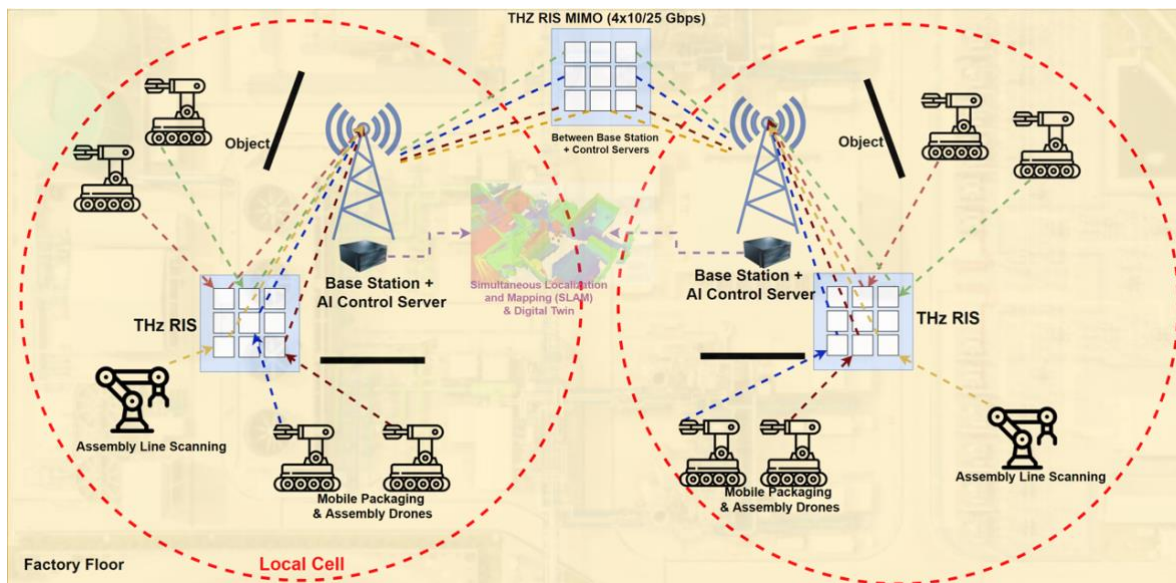
Figure 5-3: Diagram showing robot to server communication utilising a THz RIS and server-server connection between local cells using THz RIS MIMO

In terms of the local factory environment that this use case is based on, a section of the factory can be seen below in Figure 5-4. Note that the manufacturing machines are not present in the image but are marked with a blue outline on the floor. It can be seen from this figure that the overall general layout of the factory features consistent rows and columns of pillars approximately 10 meters apart.

Figure 5-4: Factory floor design

These pillars (in addition to possible supplemental RIS'es mounted on the ceiling) serve as a good location from which to mount THz RIS devices in order to cover the vast majority of the factory floor. This RIS deployment strategy can be seen below in Figure 5-5, where RISs could be mounted on each side of the pillar at an angle that maximises the total area of coverage. This angle could change depending on the type of RIS being deployed.
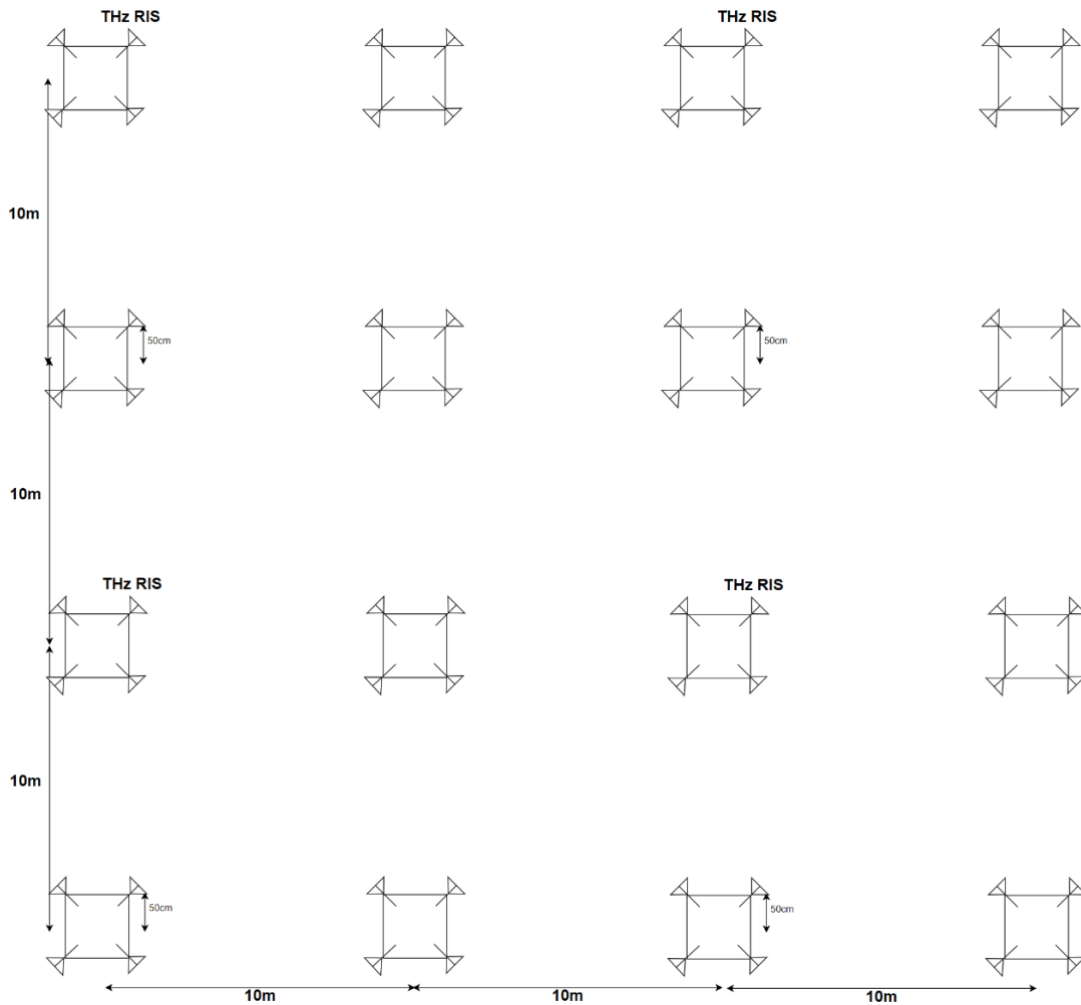
Figure 5-5: Possible THz RIS deployment strategy

This RIS deployment strategy will be further refined but serves as the basis for defining minimum requirements and KPI's in order for the use case to implement a successful demonstration and determine the use case viability via link budget calculations and system simulations in subsequent sections and Work Packages [5].

5.1. Optimising RIS Deployment on Pillars

Mounting RIS on pillars can provide several advantages along different dimensions:

Strategic Placement and Coverage Maximisation: Mounting RIS on pillars offers a strategic advantage due to their elevated position and even spacing throughout the factory floor. This setup ensures that the RIS can cover a wide area with minimal obstructions. By mounting RIS on each side of the pillar, it is likely possible to reach the greatest THz signal coverage of the factory floor, for the least number of RIS' required, as the elevated position helps in avoiding many ground-level obstacles and machinery that might otherwise block the signal.

Adjustable Angles for Diverse Requirements: The angle at which RIS devices are mounted can be adjusted to suit different types of RIS technology and coverage requirements. For example, in environments where the signal needs to penetrate deeper into machinery clusters, a steeper angle might be necessary. Conversely, a more horizontal deployment (or ceiling mounted) might be required in open areas to extend coverage across a wider plane. Customising these angles ensures that the coverage area is optimised for specific sections of the factory, thereby enhancing overall network efficiency.

Dynamic Adaptation to Layout Changes: The dynamic nature of manufacturing environments often necessitates reconfiguration of the network layout. Pillar-mounted RIS can be easily re-angled or repositioned as the factory layout changes (by designing the signal interface for RIS to be based on

modular connectors from the outset), such as during retooling for new production lines. This adaptability is crucial for maintaining complete coverage for manufacturing use cases and minimising downtime during transitions.

Enhanced Deployment Strategies Beyond Pillars

Mobile RIS Platforms: To address the limitations of fixed pillar-mounted RIS, mobile platforms equipped with RIS devices could be introduced. These platforms can move autonomously or be manually positioned to provide targeted coverage in areas where the signal quality is compromised. Mobile RIS units can navigate around large machinery or densely packed areas, ensuring consistent signal strength and network reliability even in the most challenging environments. It may be feasible for these mobile RIS platforms to be integrated with existing mobile robots on the factory floor, thus enabling the manufacturing robots (which are the most critical devices to keep connected to the THz network) to become the most adaptable for controlling THz link management with a built-in RIS to maintain their own and other local devices connections in built-up environments. An example of this can be seen in Figure 5-6, showing RIS-enabled robots integrated with the pillar design network architecture to maximise performance and availability.
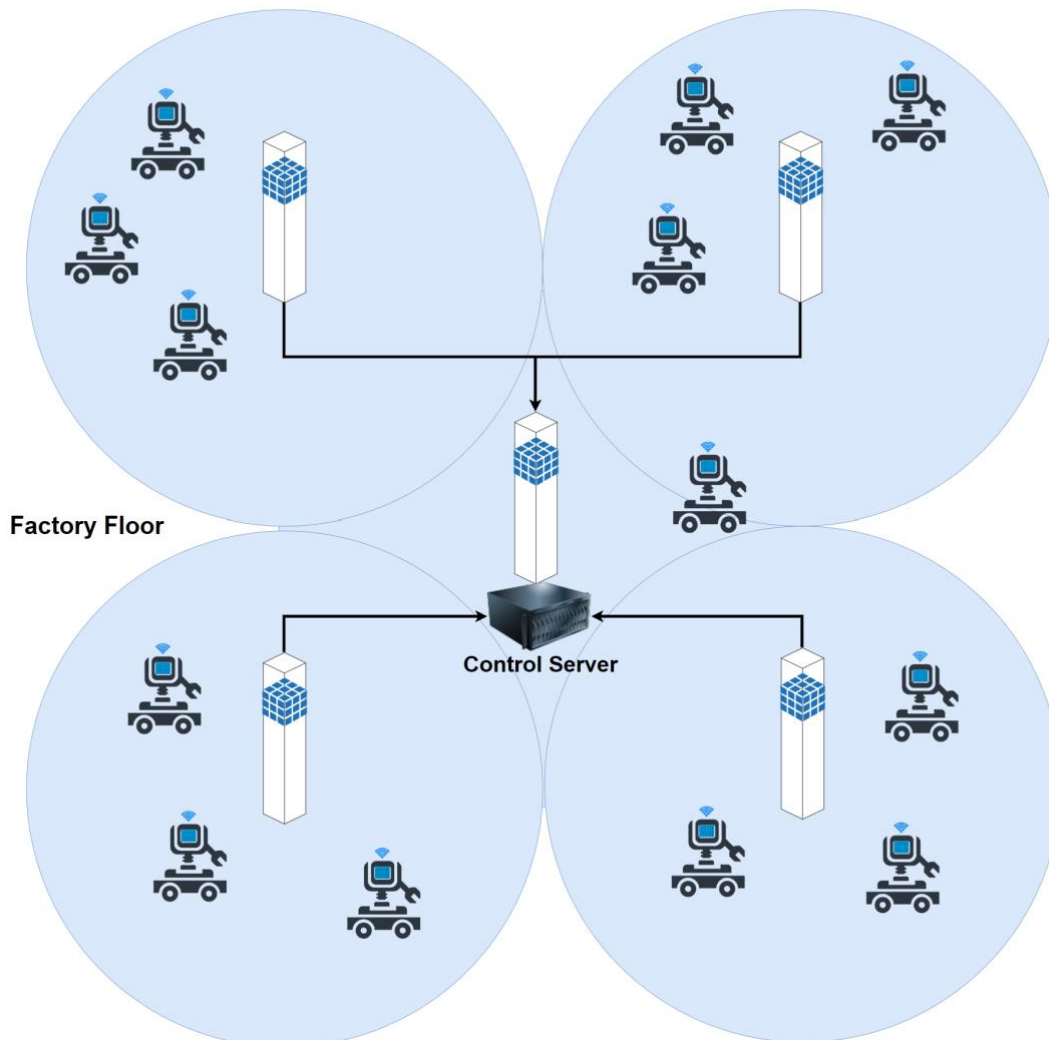
Figure 5-6: Isometric representation of RIS deployment strategy and network architecture

Overhead Gantries and Ceiling-Mounted RIS: Overhead gantries and ceiling-mounted RIS offer another layer of flexibility. Gantries, which can move along predefined paths, provide an excellent vantage point for wide-area coverage. Ceiling-mounted RIS can complement this setup by covering

areas that might otherwise experience signal shadowing due to obstacles on the factory floor. This multi-layered approach ensures comprehensive coverage and robust network performance.

Wall and Floor-Integrated RIS: Integrating RIS into the walls and floors of the factory can significantly enhance signal reflection and penetration, especially in hard-to-reach areas. Wall-integrated RIS can reflect signals around corners and into enclosed spaces, while floor-integrated RIS can ensure coverage in areas where movement is restricted and/or obstructed by large equipment. This approach requires careful planning and installation but offers substantial benefits in terms of network coverage and reliability.

5.2. Robust Communication Protocols for Seamless Connectivity

To support these varied RIS deployment strategies, and use cases intending to use THz and RIS technology, the following robust communication protocols and techniques are essential:

Handoff Protocols

Seamless Handoff Mechanisms: Developing handoff protocols that manage the transition of mobile devices between different RIS and APs is critical for maintaining uninterrupted connectivity. These protocols should include predictive algorithms that can anticipate device movement based on historical data and real-time monitoring. By pre-emptively adjusting beamforming and channel allocations, the network can ensure a seamless handoff, minimising latency and avoiding dropped connections, particularly important for the TCP protocol [6].

Machine Learning for Predictive Handoff: Machine learning algorithms can be employed to enhance the accuracy of predictive handoff mechanisms. By analysing patterns in device movement and network usage, these algorithms can make more accurate predictions about future device locations and network requirements. This allows for more efficient resource allocation and improved overall network performance [7].

Context-Aware Handoff: Incorporating context-aware handoff strategies can further enhance seamless connectivity. These strategies can use contextual information, such as the type of task a robot is performing or its expected path, to optimise handoff decisions. By understanding the operational context, the network can prioritise critical connections and allocate resources more effectively [8].

Beam Management

Dynamic Beam steering: Implementing dynamic beam steering techniques allows RIS to steer beams towards moving devices in real-time. This requires the deployment of adaptive algorithms that can adjust the direction and shape of the beams based on feedback from the network. Real-time feedback mechanisms, such as sensors and monitoring tools, provide the necessary data to make these adjustments, ensuring that devices receive a strong and stable signal as they move through the factory [9].

Advanced Beam Shaping Techniques: Advanced beam shaping techniques can be used to optimise the signal strength and coverage area. By adjusting the amplitude and phase of the transmitted signals, RIS can create focused beams that deliver higher signal quality and reduced interference. This is particularly important in environments with a high density of devices and potential sources of interference [10].

Multi-Beam Management: The ability to generate and manage multiple beams simultaneously can significantly enhance network efficiency. Multi-beam management (and/or beam splitting) allows RIS to support multiple devices or areas with different beams, optimising resource utilisation and improving overall coverage. This is especially useful in scenarios where multiple robots or devices are operating in close proximity [11].

Channel Allocation

Dynamic Channel Allocation: Designing dynamic channel allocation protocols is essential for optimising the use of available THz spectrum. These protocols should be capable of adjusting to real-time network conditions, such as changes in device density and interference levels. By dynamically allocating channels to devices based on current network requirements, the protocols can maximise throughput and reduce the likelihood of interference. It would be very useful in a mesh network

environment for each THz RIS AP to be aware of the channel utilisation of mobile devices as they travel through the mesh on the factory floor [12].

Interference Management: Effective interference management techniques, such as adaptive power control and frequency hopping, are crucial for maintaining high network performance. These techniques can mitigate the impact of co-channel interference, ensuring that each device receives a clear and reliable signal. Adaptive power control adjusts the transmission power based on the distance and interference levels, while frequency hopping reduces the chance of sustained interference on any given channel. AI algorithms may even be implemented to manage this in real-time [13].

Quality of Service (QoS) Optimisation: Implementing QoS optimisation strategies can ensure that critical applications receive the necessary bandwidth and low-latency connections. By prioritising traffic based on its importance, the network can provide consistent performance for essential tasks while managing less critical data streams efficiently [14].

Mobility Support

Low-Latency Handoff Mechanisms: To support high-speed mobility, the network must integrate low-latency handoff mechanisms that maintain high signal quality during transitions. These mechanisms should leverage the directional nature of THz communications and the flexibility of RIS to quickly adapt to changes in device positions. Low-latency handoff is particularly important in environments where devices move rapidly or frequently change locations and may make use of real-time AI during their operation [15].

Continuous Connectivity in Dynamic Environments: Ensuring continuous connectivity in dynamic manufacturing environments requires a combination of advanced handoff protocols, dynamic beamforming, and real-time feedback mechanisms as previously mentioned above. By integrating all of these elements into a comprehensive THz wireless AP system, the network can provide consistent performance and minimise disruptions, even in highly dynamic settings.

Mobility-Aware Resource Allocation: As also mentioned above, resource allocation strategies that consider the mobility patterns of devices can further enhance network performance. By anticipating the movement of devices, the network can allocate resources proactively, ensuring that the high-bitrate requirement of mobile robots in a factory environment can maintain strong connections and optimal performance.

Consider the example below in Figure 5-7, showing a single robot and an expanded view of the factory floor. Consider that each pillar (or even a group of 4 pillars) is treated as an Access Point, controlling a number of THz RIS. As the robot performs its normal manufacturing operations, it may first move from RIS to RIS within the same AP, and then later also transition from AP to AP in a mesh network as it moves across the factory floor.
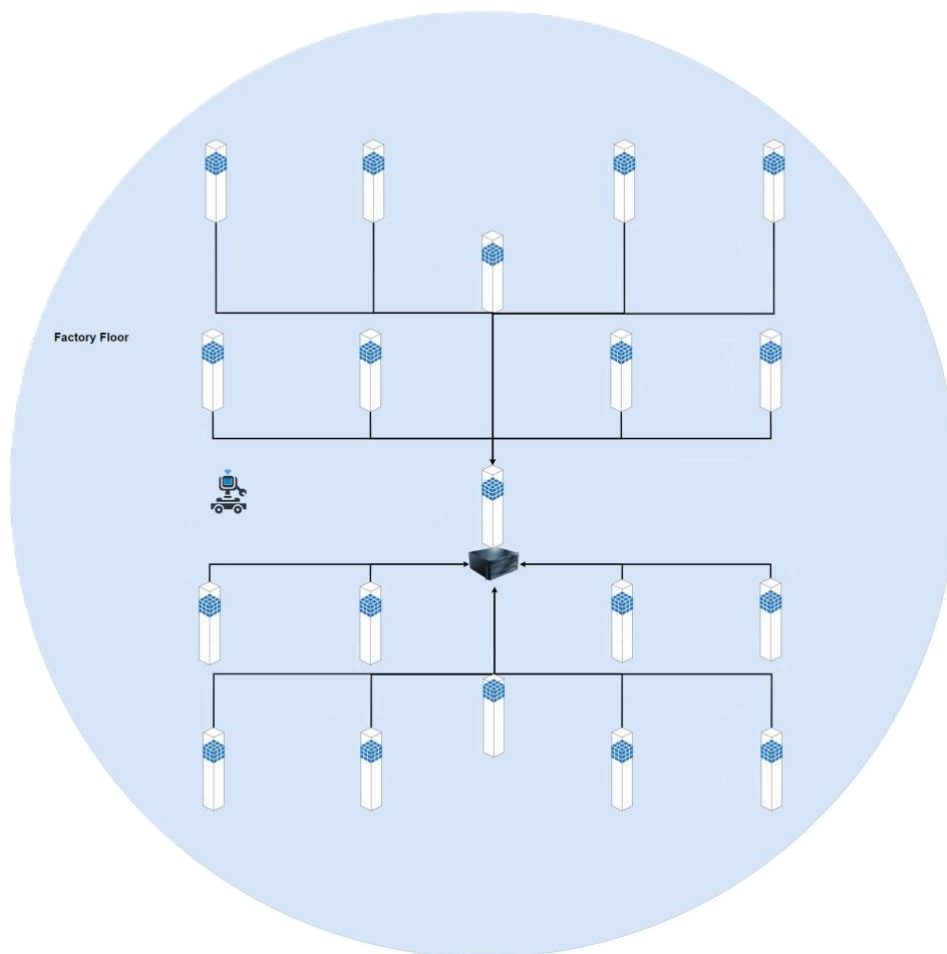
Figure 5-7: Expanded isometric view of architecture.

Enabling seamless connectivity for this device, and potentially hundreds of these and other mobile devices in the network is a far greater challenge for a directional THz network compared to traditional omni-directional WiFi. Special considerations need to be made to enable the types of functionalities listed above, which need to be integrated into future standards of network protocols that utilise high frequency communications.

5.3. IEEE 802.15.3d and 802.11 Adaptation for Factory Use Cases

To implement an effective THz network for a software-defined factory, we propose following the IEEE architecture, specifically adapting IEEE 802.15.3d standards towards IEEE 802.11 type standards for Wireless Local Area Networks (WLANs) at 300 GHz. This section details the rationale, design considerations, and proposed adaptations necessary to achieve this integration [16]. The rationale behind merging functionalities from both standards is to combine the required functionality from both standards towards a result that maximises the benefits and performance of THz and RIS wireless links. IEEE 802.15.3d provides the necessary framework for 300GHz PHY and MAC communication with low latency over short distances, making it ideal for the high-speed, localized communication requirements of a factory environment. However, IEEE 802.11 standards offer mature and widely adopted solutions for networking and security, which are essential for building a reliable and secure WLAN infrastructure.

In future THz systems, it is also expected for improvements in device power and RIS design to greatly increase the effective range of communication links above and beyond 100 m. This also coincides with 802.11 WLAN standards in both range, and intention to connect devices to a larger local area network. 802.15 on the other-hand is designed for personal area networks (WPAN), with distances of 10 m or less, and intended for device-to-device communication (e.g., Bluetooth). While current THz device technology has this kind of range performance, both the range and intent for this factory use case aligns

with the use of future higher-performing devices in an 802.11 standard, rather than 802.15. By integrating aspects from both 802.11 and 802.15 however, we can ensure that the THz network not only meets performance requirements but also benefits from the extensive security measures, interoperability, and ease of integration associated with IEEE 802.11. Using 802.11 standards also allows for a more seamless integration with existing network infrastructure, facilitating the deployment of THz technologies in environments where IEEE 802.11 is already in use, which is true for the manufacturing environment of Dell Technologies and many other manufacturing environments. This approach ensures that the new THz network can be managed using familiar tools and protocols, reducing the learning curve and operational complexity for network administrators.

IEEE 802.15.3d Overview

The IEEE 802.15.3d standard specifies the physical (PHY) and medium access control (MAC) layers for THz communication systems operating in the 252-325 GHz frequency range. The frequency and channel list can be seen in Figure 5-8. It is designed to support ultra-high-speed data rates and is particularly suitable for short-range, high-capacity wireless communication applications. Key features of the IEEE 802.15.3d standard include:

- **High Data Rate Support:** The standard supports data rates up to 100 Gbps, which is essential for applications requiring the transfer of large volumes of data in real-time.
- **Directional Communication:** IEEE 802.15.3d leverages highly directional antennas to minimise interference and maximise signal strength over short distances, typically within 10 meters.
- **Low Latency:** The standard is optimised for low latency communication, which is critical for real-time industrial applications.

The 802.15.3d standard is foundational for THz communications because it addresses the unique challenges and requirements of operating at such high frequencies. These include the high path loss, atmospheric absorption, and the need for precise alignment due to the directional nature of THz waves. By leveraging these standards, we can ensure a robust framework that supports the high-speed, high-capacity needs of a modern factory environment.
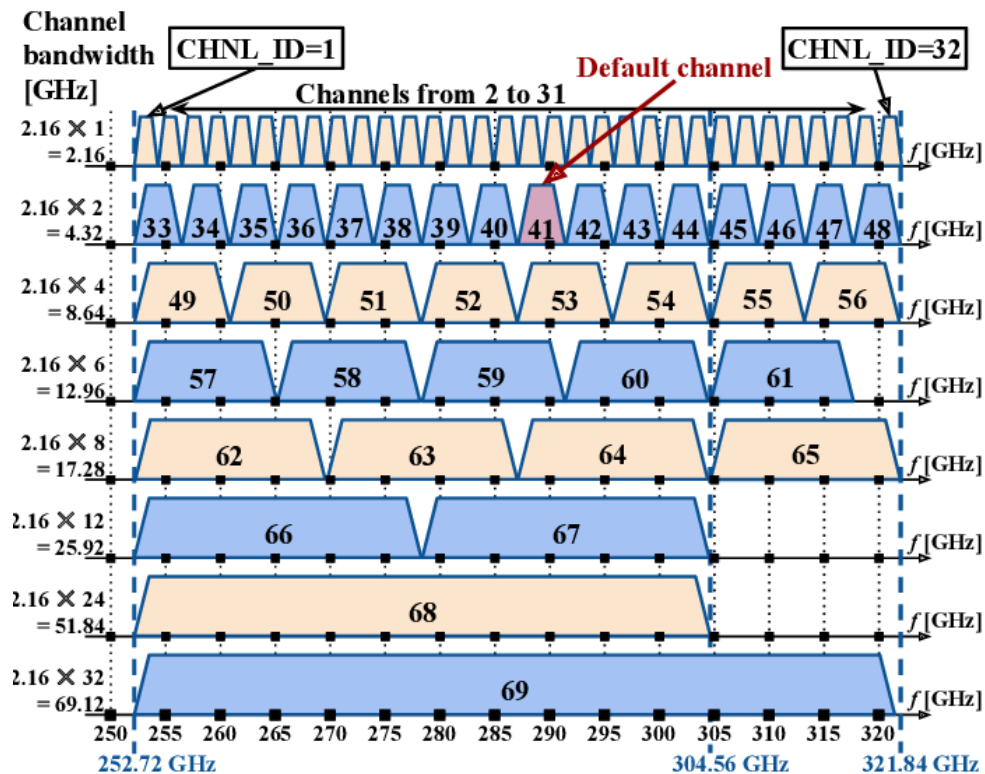
Figure 5-8: IEEE 802.15.3d Frequency and Channel structure [16]

Adapting IEEE 802.15.3d into IEEE 802.11 Standards

Adapting IEEE 802.15.3d into IEEE 802.11 standards involves integrating the high-speed, short-range capabilities of 802.15.3d with the established networking and security frameworks of 802.11, while also including additional functions necessary for the use cases intending to utilise real-time high frequency communications. The goal is to create a standard that leverages the strengths of 802.15.3d, providing a robust and flexible solution for high-speed WLANs in industrial environments.

Physical Layer (PHY) Adaptation

The physical layer of the IEEE 802.15.3d standard includes various modulation and coding schemes designed to operate efficiently at THz frequencies. For adaptation into IEEE 802.11 standards, the following considerations are proposed:

- **Modulation Schemes:** Incorporate high-order modulation schemes such as Quadrature Amplitude Modulation (QAM) to support high data rates. The modulation schemes from 802.15.3d (e.g., On-Off Keying (OOK), Binary Phase-Shift Keying (BPSK), and Quadrature Phase-Shift Keying (QPSK)) will be integrated into the 802.11 framework to ensure compatibility with THz communications. Higher-order modulations like 16-QAM, 64-QAM, and 256-QAM can be used to maximise data throughput where possible while maintaining robust error performance.
- **Channel Coding:** Employ advanced error correction codes such as Low-Density Parity-Check (LDPC) and Turbo codes to enhance data reliability and robustness against noise and interference. These coding schemes are critical for maintaining data integrity over the challenging THz frequency channels [17].
- **Spectrum Utilisation:** Define specific frequency bands within the 300 GHz range for public/industrial WLAN applications, ensuring optimal spectrum utilisation and minimal interference with existing wireless systems. This involves coordinating with regulatory bodies to secure the necessary spectrum allocations and establishing protocols for dynamic spectrum access to maximise efficiency.

Medium Access Control (MAC) Layer Adaptation

The MAC layer of the IEEE 802.11 standard is well-established for managing wireless communications, providing mechanisms for channel access, collision avoidance, and data security. Adapting the MAC protocols to support THz frequencies involves the following enhancements:

- **Directional MAC Protocols:** Incorporate directional MAC protocols that can manage highly directional THz links. This includes mechanisms for beamforming, beam tracking, and adaptive beam steering to maintain optimal communication links. Directional MAC protocols must efficiently handle the discovery and maintenance of directional links, including managing handovers and mitigating interference from other devices [18].
- **Channel Access Mechanisms:** Adapt the carrier sense multiple access with collision avoidance (CSMA/CA) protocol to operate effectively at THz frequencies. This includes modifications to account for the directional nature of THz communications and the shorter communication range. For THz links, new or additional mechanisms such as time-division multiple access (TDMA) and frequency-division multiple access (FDMA) can also be integrated to enhance channel access efficiency [19].
- **QoS and Latency Management:** Enhance quality of service (QoS) protocols to prioritise low-latency, high-priority traffic, ensuring that critical industrial applications receive the necessary bandwidth and minimal delay. This includes implementing traffic prioritisation, dynamic resource allocation, and advanced scheduling algorithms to meet the stringent performance requirements of industrial applications [20].

The IEEE 802.15.3d standard specifies the PHY and MAC layers for THz communication systems, providing a robust framework for high-speed, short-range communications. To integrate THz and RIS technologies into broader wireless local area network (WLAN) applications, particularly those defined under IEEE 802.11 standards, it is essential to adapt and extend the existing Layer 2 header structures

from both IEEE 802.15.3d and 802.11, and also incorporate additional header information to aid with RIS communications. An example of the IEEE 802.15.3d header structure can be seen in Figure 5-9.
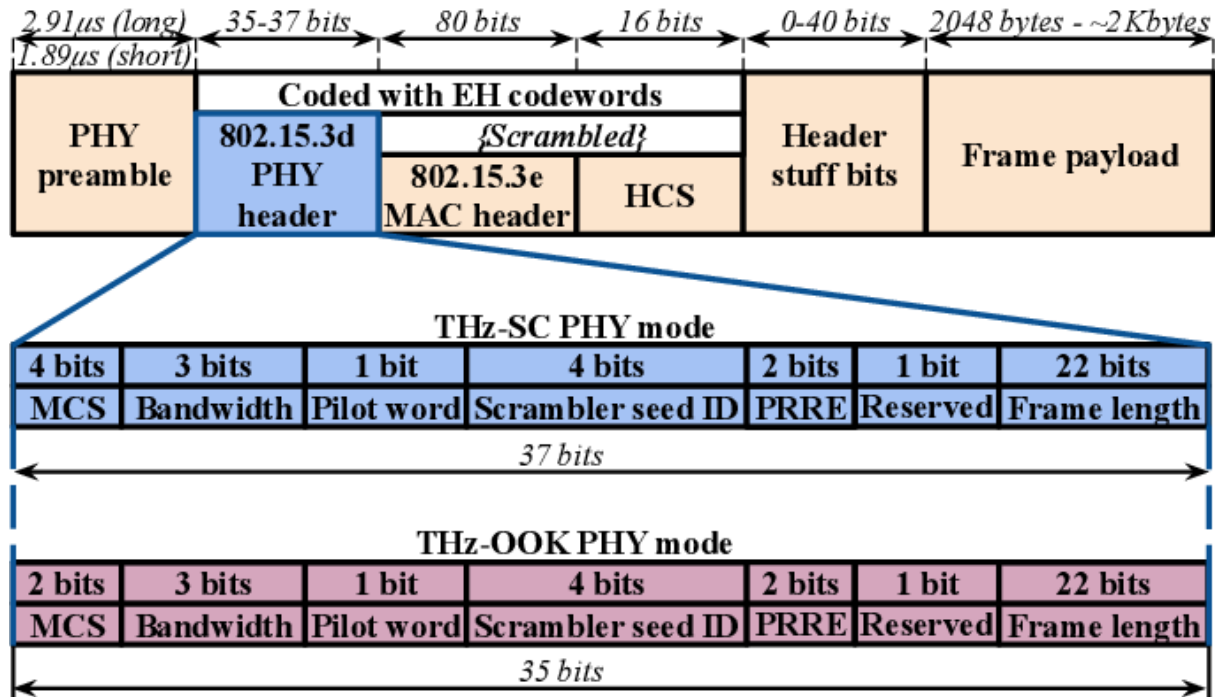
Figure 5-9: 802.15.3d Header structure [16]

Proposed Adaptations to IEEE 802.11 Headers

Beam Steering Control: The integration of RIS into WLANs necessitates precise control over beam steering functionalities. By modifying the L2 header, specific bits can be designated for beam steering commands. This includes parameters such as the angle of departure (AoD) and angle of arrival (AoA), allowing real-time adjustments to the beam direction based on the current network topology and user locations. This field can include subfields for azimuth and elevation angles, allowing the AP or RIS controller to dynamically adjust the beam direction. For example, 8 bits could be allocated for azimuth and another 8 bits for elevation, providing 256 discrete levels of control for each parameter. A higher resolution of discrete states can be supported with additional bits, at the cost of slightly reduced overall network layer throughput.

RIS Configuration Commands: To enable dynamic reconfiguration of the RIS elements, the L2 header can be extended to include RIS configuration commands. These commands would allow the controller to adjust the phase shifts and amplitude settings of individual RIS elements to optimise signal reflection and transmission. This field could be subdivided into multiple subfields, each corresponding to a different configuration parameter (e.g., phase shift, amplitude adjustment). By using a combination of bits to represent these parameters, the controller can send complex reconfiguration commands in real-time within the standard frame structure.

Channel State Information (CSI) Feedback: Incorporating real-time CSI feedback into the L2 header, can significantly enhance the network's ability to adapt to changing environmental conditions. This information is crucial for optimising beamforming and other adaptive techniques. This field can carry condensed CSI reports, such as the estimated signal-to-noise ratio (SNR), channel quality indicator (CQI), and other relevant metrics. This allows the AP and RIS to make informed decisions about beamforming and resource allocation.

Quality of Service (QoS) Enhancements: To support applications with stringent latency and bandwidth requirements, the L2 header can be extended to include enhanced QoS parameters. These parameters help prioritise traffic and ensure that critical data receives the necessary resources. This

field could include bits for priority level, latency requirements, and bandwidth allocation. By encoding these parameters directly into the frame, the network can dynamically adjust its resource management to meet the needs of different applications.

Example L2 Header Extension for IEEE 802.11

Below is an example of how the L2 header might be extended to incorporate these new functionalities:

Table 1 Example of IEEE 802.11 adaptation to support RIS control.

Field	Size (bits)	Description
IEEE 802.15.3d PHY	37	PHY Header adapted for 802.11
Frame Control	16	Standard IEEE 802.11 frame control
Duration/ID	16	Duration or ID field
Address 1	48	Receiver address
Address 2	48	Transmitter address
Address 3	48	Filtering address
Sequence Control	16	Sequence number for tracking frames
Beam Steering Control	16	Azimuth and elevation angles for beam steering
RIS Configuration	32	Configuration commands for RIS elements
CSI Feedback	16	Condensed channel state information
Enhanced QoS	16	Priority, latency, and bandwidth requirements
Address 4	48	(Optional) Used in some frame types
Frame Body	Variable	Data payload
FCS	32	Frame check sequence for error detection

The benefits of adapting the IEEE 802.11 L2 header to include beam steering controls, RIS configuration commands, enhanced QoS fields, and CSI feedback are significant. These adaptations enable the network to achieve precise and responsive beamforming, crucial for maintaining high-quality THz links in dynamic environments. Embedding RIS configuration commands facilitates real-time adjustments to RIS elements, optimising signal propagation and overall network performance. The extended QoS fields ensure better resource management, guaranteeing that critical applications receive the necessary bandwidth and low-latency connections. Additionally, incorporating CSI feedback allows the network to continuously adapt to changing conditions, maintaining optimal performance and reliability. By extending the IEEE 802.11 L2 header with these new fields, we can effectively integrate THz and RIS technologies into WLANs, providing the control and communication functionalities needed for high-speed, reliable, and adaptive wireless networks.

5.4. Role of Reconfigurable Intelligent Surfaces (RIS)

The integration of RIS is critical for the deployment of reliable THz links in a factory setting. RIS can enhance the performance of THz wireless networks by dynamically controlling the propagation environment, thus mitigating the challenges posed by the highly directional nature of THz signals.

RIS as a Key Enabler

RIS can be used to:

- **Improve Coverage:** By reflecting THz signals around obstacles, RIS can extend coverage in areas where direct line-of-sight (LoS) paths are blocked. This is particularly important in factory environments with numerous machines and structural elements that can obstruct signals.
- **Enhance Link Reliability:** Through intelligent beam steering, RIS can dynamically adjust the direction of the reflected beams to maintain a reliable link as devices move or as the environment

changes. This ensures continuous, high-quality communication even in dynamic and cluttered environments.

- **Optimise Spectrum Reuse:** By controlling the direction of signal propagation, RIS can enable efficient spectrum reuse, increasing the overall network capacity. This is achieved by directing beams to specific devices, minimising interference, and allowing multiple devices to operate in close proximity without degrading performance.

Core RIS Functions

For effective integration into the IEEE architecture, a core set of RIS functions should be defined and embedded into future wireless Access Points (APs) supporting THz frequencies. These functions include:

- **Beam Steering:** The ability to dynamically adjust the direction of the reflected beam to maintain a high-quality link. This involves algorithms for precise control of the phase and amplitude of reflected signals to steer beams towards intended targets.
- **Channel Control:** Managing the THz channels to optimise data throughput and reduce interference. This includes dynamically allocating channels based on real-time network conditions and implementing frequency hopping techniques to mitigate interference.
- **RIS Discovery:** Enabling APs to detect and integrate nearby RIS into the network to enhance coverage and performance. This function will involve protocols for discovering, authenticating, and configuring RIS elements. Discovery protocols must be efficient and robust, ensuring seamless integration of new RIS elements as they are deployed.
- **Adaptive Beamforming:** Utilising feedback from user devices to adapt the beam patterns in real-time, ensuring optimal signal delivery. This includes mechanisms for real-time beam adjustment based on device movement and environmental changes. Machine learning algorithms can be employed to predict optimal beam patterns based on historical data and real-time feedback.
- **Energy Efficiency Management:** Optimising the power consumption of RIS elements to enhance overall network energy efficiency. This function will include dynamic power management based on network load and environmental conditions. Energy-efficient designs and power-saving strategies will be critical for minimising operational costs and extending the lifespan of RIS elements.
- **Security Enhancement:** Using RIS to create secure communication paths and prevent eavesdropping. This includes implementing encryption and authentication protocols specific to RIS-enabled communications. Secure beamforming techniques can be used to direct signals in a manner that minimises the risk of interception.

Integrating RIS Functions into Wireless APs

Future wireless AP designed to support THz frequencies should incorporate a dedicated RIS Control Unit (RCU) to manage the integration and functionality RIS. This specialized module within the AP will play a crucial role in ensuring efficient operation and seamless integration with the broader network. The RCU will encompass a variety of functions necessary for optimizing the performance of RIS-enabled wireless networks. The RCU should have the following functions:

Configuration Management: The RCU will manage the initial setup and ongoing configuration of RIS elements. This includes defining the phase shifts and amplitude adjustments required for optimal signal reflection and transmission. The configuration management system will support various operational modes of the RIS, such as transmissive, reflective, and hybrid modes, allowing for flexible deployment based on the specific use case requirements.

Real-time Monitoring and Feedback: Continuous monitoring of RIS performance and environmental conditions will be a key function of the RCU. This involves collecting real-time data from RIS elements and the surrounding network environment. The RCU will analyse this data to detect any performance degradation or changes in the network conditions, allowing for proactive adjustments to maintain optimal performance.

Beam Management Algorithms: The RCU will include advanced beam management algorithms to control beamforming and beam steering in real-time. These algorithms will leverage machine learning

techniques to predict and adapt beam patterns based on historical data and real-time feedback. By dynamically adjusting the beam direction and shape, the RCU will enhance the network's ability to maintain high-quality links, even in highly dynamic and cluttered environments.

Channel State Information (CSI) Analysis: A crucial component of the RCU will be the CSI module, which continuously collects and analyses channel state information. This data is essential for understanding the current channel conditions and making informed adjustments to the RIS configuration. Accurate and real-time CSI analysis will enable effective beam steering and channel control, ensuring that the network can adapt to changing conditions and maintain reliable communications.

Power Management: The RCU will implement intelligent power management strategies to optimize the energy efficiency of RIS elements. This includes adjusting the power usage based on network load and operational requirements. Energy-efficient designs and power-saving strategies will be key to reducing operational costs and extending the lifespan of RIS components.

Security and Authentication: Ensuring secure communication between the AP and RIS elements will be a critical function of the RCU. This involves implementing encryption and authentication protocols to protect against unauthorized access and potential cyber threats. Secure beamforming techniques will also be employed to minimize the risk of interception and ensure that data transmission remains confidential and protected.

Figure 5-10 illustrates a typical WLAN router block diagram with extensions added for a RIS control chip. This diagram highlights how the RCU integrates into the existing AP architecture, enabling seamless communication and control of RIS elements. The inclusion of the RCU within the AP's design ensures that all RIS-related functions are managed efficiently and effectively, contributing to the overall performance and reliability of the wireless network. By incorporating these advanced functions into the RIS Control Unit, future wireless APs will be well-equipped to handle the complexities of THz and RIS technologies, providing high-speed, reliable, and adaptive wireless communications.
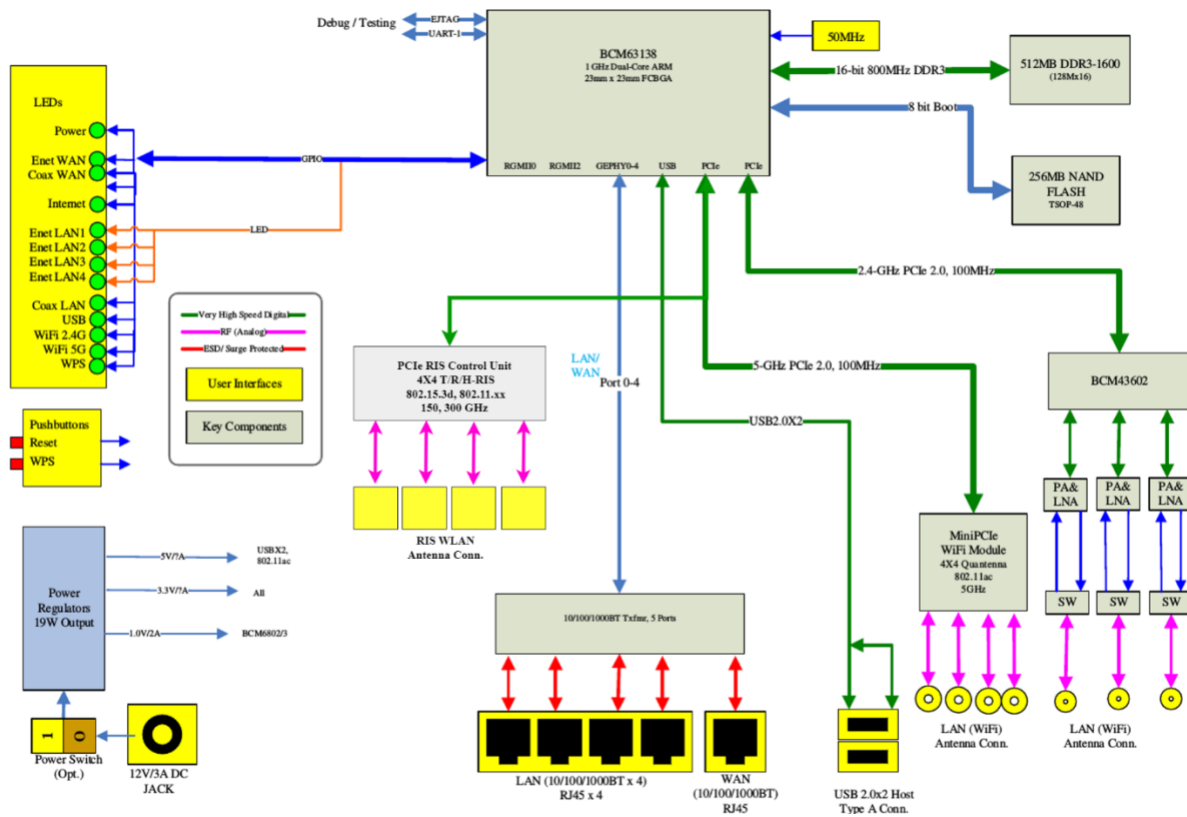
Figure 5-10: Typical WLAN router block diagram with THz and RIS controller adaptations

Figure 5-11 presents a conceptual diagram of a THz System on Chip (SoC), illustrating the potential future design of a wireless access point that integrates both THz and RIS technologies. This SoC device resembles existing Wi-Fi routers in form and function but includes advanced features for managing THz links and RIS. The SoC is designed to control not only the THz and RIS functionalities but also traditional Wi-Fi signals across 2.4 GHz, 5 GHz, and 6 GHz bands. By integrating these capabilities into a single chip, the device can seamlessly manage diverse frequency operations, providing robust and adaptive wireless communication. This conceptual design serves as a forward-looking example of how future products might incorporate THz and RIS technologies within the IEEE architecture, offering enhanced performance and flexibility for next-generation wireless networks.
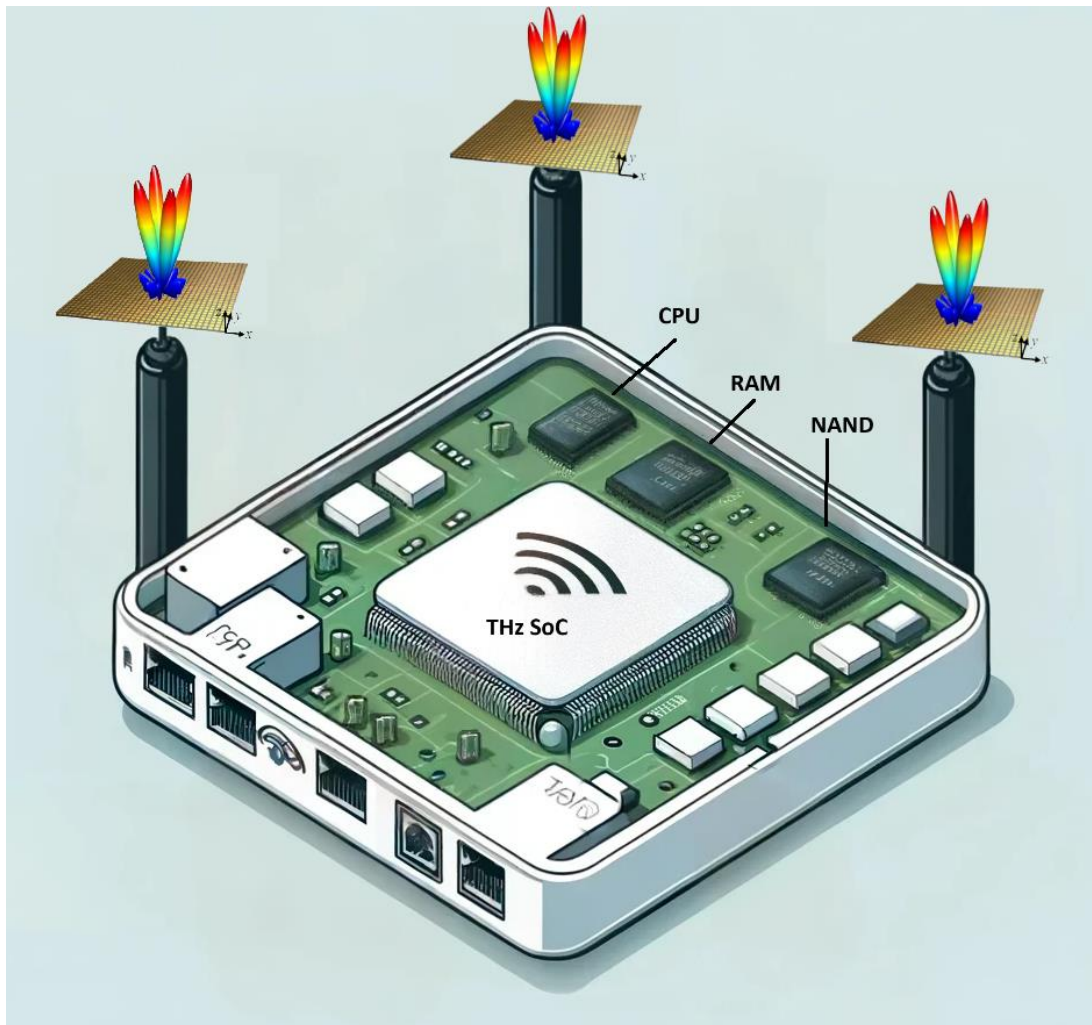
Figure 5-11: Conceptual figure of what a future IEEE WLAN-based THz and RIS Access Point may look like

5.5. Use Case Network Architecture

The proposed network architecture for a software-defined factory utilising THz links and RIS involves several key components:

THz Wireless APs: These APs will support THz frequencies, integrated with RIS control capabilities, and adhere to the adapted IEEE 802.15.3d to 802.11 standards. Strategically placed throughout the factory, these APs will ensure optimal coverage and performance, equipped with advanced beamforming capabilities, high-gain antennas, and robust security features.

Edge Servers: Localized processing units will handle data generated by factory devices, ensuring low-latency processing and control. These servers will be interconnected using high-speed THz links and

fibre optic cables, providing real-time processing capabilities. This will reduce latency and enhance the performance of industrial applications.

RIS Elements: These will be strategically placed throughout the factory to ensure optimal coverage and performance, controlled by the THz APs. Their placement will be based on thorough site surveys to identify the best locations for coverage enhancement. Designed to be energy-efficient and durable, these RIS elements will be capable of withstanding the harsh factory environment.

Backhaul Network: The backhaul network will consist of a combination of fibre optic and THz wireless links to connect the factory network to the broader enterprise network. This network will ensure high-speed, reliable connectivity for data-intensive applications, with redundant backhaul links and failover mechanisms to enhance network reliability and resilience.

Network Topology

The network topology in a software-defined factory will feature a hierarchical, multi-tiered architecture. The access layer will comprise THz wireless APs and edge servers, providing high-speed connectivity to factory devices and handling initial data processing. This layer will include multiple APs strategically placed for comprehensive coverage and seamless handovers for mobile devices. The aggregation layer will connect multiple access layer networks, typically through THz or fibre optic backhaul links, aggregating data from multiple access points and routing it to the core layer. High-capacity switches and routers in this layer will manage increased data traffic. The core layer will serve as the main network backbone, connecting the aggregation layer to external networks and data centres, handling bulk data traffic, and providing connectivity to external systems. High-performance routers and switches in this layer will ensure low-latency and high-reliability connectivity.

Redundancy and Reliability

To ensure the highest level of reliability and availability, the network architecture will incorporate redundancy at multiple levels. Redundant APs will be deployed in overlapping coverage areas to ensure seamless connectivity in case of an AP failure. Multiple THz links and fibre optic connections will provide failover capabilities for the backhaul network, ensuring continuous operation. Redundant edge servers with load balancing will distribute processing tasks and provide backup in case of server failure.

Security Considerations

The proposed network architecture will include robust security measures to protect against potential threats. All data transmitted over THz links and within the network will be encrypted using strong encryption algorithms. Strict access control policies will regulate which devices can connect to the network and what resources they can access. Continuous monitoring of network traffic will detect and respond to potential security threats in real-time, and intrusion detection systems will identify and mitigate malicious activities within the network.

Example Use Case: SLAM with THz Links

One critical application in a software-defined factory is SLAM using mobile robots. This use case leverages high-bitrate THz links to ensure real-time data transmission between mobile robots equipped with THz communication modules and local edge servers. The high data rates and low latency of THz links are ideal for the bandwidth-intensive and time-sensitive nature of SLAM data. Equipped with directional antennas and beamforming capabilities, the robots maintain robust connections with APs and THz RIS.

RIS elements play a crucial role in supporting mobility by dynamically adjusting the beam direction to maintain reliable links as robots move throughout the factory. This ensures continuous, high-quality communication even in complex and changing environments. Strategically placed to cover key areas, RIS elements adapt in real-time to the movement of the robots, ensuring seamless connectivity.

Local edge servers process the SLAM data, collaborating to build a comprehensive map of the factory environment. The distributed nature of edge processing reduces latency and enhances the efficiency of SLAM operations. These edge servers perform real-time data analysis, machine learning, and decision-making, supporting autonomous robot navigation.

The network design for supporting SLAM involves critical components such as the strategic placement of APs to ensure optimal coverage and minimal signal interference. AP placement considers the factory layout, including obstacles and high-traffic areas. RIS elements are deployed in areas where direct line-of-sight (LoS) is not feasible or where signal enhancement is required, ensuring seamless coverage and dynamic beam steering support. Edge servers are configured to handle the processing load generated by SLAM applications, equipped with high-performance computing resources and efficient data storage solutions.

Real-time data processing is essential for SLAM applications. Data from multiple sensors on the robots are aggregated and transmitted to edge servers via THz links. This aggregation process ensures minimal data loss and high transmission efficiency. Edge servers perform real-time analysis of the SLAM data, generating accurate maps and localization information using advanced algorithms and machine learning techniques to enhance accuracy and reliability. The processed data is then used for real-time decision-making in robot navigation and task execution, including obstacle avoidance, path planning, and task scheduling.

To enhance network performance supporting SLAM applications, several strategies are employed. Quality of Service (QoS) protocols prioritize SLAM data traffic, ensuring minimal latency through dynamic bandwidth allocation and traffic shaping techniques. Advanced interference mitigation techniques, such as adaptive frequency hopping and beamforming strategies, minimize the impact of signal interference on SLAM data transmission. Continuous monitoring and optimization of network performance ensure optimal operation through real-time adjustments to AP configurations, RIS settings, and network routing.

In a typical use case scenario, multiple mobile robots equipped with THz communication modules and sensors navigate the factory floor. Upon startup, the robots connect to the nearest AP and establish THz links, with APs and RIS elements dynamically adjusting beams to ensure optimal connectivity. The robots continuously collect sensor data and transmit it to the edge servers via THz links, where the data is aggregated and processed in real-time. Edge servers perform SLAM processing, generating accurate maps and localization information, which are used to update the robots' navigation paths. As the robots move, the network dynamically adapts to maintain optimal connectivity, with RIS elements adjusting their beam directions and APs managing handovers to ensure seamless communication. The robots execute their tasks based on the processed data, navigating the factory floor, avoiding obstacles, and interacting with other machines and equipment.

Integrating IEEE 802.15.3d into 802.11 standards and leveraging RIS technology offers a robust solution for the network demands of a software-defined factory. This hybrid approach combines the high data rates and directional communication capabilities of THz links with the flexibility and scalability of IEEE 802.11-based WLANs. By embedding RIS functions directly into wireless APs, the network can dynamically adapt to the challenging factory environment, ensuring high performance, reliability, and energy efficiency. This proposed network architecture supports the advanced manufacturing processes of Industry 4.0, paving the way for the future of smart factories.

6. Telco Use Case Network Architecture

6.1. THz RIS Architecture in ORAN

The deployment of THz RIS units will lead to some key architecture choices in order to realise efficient implementations. For a future 6G network to support a THz RIS, a break from traditional deployments is essential. It is expected that these future 6G networks will be disaggregated in nature which will leverage an Open Radio Access Network (O-RAN) architecture.
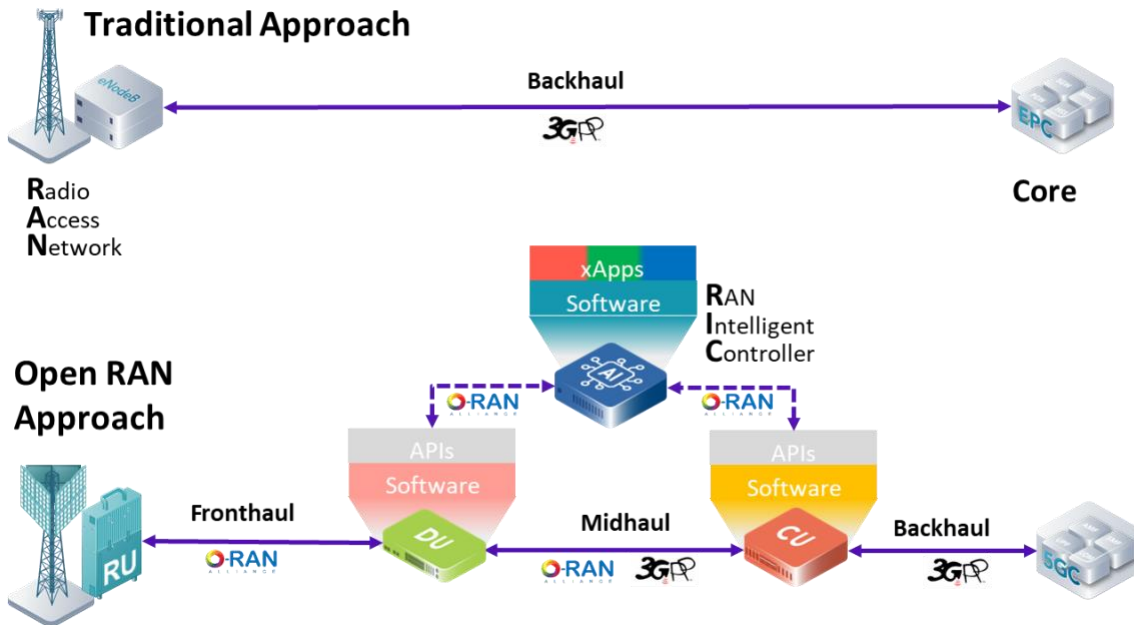
Figure 6-1: Traditional vs ORAN deployments

The RAN has for a long time been proprietary in nature, meaning a single vendor typically provided the antenna, baseband processing, and the management plane (as shown in Figure 6-1). This trend has resulted in stifled innovation, with the existing RAN market being made up of a few select vendors. Disaggregating the RAN into interoperable components can provide a number of benefits including (1) increased innovation through picking the best vendor in the mix for each component and (2) increased scope for virtualisation of software/hardware components. Both of these benefits could also provide greater flexibility and highly customised networks for bespoke use cases that service providers, operators, and their customers may have.

The impact of radio performance will be considered in the context of required changes to the RAN architecture and deployment techniques. ORAN architecture follows 3GPP architecture and interface specifications to the possible extent. The main network functions implemented in ORAN are related with the 5G-NR gNB and consist of one Open-RAN Centralised Unit (O-CU) that connects to and controls at least one Open-RAN Distributed Unit (O-DU) via the F1 interface. The O-DU connects to at least an Open RAN Radio Unit (O-RU), via an Open Fronthaul CUS-Plane, to implement the Uu interface. The Open Fronthaul M-plane exist for the implementation of the Management Plane towards the O-RU via the O-DU

ORAN High level Architecture
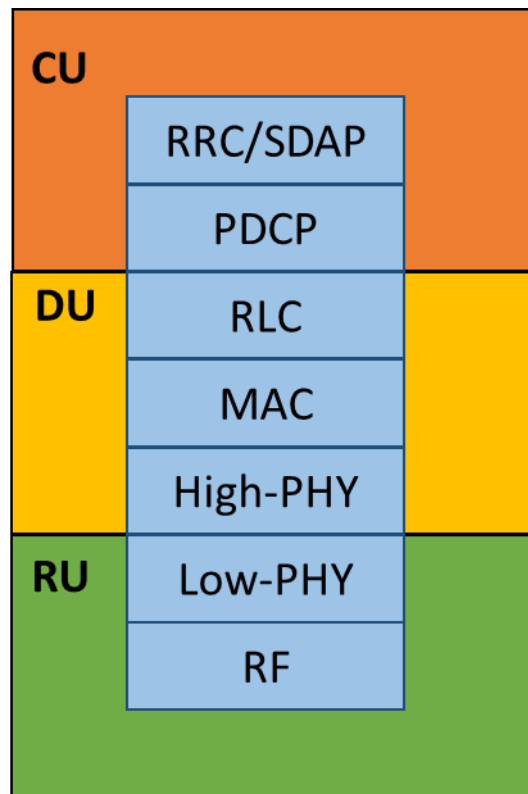
Figure 6-2: High Level ORAN Architecture

To accommodate more flexibility in the design of radio access networks, the O-RAN Alliance has developed ORAN protocols, allowing the baseband and radio units to be split into three different modules and their protocol layers, each of which can be provided by different vendors. A diagram of the architecture can be seen in Figure 6-2 above. It is split into the following over-arching functional blocks:

- **RU** (radio unit), which processes the RF and lower part of the physical layer (Low-PHY)

- **DU** (distributed unit), which takes on tasks of the upper part of the physical layer (High-PHY), medium access control (MAC), and radio link control (RLC)

- **CU** (central unit), which manages the packet data convergence protocol (PDCP), service data adaptation protocol (SDAP), and radio resource control (RRC) protocol entities.

In the ORAN context, the interface between CU and the core network is known as backhaul, the interface between DU and CU is known as mid-haul, and the interface between DU and RU is called fronthaul.

Function Splits

In terms of addressing the long-term capacity growth in radio access networks, it is the evolution of deployment architecture that is perhaps the most forward looking. The specification and part standardisation of new 'functional splits' in 5G standards have paved the way for greater flexibility and improved scalability of deployment through realisation of centralised and virtualised radio access networks. Whilst ORAN architectures are able to support a range of new deployment scenarios from consolidation or disaggregation of macro cell baseband capability to low-cost cell

densification built on street level small cells, they are underpinned by new high capacity, low latency fronthaul transport interfaces.
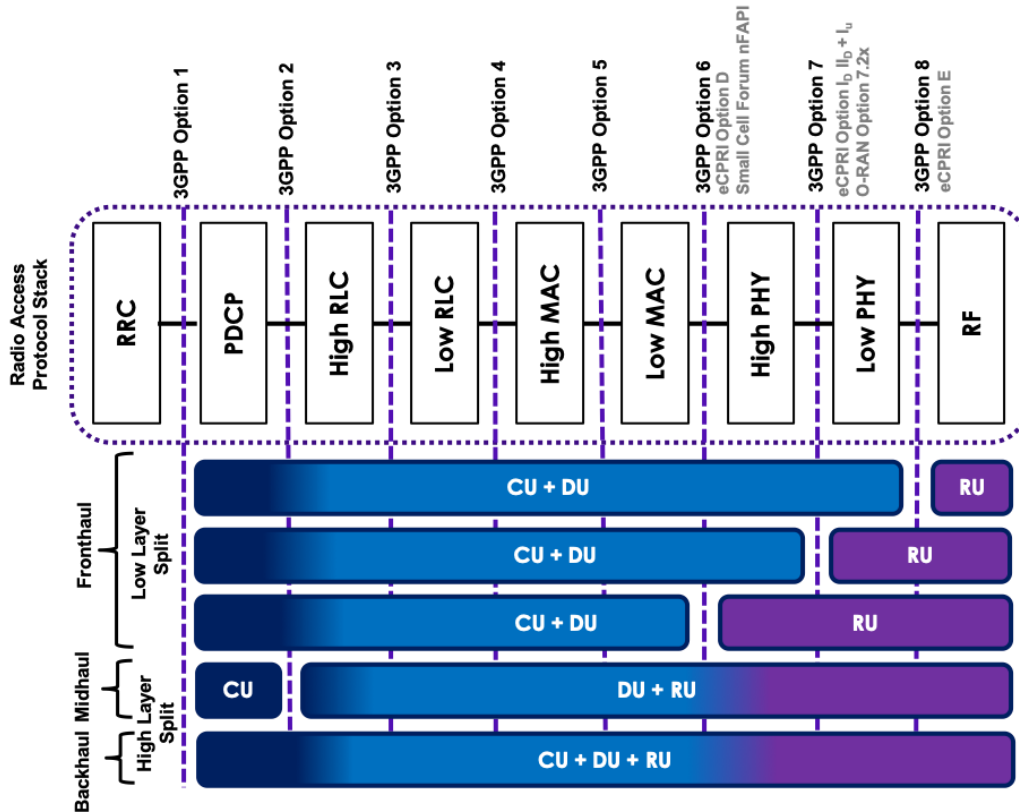
Figure 6-3: Functional Split options

There are eight split options that are defined by 3GPP [21] and are presented in Figure 6-3. Each one of these splits offers a different trade-off between centralisation benefits and fronthaul network requirements. There is no single, ideal functional split because different options will suit different applications. However, it is unlikely that the industry could practically support all eight options. Some of these functional splits are championed by key standardisation bodies such as 3GPP, ORAN, SCF, and NGMN. To ensure scale and openness, various industry alliances are working to gain consensus on the best options to be adopted. 3GPP has recommended Option 2 for highly centralised applications such as fixed wireless access, (FWA), where cell-site coordination is not required and latency and bandwidth requirements on the transport network are relatively relaxed.

Functional splits considered in network deployments

The so-called lower layer split (LLS) is a functional split between a baseband unit and a radio unit. The 3GPP study (3GPP TR 38.816) on functional splits included the "Option"-alternatives shown in the picture. Option 6 is a split between the media access control (MAC) layer and the physical (PHY) layer. The payload information conveyed over that split consists of transport blocks per layer. Options 7-1, 7-2 and 7-3 are different splits within the PHY layer. Option 8 is a split between the PHY layer and radio processing (which can include both digital and analogue processing). The payload information conveyed over that split consists of time domain IQ samples per radio chain.

THz RIS envisioned architectures
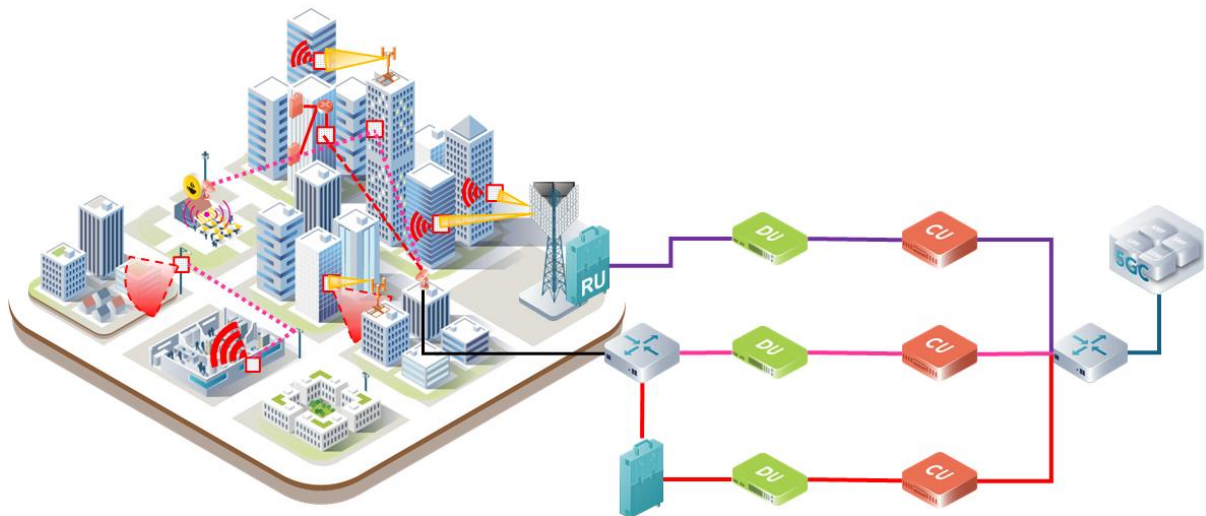
Figure 6-4: THz RIS deployments

The proposed THz RAN architecture incorporates modular and interoperable RAN components with existing open interfaces, namely Open-RAN, enabling seamless integration of sub-THz and THz frequency ranges. The flexibility of this type of architecture primarily focuses on improving network efficiency and performance in high-frequency bands, which are characterised by their limited propagation, high directionality, and high attenuation rates. A number of architectural changes are proposed:

1. **Modular THz RAN Components:** The architecture adopts a disaggregated RAN approach, where radio units (RUs) designed for lower frequencies can be easily replaced or augmented with ones operating in the sub-THz/THz bands. This flexibility supports dynamic network adaptation to varying demands and environmental conditions, promoting efficient spectrum utilisation.

2. **Enhanced Beamforming Techniques:** To address the challenges associated with THz communications, such as severe path loss, beam alignment issues and beam-squint effects, new beamforming algorithms are optimised for the wide bandwidths and high propagation losses typical of THz frequencies and integrated into the network architecture.

3. **Integration of THz RIS with Dual-Role Functionality:** RIS tailored for THz frequencies are integrated into the network infrastructure. These RISs are not only deployed to augment signal coverage and network capacity, but they also incorporate sensing capabilities. By enabling the RIS to perform environmental sensing, the architecture facilitates a robust feedback loop where sensing data informs RIS configurations, enhancing both communication efficiency and environmental awareness. This dual functionality is particularly advantageous in urban and information-dense settings where direct transmission paths are frequently obstructed, or high-performance mobile links are essential for ultra-high-speed data transfer.

These innovations tackle the barriers of leveraging THz spectrum utilisation by enhancing network flexibility and intelligence, which aligns with the overarching aspects of 6G. By improving the capability of networks to handle future radio access, this architecture supports a wide array of usage scenarios, paving the way for ubiquitous connectivity and integrated sensing and communication capabilities in 6G networks.

Typical Deployment Scenarios for 6G THz RIS
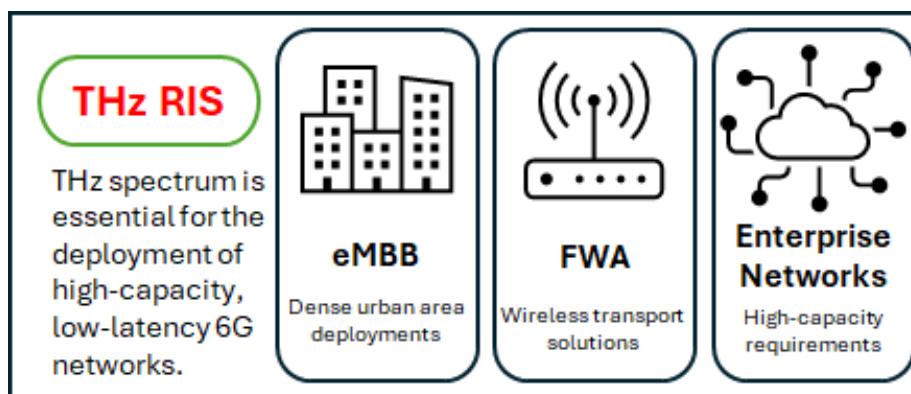
Figure 6-5: Key THz RIS deployments

Key deployment scenarios for THz RIS

- Fixed Wireless Access Networks
    - Wireless transport
    - Coverage enhancements
- Mobile broadband Networks (eMBB)
    - High-capacity networks
    - High-speed broadband
    - Network densification
- Private or Enterprise Networks
    - Indoor enterprise applications
    - Industrial applications

THz RIS enabled xHaul

Due to the challenging transport requirements of fronthaul interfaces, it is generally assumed that only ubiquitous fibre networks can practically support Open RAN deployments. The use of fibre, however, can often be too costly or time consuming to deploy at scale. In addition, wireless transport solutions have historically, found favour in conventional backhaul-based distributed RAN (D-RAN) architectures for the same reasons. In today's mobile networks over 50% of existing macro cellular base stations worldwide utilise a wireless transport solution. As a result, next generation wireless transport solutions are seen as a key technology enabler necessary to realise new centralised architectures and offer a viable deployment alternative to fibre transport. While the vast majority of traditional backhaul links operate in conventional fixed service microwave bands (typically 6-42 GHz), the performance criteria of new Ethernet-based fronthaul pose challenges for such bands [22]. To address these new deployment requirements, the migration to promising new high frequency sub-THz/THz transmission bands, such as the D-band (130-174.8 GHz), is being considered for future wireless xHaul scenarios. These fixed service bands promise low latency, high-capacity capability owing to the large channel bandwidths that are possible. Crucially, such bands have the potential to support fronthauling of lower layer functional split interfaces as well as the higher layer functional splits of midhaul and backhaul interfaces.

In traditional systems, backhaul was implemented via a fibre/wired connection or a microwave link. In Open RAN, where the radio unit may be separate from other components of the gNodeB (e.g., DU and CU) there still needs to be a way of connecting the parts together. The terms used are commonly fronthaul, midhaul and backhaul, known collectively as xHaul.

The components of xHaul in the context of splits are defined as:

- Complete gNB to core refers to the backhaul
- gNB-DU (RU/DU) to CU refers to midhaul
- RU to DU refers to the fronthaul

(a)

(b)

(c)
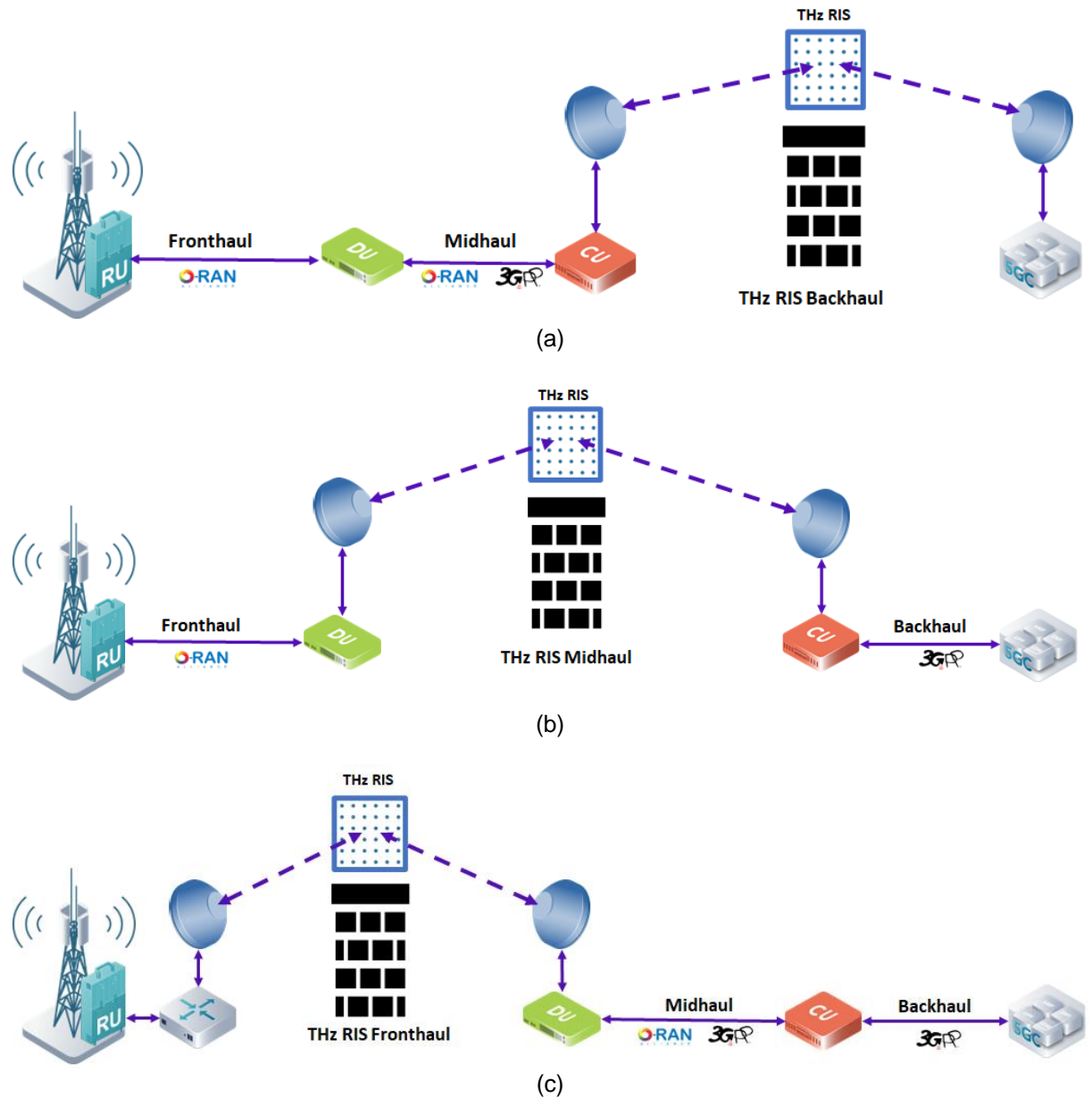
Figure 6-6: THz RIS xHaul deployments

Figure 6-6 illustrates typical deployments using THz RIS for xHaul leveraging split architectures. Figure 6-6 (a) depicts a THz RIS backhaul scenario where the gNB CU is connected to the mobile core via a wireless link supported by THz RIS in a NLOS scenario. Figure 6-6 (b) depicts a THz RIS midhaul scenario where a DU is connected to a CU via a wireless link enhanced by THz RIS for NLOS. Figure 6-5 (c) depicts a THz RIS fronthaul scenario where a RU is connected to a DU via a wireless link enhanced by THz RIS for NLOS.

THz Access

A THz RIS-enabled network is presented in the network architecture diagram in Figure 6-7 which is Open RAN-based and leverages the flexibility of RAN disaggregation. It consists of a core network, the RAN (CU+DU) which can be integrated or disaggregated, and a THz-enabled RU.

The core is typically hosted by the MNO or private tenant, and the other components of the RAN can be distributed geographically throughout the network. By leveraging an ORAN architecture for 6G, this will provide mobile operators with the flexibility to pick and choose different splits based on the deployment requirements. This flexibility comes from using different hardware or software implementations within various network components. This disaggregated approach of Open-RAN also provides a mechanism for providing effective network customisation.
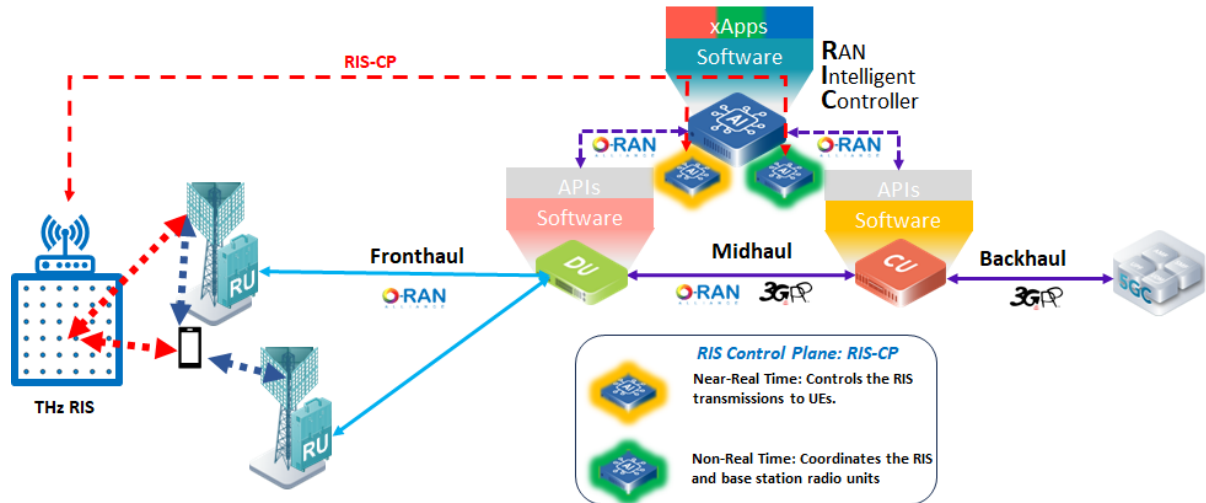
Figure 6-7: THz RIS deployments

The proposed THz RAN architecture incorporates modular and interoperable RAN components with existing open interfaces, namely Open-RAN, enabling seamless integration of sub-THz and THz frequency ranges. The architecture adopts a disaggregated RAN approach, where radio units (RUs) designed for lower frequencies can be easily replaced or augmented with ones operating in the sub-THz/THz bands. This flexibility supports dynamic network adaptation to varying demands and requirements. A RIS control plane is proposed to support RIS in an ORAN architecture. The introduction of the RIS control plane (RIS-CP), is a new control signalling which is processed in a RAN intelligent controller (RIC), separating the RIS-to-BS signalling and the RIS-to-UE signalling. The RIS units are fully integrated into the network architecture, contributing to a new control plane layer within the standard RIC. This integration allows for the orchestration of both communication and sensing operations, making RIS a pivotal component in the overall network management and a key enabler for applications requiring simultaneous data communication and environmental sensing.

6.2. RIS Control Architecture

To fully realise their potential as a key enabler in the envisioned 6G and THz networks, RIS devices require smooth integration with the existing infrastructure and network components. To that goal, the aim of this section is to provide a description of the RIS architectures, in an effort of harmonisation with the equivalent ORAN and 3GPP specifications.

As a first step, a layered control architecture is defined below, building on top of the network architecture proposal from [23], by adapting the previously defined entities to the needs of the THz networks, and by extending their definitions to account for the increased technological maturity level under TERRAMETA. Specifically, the control plane of the RIS from an architectural point of view is structured along the following entities: The RIS Orchestrator (RISO), the RIS Controller (RISC) and the RIS Actuator (RISA). Each entity implies different capabilities in terms of computation, communication (interaction with the rest of the network), and therefore control response time. The corresponding layers, as depicted in Figure 6-8 roughly correspond to the Non-RT RIC, Near-RT RIC, and gNB layers of the ORAN architecture.

From the lower hierarchical level to the highest, the description of the different control modules are given as below:

- **The RISA** is in charge of actuating the logical commands received by the RIS Controller, i.e., of translating them into physical configurations to be applied to the RIS device. In particular, such configurations might be envisioned as phase shifts or ad-hoc meta-material state changes. Additionally, the support for pre-stored codebooks is envisioned, under which the RISA is responsible for cycling through the codebook configurations without further commands. The RISA is controlled by the RISC with an action time granularity in the order of microseconds, allowing real-time operation. The RISA is assumed embedded to the RIS device for simplification, and its design should be dependent on the type of the device (e.g., operating bands, receiving/transmitting/reflecting modes), allowing device-specific operations to take place, such as CSI estimation. We make use of the term "Open Environment" to refer to the support of such heterogeneous devices as well as their encapsulation under RISA. In essence, this strategy of hierarchical control modules definitions is instrumental in the deployment of sophisticated smart radio environments, as described in this deliverable.

- **RISC** – It is the module associated to a RISA (that can be either collocated or external to the RIS device). It is responsible for generating the logical commands associated to the switching operations between the configurations/states of the RIS elements (e.g., predefined phase shifts). Algorithmic operations (e.g., signal processing or AI-based) take place at that level, implying various levels of computational capabilities. The RISC may also need to operate in sync with other parts of the network, or being in standalone operation mode (e.g., by illuminating pre-defined areas). The expected action time delay should be no more than 100 ms, with the intention of near real-time operation.

- **RISO** – It is placed on the highest (hierarchical) layer, and it orchestrates multiple RISCs. Its action time granularity is expected to be between 100 ms and a few seconds. The RISO is designed to capture the overall system objective, in terms of KPIs, and other operation parameters, as well as to coordinate multiple RISs.
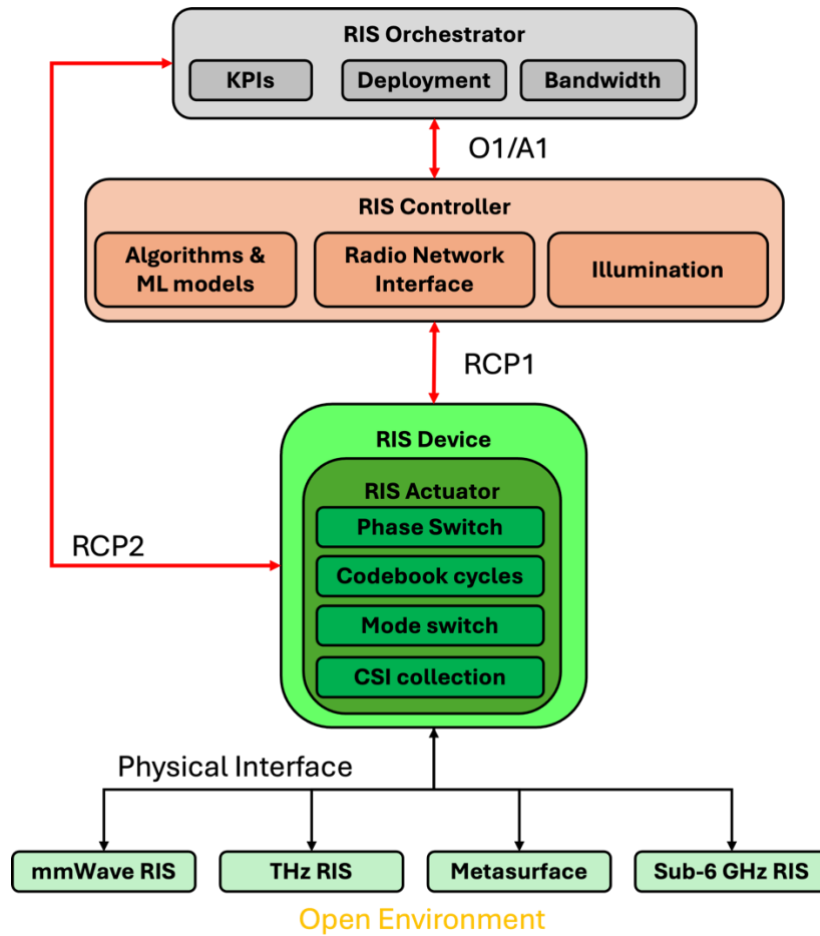
Figure 6-8: Proposed hierarchical architecture for RIS control with three different levels of control modules and accompanying interfaces, supporting different device types.

Having specified the control modules, it is important to define appropriate communication interfaces between them. In Figure 6-8, the "vertical" communication stack is illustrated from the RISA up to the RISO, by defining interfaces similar to O-RAN and 3GPP. In particular, RISO and RISC communicate via the use of an O1 or A1 interface, as it is defined under O-RAN for the SMO and Near-RT RIC layers. The RISC talks to the RISA via the interface referred to RIS Control Plane 1 (RCP1), which is an interface of similar nature to that of E2 of O-RAN. It is also possible for the orchestrator to communicate directly with the RISA, e.g., for changing the operation mode of the device or to obtain CSI. To facilitate such exchanges, the RCP2 interface is defined, which is similar to the O1/O2 interfaces of O-RAN for SMO-gNB communication.

Finally, the intention behind this "vertical" control requires commenting: By following the aforementioned control stack, one is able to deploy and operate RIS devices without the involvement of, or even awareness by the rest of the network control functions. While it is highly likely that at least some level of coordination will be required for most cases, a lot of the high-level functionalities can be isolated at the orchestration level, allowing for automaticity in the lower levels, where time granularity is of importance. In the following section, the proper integration to the O-RAN and 3GPP architecture is discussed.

6.3. Integrated RIS and O-RAN Architecture

O-RAN specifies a number of relevant functional architecture blocks and accompanying interfaces that are designed to be applicable to the 3GPP interfaces. The overall architecture, and its integration with the previous sub-component is given in Figure 6-9, while the terminology is explained below.
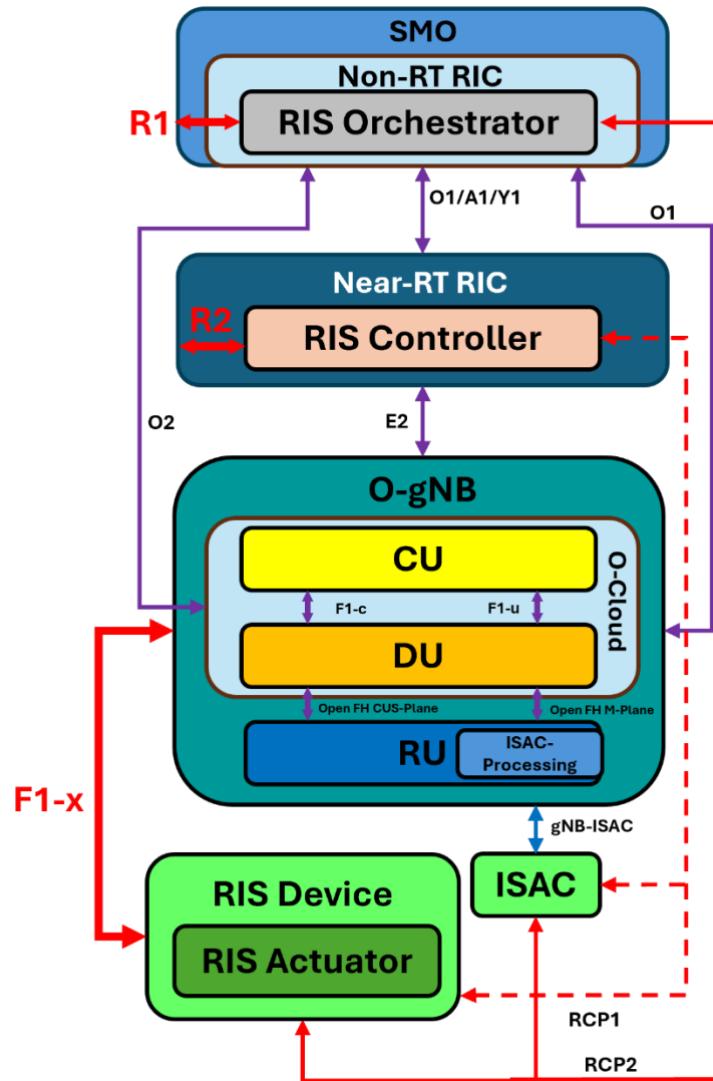
Figure 6-9: Integration of the RIS architecture to ORAN/3GPP with the definition on new horizontal RIS-ORAN interfaces (R1, R2, F1-x).

- At the higher level, the Service Management Orchestration (SMO) involves Non-Real Time (RT) RAN Intelligent Controllers (RICs), communicating via R1 interfaces. The RISO is seen as a non-RT RIC and is integrated under SMO alongside other rApps.
- At the second level, Near-RT RICs are responsible for controlling deployed gNBs via the use of xApps and other functionalities. The RISC is designed to interact with this layer to support joint optimisation, QoS management, etc. To that end, we define the R2 interface between the two parallel layers.
- The lower layer of the O-RAN architecture is the direct control of RAN elements. Each RAN element, namely eNB or gNB according to 3GPP, can be split into a Centralised Unit (CU), a Distributed Unit (DU) and a Remote Unit (RU). This layer communicates with the RAN Controller via the E2 interface. The lowest physical layer functions are left to the RU that represents the RF device and shall be placed at the remote cell site. DU functions can be placed on an edge cloud with very-high-capacity connection to assist and support real-time operations between RLC/MAC layers and the physical layers. CU functions can also be placed on edge clouds and shall be split into control plane (CP) and user plane (UP) functions. CUs and DUs are connected through the F1 interface (F1-c and F1-u for control plane and user plane respectively). Finally, DUs are connected to RUs via the open fronthaul (O-FH) protocol that includes four different planes: user (U-) and control (C-) planes to transport physical layer and control commands, synchronisation plane (S-plane) to manage synchronisation among DUs and RUs, and management plane (M-plane) to configure RU features.

- In this integrated architecture, we further define the F1-x interface between gNBs and RISA with the following intentions: (a) Many applications and RIS deployment strategies require precise and reliable synchronisation between gNBs/eNBs (mainly RUs) and the RIS in order to facilitate operations such as channel estimation procedures, (b) direct gNB/eNB – RIS communication may offer much more flexible options in terms of RAN deployment and operation, that what is achievable by communicating through the Near-RT RIC (E2 interface), next through the RISC (R2 interface), ultimately reaching RISA via RCP1.
- We have accounted for a new functionality within the RU that is ISAC processing. The RUs will gather sensing data and process them, essentially acting as fusion centres for either centralised or distributed sensing depending on the information shared (local or global). Then the whole gNB communicates via the gNB-ISAC link to an entity that gathers information from the RIS(s) as well and realises an ISAC objective such as SLAM of the environment.

7. Use Case THz and RIS HW Integration Architecture

7.1. ICOM's Baseband Solutions and Integration Architecture

The developed RISs and the different sub-THz components for the RF front-end along with the baseband units from ICOM, will be integrated in order to efficiently serve the use cases of TERRAMETA targeting demos in a telecommunications setting as well as in a factory scenario. The main architecture that will be followed is depicted in Figure 7-1. As can be seen in this figure, two main demos will be showcased, the first one at BT for the Fronthaul use case facilitating the link between the CU/DU and RU and the second at DELL for an enhanced throughput use case in the factory environment.
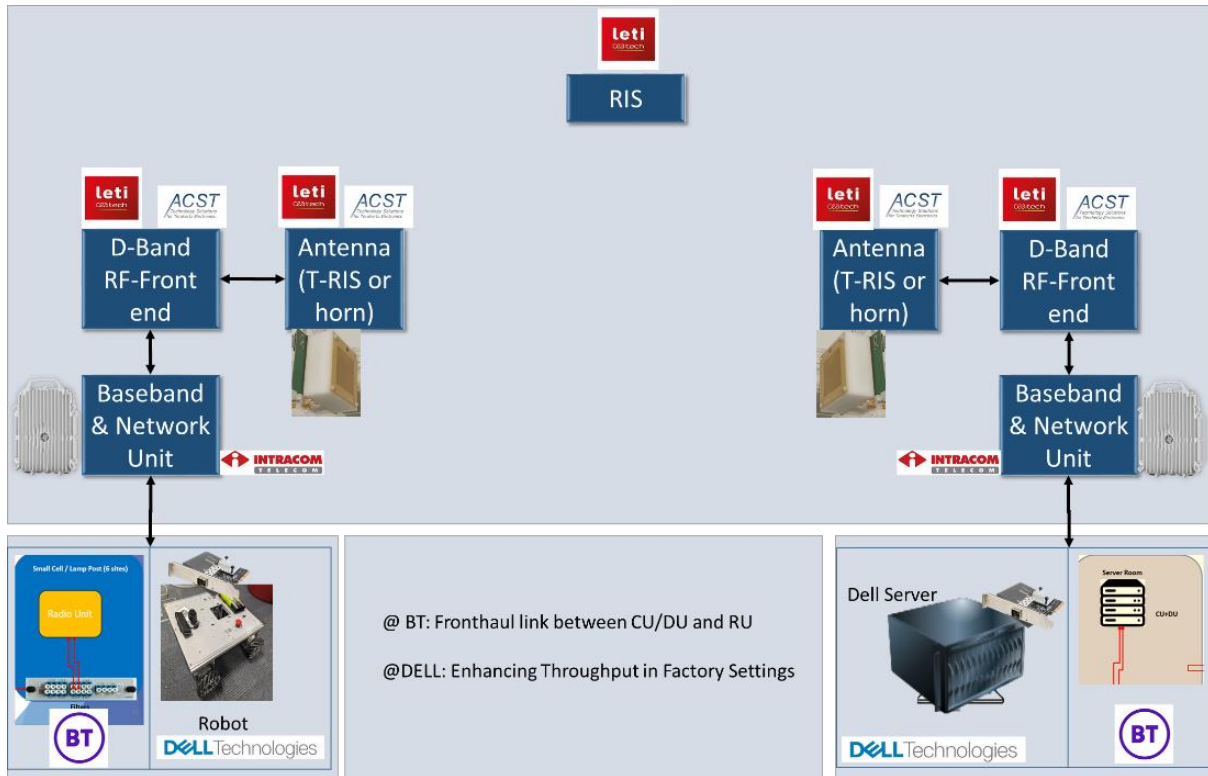
Figure 7-1: The architecture of the proposed/planned use cases at DELL and BT

As depicted in Figure 7-1, the main building blocks for these demos are:

- ICOM's baseband units will transform the digital data traffic to I/Q data signals using a channel bandwidth of 2 GHz and constellation size up to 512-QAM.
- The required RF front-end is provided by TERRAMETA partners CEA-Leti and/or ACST for the up/down conversion to sub-THz frequencies.
- The required metasurfaces that will be used as transmissive and/or reflective surfaces are provided by TERRAMETA partner CEA-Leti. Other types of RIS such as the micro-fluidic based RIS will be considered as the project progresses in WP6.
- The necessary equipment from TERRAMETA partners BT (CU/DU, RU) and DELL (Robots and Servers) supporting the fronthaul and factory use cases, respectively.

The baseband units for these demos are based on ICOM's E-Band commercial platforms mainly used in X-haul applications. ICOM will provide two different baseband solutions. In the first solution, a baseband system with dual modem will be offered achieving bit rates up to 30 Gbit/s. It consists of the baseband unit (BBU) with the FPGA-based modems and the digital-to-analogue (D/A) and analogue-to-digital (A/D) converters board. As a second solution, a single-modem baseband unit will be provided, able to achieve bit rates up to 10 Gbit/s using 256-QAM constellation size. Similarly, to the first solution, the required DA/AD converter board will be provided to generate the QAM data signals at Tx and to receive the intermediate frequency (IF) produced signals from ACST's RF front end at Rx side.

These units can host the demanding Digital Signal Processing (DSP) algorithms for the proper generation, reception, and demodulation of the QAM signals after the wireless transmission. The achievable bit rates will depend on the RF front-ends and wireless transmission characteristics.

7.2. CEA-Leti's RF Front-end

The RF front-end architecture is shown in Figure 7-2. The RX circuit implementing the two-channel architecture illustrated in Figure 7-2, is fabricated in a 45-nm CMOS technology and mounted on a low-cost printed circuit board (PCB), where the feed antennas, i.e. two pairs of aperture-coupled patches, are realised. The RX covers simultaneously two sub-bands: the lower band (LB), from 139 to 148 GHz, and the upper band (UB), from 148 to 157 GHz. Two LNAs are designed with a four-stage topology similar to [24]. Their input matching is optimised at the centres of the corresponding sub-band (LB or UB). The following mixer and Intermediate Frequency (IF) amplifier are identical in the two channels and are optimised to cover the 57- 67-GHz IF band. The design of the TX of the proposed point-to-point wireless link has been partially presented also in [24]. It comprises the same antenna-in-package (AiP) of the RX. The IC output power at the antenna input ports is 0 dBm. The equivalent isotropic radiated power (EIRP) is 27 dBm at the output 1-dB compression point (OCP1dB) of the TX integrated circuit (IC). Due to the multi-channel signal, a back-off of 9.4 dB is used, so that the EIRP for a modulated signal covering the full system band, i.e., from 139 to 157 GHz, is 15.4 dBm. The emitted signal is composed of eight BB channels, spaced by 2.16 GHz, which are up-converted to the D-band, as illustrated in Figure 7-2. The TX circuit has two channels, as the RX, providing two sub-bands (LB and UB) to the two ports of the AiP. The full-band signal is obtained by the over-the-air power recombination of the two sub-band signals, performed by the transmissive RIS.
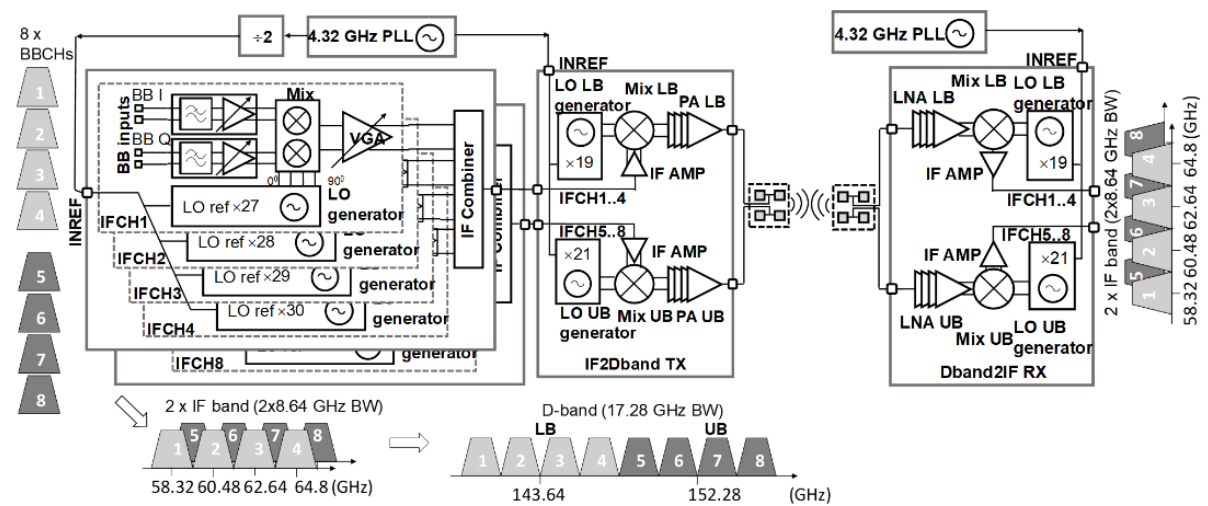
Figure 7-2: CEA-Leti BB to D-band TX and D-band RX front-end architecture.

To explore other possibilities regarding architecture at the RF front-end, ACST has proposed an alternative solution at D-Band. This consists of packaging an MMIC in the 71-76 GHz range, that generates IQ modulated signals, given an appropriate LO frequency and I and Q base-band signals. The up-conversion of the generated E-Band IQ modulated signals to D-Band would happen by doubling the frequency with a Schottky-diode based frequency multiplier. The last multiplication stage could provide a modulated output power in the +20 dBm range.

This D-Band RF front-end could be used in the architecture depicted in Figure 7-1 and provide a good comparison between a link with higher and lower power levels at mmWave frequencies.

For this front-end to perform appropriately, the input constellation in the first E-Band hardware needs to be modified, since the frequency doubler will not only double the frequency, but also the phase of the signal. Therefore, instead of a standard 4-QAM constellation, a specific distribution of symbols needs to be used to correct the phase doubling effect introduced by the last multiplication stage.

7.3. D-band metasurface based antenna module

The antenna modules integrated on the actual D-band TX and RX front-end presented in Figure 7-2 are based on a focal-plane antenna module illuminating a fixed-beam metasurface. (T-RIS). Note, that a reconfigurable metasurface architecture based on CMOS is being developed in WP4. This advanced smart system is totally compatible with the actual setup.

At the TX side, the antenna system comprises two primary antenna feeds, realised in the same package where the TX IC is assembled, which illuminate a transmit array antenna (TA) or transmissive-RIS (T-RIS). Each antenna feed is connected to one of the two IC outputs and radiates a signal only in the corresponding band, i.e., LB (139.3-148 GHz) or UB (148-156.6 GHz). The T-RIS operates over both bands. It forms a high-directivity beam at boresight (link direction) and, at the same time, performs frequency multiplexing, aggregating LB and UB signals. The design and characterisation of two different TA configurations, shown in Figure 7-3, are presented: a standard TA and TA folded TAT-RIS architecture, in which the distance F between the feed and the planar lens is reduced by a factor of 3 with respect to the former one. Both systems use the same flat lens classical T-RIS architecture. The principle of operation of the folded TAT-RIS is schematically illustrated in Fig. Figure 7-3(a). A reflective polarisation rotating surface (RPRS) is realised in the AiP, around the antenna feeds. With respect to the standard TA system, the planar lens is rotated by 90°. In this way, the x-polarised field radiated by the feeds is first reflected by the lens, then converted to a y-polarisation and back-reflected towards the lens by the RPSR. In the geometrical optics (GO) approximation, the system works as the flat lens was illuminated by a virtual feed at a distance $F_0 = 3F$. The fabricated T-RIS is presented in Figure 7-3(b).

The primary feed module comprises two pairs of aperture-coupled microstrip patch antennas, radiating the LB and UB signal, respectively. The fabricated antenna module is shown in Figure 7-4. The TX IC is flip-chipped on the backside (m1) of a low-cost four-layer PCB (Isola Astra MT77, $\varepsilon r = 3$, tan δ =0.0017 at 10 GHz) embedding the patch antennas and related feed networks. The center-to-center distance between the two patch arrays, along the y-axis, and that between the two patches in each array (along x-axis), are both 1.25 mm. The patches are excited by microstrip lines, through rectangular slots in the ground plane realised on one inner layer of the dielectric stack-up. The two feeding lines are connected to the IC outputs. The distance between the patches and the ground is 0.254 mm. The patches are surrounded by a cavity with through-hole vias, which has a size 3.3 mm × 2.9 mm, to mitigate the impact of the TM_0 surface wave.

(a)   (b)
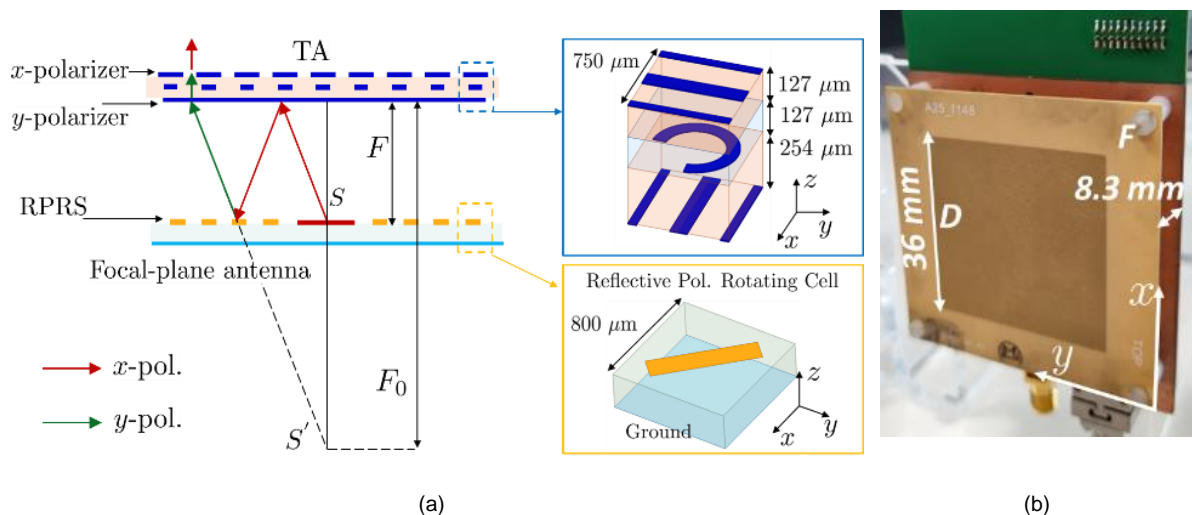
Figure 7-3: (a) Schematic view of the folded T-RIS architecture. The distances between the AiP and the T-RIS are F = 8.33 mm.

An RPRS around the antennas is employed to realise the folded T-RIS system. This structure reflects and converts an incident x-polarised plane wave, parallel to the main far-field component of the antenna, into a y-polarised one. The unit cell (UC) of the RPRS UC comprises a rectangular strip oriented at 45°,

over the ground plane. The RPRS occupies an area of 40 mm × 40 mm and has a periodicity of 0.8 mm, along both x- and y-axis. The simulated reflection coefficients (from x- to y-polarisation) of the UC, enforcing periodic boundary conditions, for a plane wave impinging at boresight and at 45° are greater than -0.2 dB and -1.2 dB, respectively, from 120 GHz to 160 GHz.

The UCs of the T-RIS are designed as asymmetric linear polarisers, using only three metal layers, without any metallised vias. The outer layers of all UCs are orthogonal wire grid polarisers. The element on the inner layer of each UC, referred to as the rotator, is designed to rotate by 90° the incident field and introduce on it the desired phase shift. The stack-up of the lens comprises the same low-cost substrate materials of the AiPs. The UC periodicity is 0.75 mm × 0.75 mm. Sixteen UCs were optimised using split rings and I-shaped patches as presented in the Deliverable D3.2 [25]. The lens for the TX systems was designed to achieve a boresight gain higher than 25 dBi. It comprises 48×48 cells, corresponding to an electrical size of $17.8\lambda_0 \times 17.8\lambda_0$, where λ_0 is the free-space wavelength at 148 GHz. The focal distance for the standard TA was set at $F_0 = 25$ mm, which provides a good trade-off among peak gain, bandwidth, and height of the antenna system.

(a)   (b)
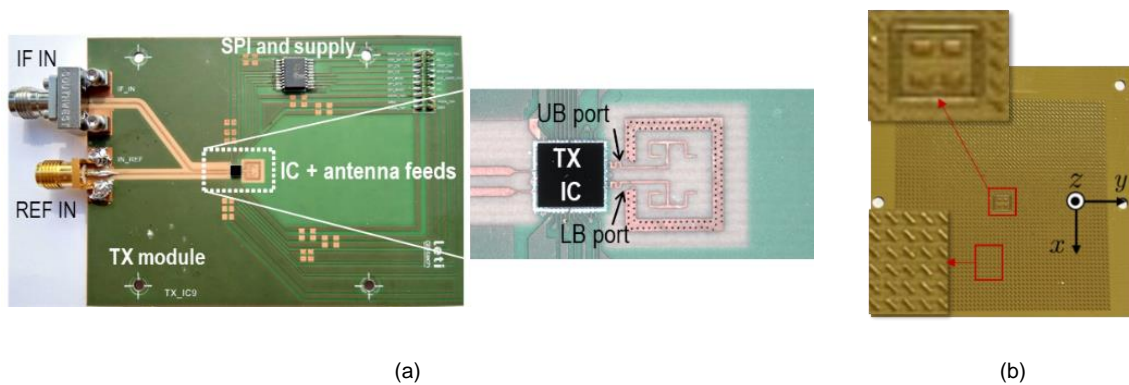
Figure 7-4: (a) Bottom side of the AiP module with the flip-chipped TX IC and detail of UB and LB outputs and microstrip feeds of the antennas. (b) Top side of the AiP for the folded T-RIS, including the RPSR.

The RX module developed for the demonstration of the point-to-point link is shown in Figure 7-5. The RX circuit implementing the two-channel architecture is fabricated in a 45-nm CMOS technology and mounted on a low-cost PCB, where the feed antennas, i.e., two pairs of aperture-coupled patches, are realised as in the case of the TX module. The RX covers simultaneously two sub-bands: the lower band (LB), from 139 to 148 GHz, and the upper band (UB), from 148 to 157 GHz. Two low-noise amplifiers (LNA) are designed with a four stages topology. Their input matching is optimised at the centre of their corresponding sub-band (LB or UB). The following mixer and IF amplifier are identical in the two channels and are optimised to cover the 57 to 67 GHz IF band. The antenna-in-package (AiP) module is placed at the focal plane of a 48×48-element T-RIS based on the same UCs than the TX module as shown in Figure 7-5. In this case, a classical T-RIS architecture without RPRS is implemented. Each of the two feed antennas in the module is connected to one of the RX inputs. The measured gain at boresight of the AiP and of the entire antenna system are shown in Figure 7-5. The RX module (without the T-RIS) is also characterised.
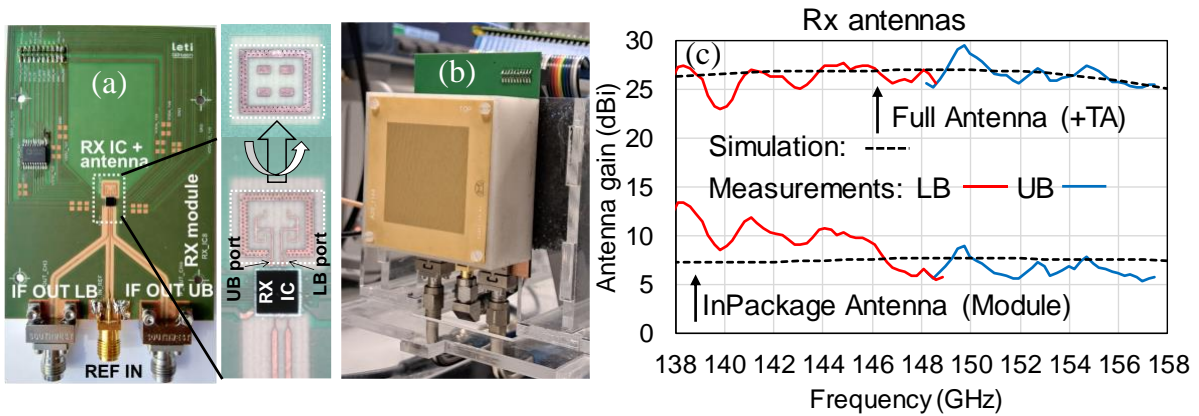
Figure 7-5: (a) Receiver module and details of the antenna-in-package. (b) T-RIS mounted over the antenna-in-package module. (c) Measured and simulated boresight antenna gain.

7.4. 300 GHz metasurface for ultra-high-gain backhauling

The 300 GHz ultra-high-gain metasurface is based on the UCs presented in Deliverable D3.2. To be compliant with the transceiver interface, a standard waveguide horn antenna is used at the focal point to illuminate a T-RIS. Optimal focal distance (F/D = 0.6) and phase distribution are calculated using a hybrid simulation tool to minimise the height of the antenna system and maximise the gain. The measurement setup of the fabricated T-RIS and the corresponding phase distribution are illustrated in Figure 7-6. Figure 7-7 presents the simulated and measured results for gain and the corresponding aperture efficiency. A peak realised gain of 43.3 dBi is achieved at 284.35 GHz, with an aperture efficiency of 39%. It is worth noting that a fabrication error in the plastic spacer causes a 5 GHz shift in the maximum gain value due to a longer focal distance of 0.5 mm compared to the simulated one.
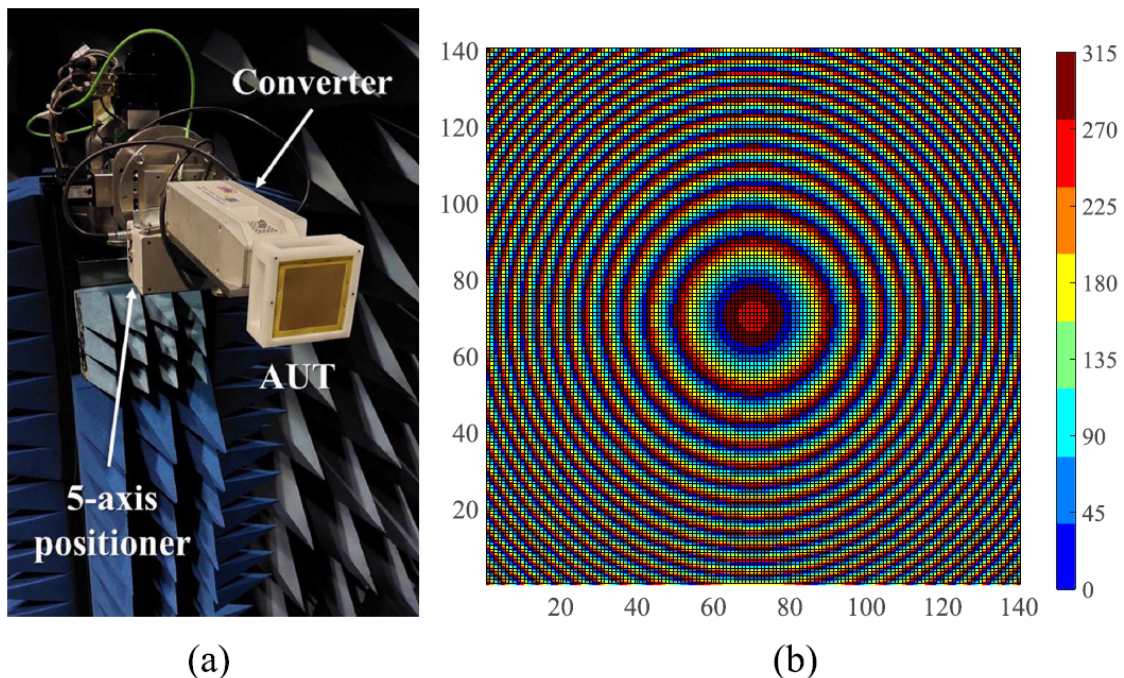
Figure 7-6: (a) The fabricated prototype of the proposed TA. (b) Phase distribution of the TA was calculated using a hybrid simulation tool.
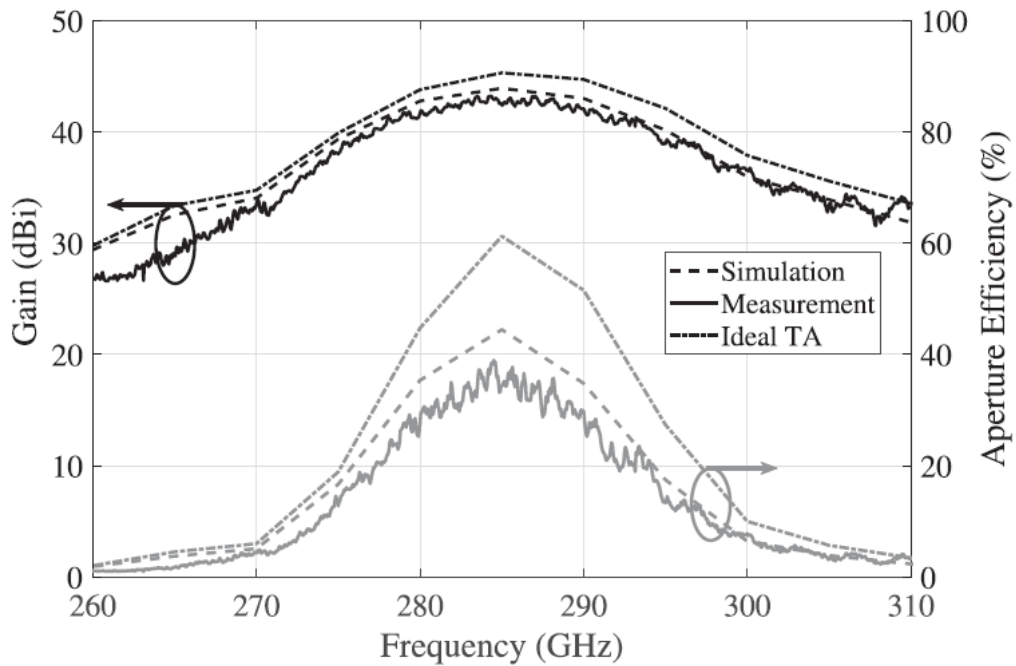
Figure 7-7: The simulated and measured gain and corresponding aperture efficiency of the TA in comparison with the results of the TA in ideal case.

7.5. Integration of ACST RF Front-end Transceiver

The RF front-end being developed by ACST at 300 GHz within WP3 consists of a direct amplitude modulator based on Schottky diode technology. The device, which will be packaged in a standard waveguide-based block, is connected directly after the 300 GHz source and should be able to provide a fast OOK modulation. Figure 7-8 shows the 300 GHz Transmitter with an example block of the amplitude modulator and a WR3.4 horn antenna:
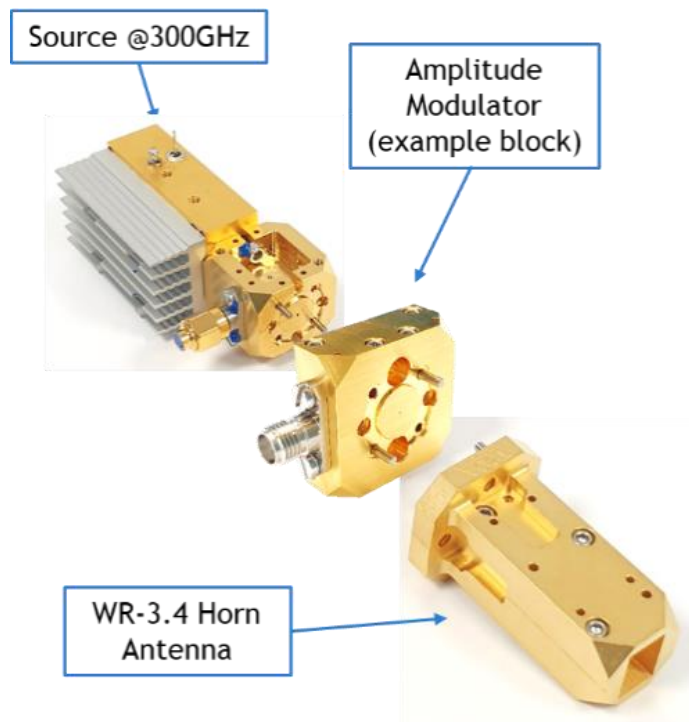
Figure 7-8: 300 GHz transmitter with envisioned direct amplitude modulator and horn antenna

Such a transmitted signal can be received by different means since there is no phase information available in the modulation. The following options are contemplated as possible solutions:

▪ Envelope detector: direct detection is the simplest available solution, which would be sufficient for the characteristics of the signal. ACST has available an ultra-broadband quasi-optical detector that can receive signals starting at 50 GHz and up to 2 THz, with different sensitivities. The received THz signal is coupled into the detector via an optical lens, which then provides a baseband or IF output signal of up to 4 GHz. Small modifications could be done in order to extend the IF bandwidth. The module is illustrated in Figure 7-9:
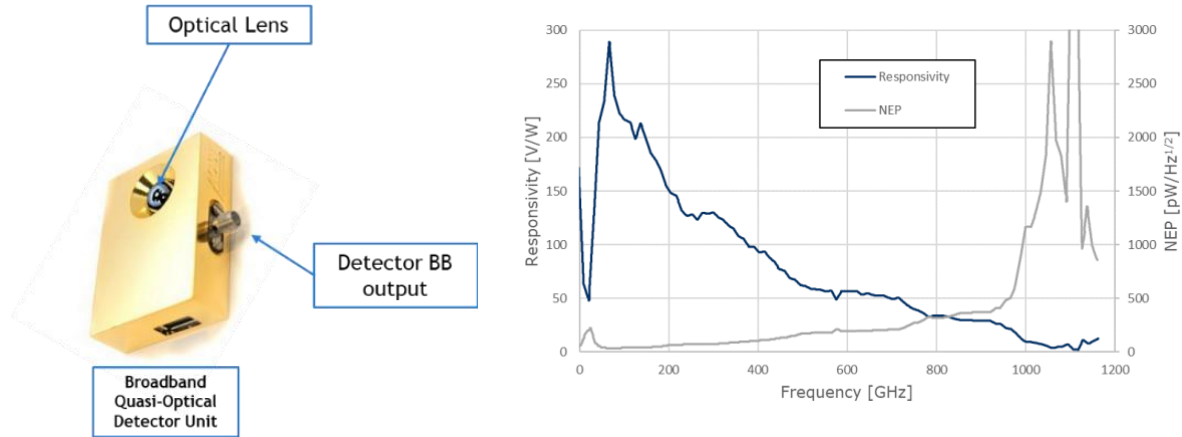
Figure 7-9: Quasi-optical direct detector and its performance

▪ Down-converter: down-conversion through a Schottky-diode based sub-harmonic mixer is traditionally used when phase information is required to be retrieved. ACST has a 220-330 GHz sub-harmonic mixer available, which presents a typical conversion loss of 10dB along the band and is capable of down-converting to an IF of up to 40 GHz. In this case, a receiver based on such technology presents different advantages in comparison to the direct detection solution: higher sensitivity and capable of receiving a high-speed modulated signal. Furthermore, the LO chain necessary to drive such a device, is also available at ACST. An image of the possible receiver is illustrated in Figure 7-10, without the necessary horn antenna.

Figure 7-10: Sub-harmonic mixer-based receiver

The block diagrams in Figure 7-11 and Figure 7-12 show the two possible front-end configurations between the amplitude modulation Tx and the different Rx solutions:
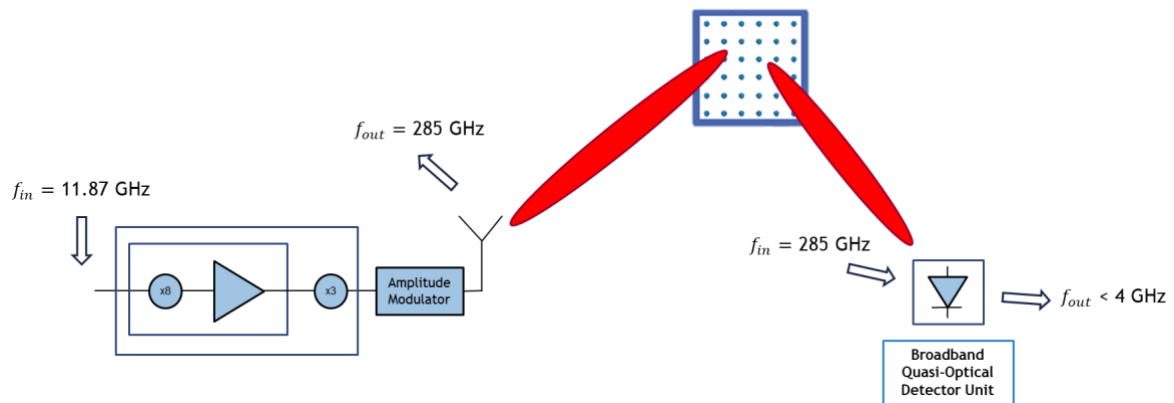
Figure 7-11: 300 GHz transmitter with direct detector (Solution 1)
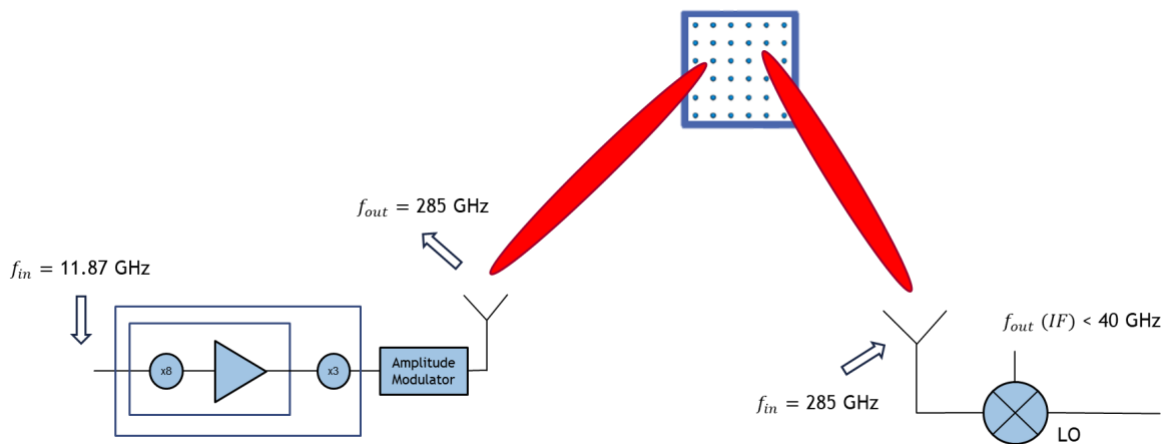
Figure 7-12: 300 GHz transmitter with sub-harmonic mixer receiver (Solution 2)

To explore the possibility of higher order modulation schemes that allow for high power transmission by the RF front-end, ACST has proposed an alternative architecture at D-Band. The idea to explore consists of a packaged MMIC in the 71-76 GHz range that generates IQ modulated signals, given an appropriate LO frequency and I and Q baseband signals. The up-conversion of the generated E-Band IQ modulated signals to D-Band would be achieved by doubling the frequency with a Schottky diode-based frequency multiplier. The last multiplication stage could provide a modulated output power in the +20 dBm range.

Such D-Band RF front-end could be used in the architecture depicted in Figure 7-13 and provides a good comparison between a link with higher and lower power levels at mmWave frequencies.
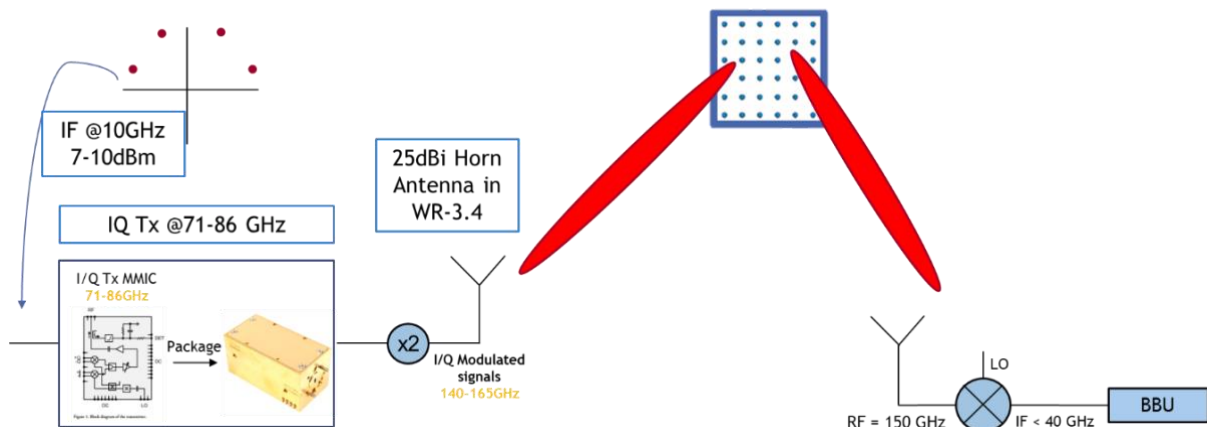
Figure 7-13: Block diagram of proposed D-Band architecture, with a mixer-based receiver

For this front-end to perform appropriately, the input constellation in the first E-Band unit needs to be modified. The reason is that the frequency doubler will not only double the frequency, but also the phase of the signal. Therefore, instead of a standard 4-QAM constellation, a specific distribution of symbols needs to be used to correct the phase doubling effect introduced by the last multiplication stage. The feasibility of this will be investigated further in WP6.

Regarding the receiver side, as proposed in solution 2 for the direct modulator at 300 GHz, a similar receiver could be used: a sub-harmonic mixer capable of down converting the RF input frequency signal to an IF of up to 40GHz. Some limitations are already previewed for such an innovative solution: constellations with a number of symbols higher than 4, can probably not be achieved.

7.6. Testbed Locations

BT Laboratories site

BT research and development campus is located at Adastral Park, Ipswich, UK. This R&D campus includes laboratories and test facilities aiming to provide a range of deployment scenarios for O-RAN and future radio access technologies. Outlined in Figure 7-14 is where the THz RIS 6G O-RAN test and integration activities can be hosted by our infrastructure for TERRAMETA. The physical infrastructures provided in the figure illustrate the sites with fibre transport connectivity to the Baseband Server Room (A) – A fully air-conditioned server room where COTS servers can be installed or hosted. The radio locations are lamp posts (C) and rooftops (D, E) where both AC and DC power distribution as well as headend fibre connectivity are available on these units. Internet connectivity and secure remote access facilities can be provided to any equipment installed. Test Lab Location (B) – This is a location suitable for desk-based working where IT services will be provided to allow remote access to installed equipment for test purposes. Each site listed has fibre connectivity and power provided to them.
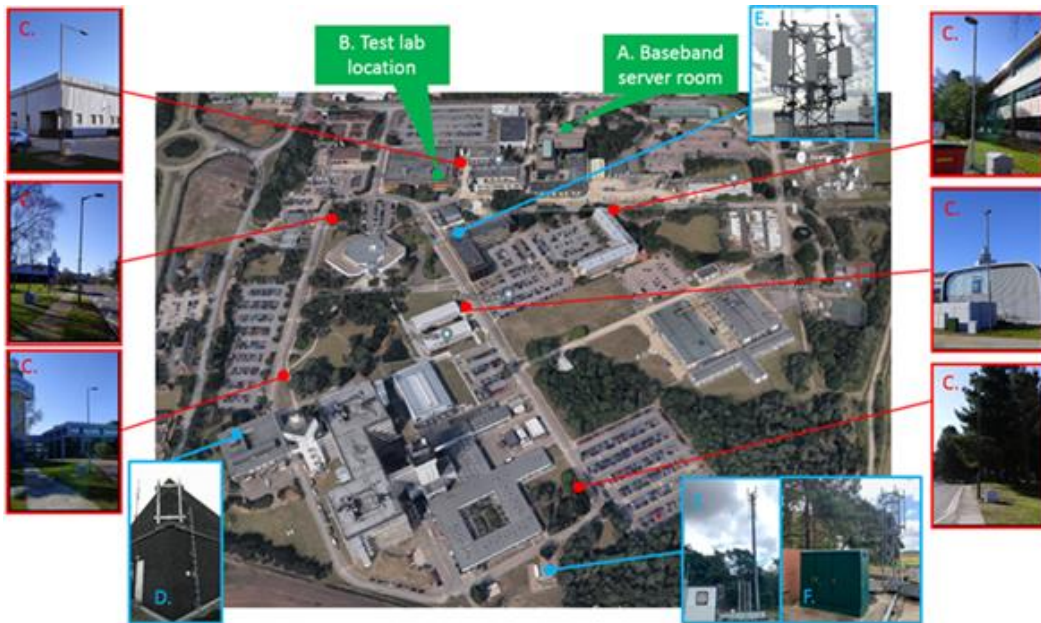
Figure 7-14: Adastral Park Outdoor Testbed

(A) Baseband Server Room; (B) Test Lab Location; (C) Lamp Post Radio Sites: there are six roadside lamp post sites available for deployment of smaller radio head unit solutions appropriate to street-level or urban deployments. It is expected that this will be the most appropriate testbed for TERRAMETA at BT Labs. (D) Rooftop Macro Site #1 – This site is a wall mounted north facing frame suitable for single sector deployments oriented towards the north. (E) Rooftop Macro Site #2 - This site is a three-faced multi-post frame, suitable for 360-degree coverage close to the centre of campus. (F) Test Mast Compound: a location suitable for low level temporary installations and outdoor test deployments.
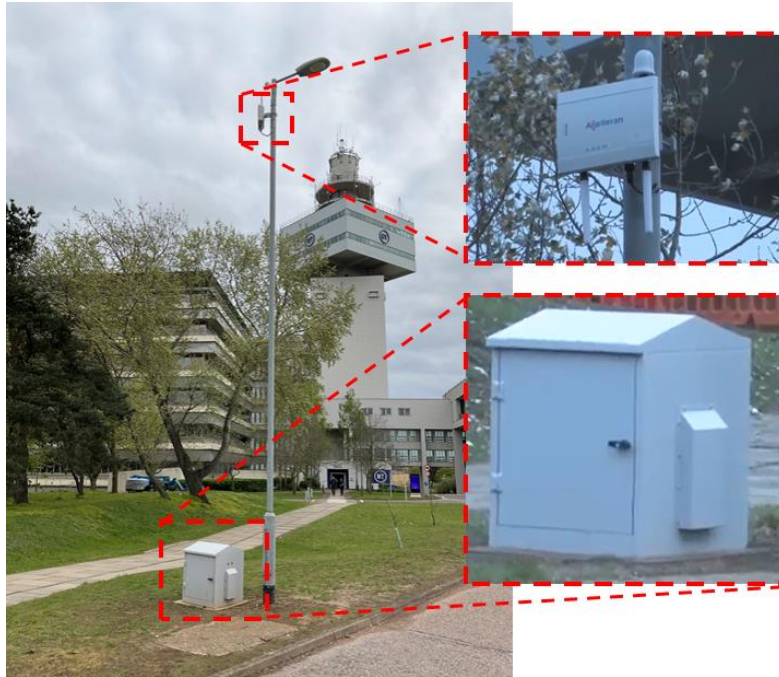
Figure 7-15: Lamppost with RU deployed

Each cell site consists of a lamp post upon which O-RUs can be fitted, GPS antennas if required and a cabinet that can be connected to the server room. The cabinet can host any power supplies required by the O-RU and has a rack-space upon which any edge processing can take place. This can allow for drive tests and walk tests. For testing with handsets, the availability and associated logging tools will vary based on radio configuration and, in particular, the spectrum bands used. Provisionally, spectrum licenses will be applied for as and when required. Advanced notice, ideally several months, is requested to allow for the spectrum license application process. Ideally, spectrum plans should be shared as early as possible so that preliminary investigations can be done to indicate if such a license is likely to be available.

DELL Technologies site

For DELL's hardware integration efforts, we focus on utilizing factory robots to transmit sensor data to a Dell PowerEdge XR4000 server for advanced analysis by AI. The data transmission will leverage high-speed THz links to ensure rapid and reliable communication, where benchmarks with Wi-Fi technology will be performed and compared. The robots involved in this integration are the Mecabot Pro and the Pickerbot Mini, both depicted in Figure 7-16, while the Dell servers are shown in Figure 7-17.
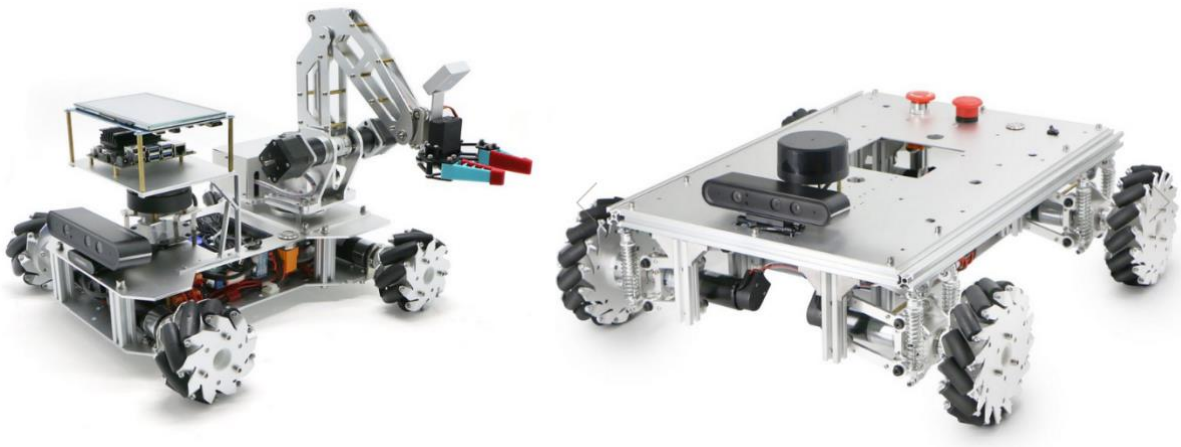
Figure 7-16: Robot devices available for testing and integration at DELL

Figure 7-17: Dell PowerEdge XR4000 servers

Mecabot Pro (Figure 7-16 right): This large robot features a flat base, providing ample space for mounting THz communication equipment. Equipped with a 3D depth sensing camera and a LIDAR unit, the Mecabot Pro utilizes Nvidia AGX Xavier boards for vision processing. These AGX nodes come with a PCIe port, to which an SFP28 NIC will be attached, enabling connection to the baseband unit for THz links. This setup ensures that the Mecabot Pro can efficiently collect and transmit detailed environmental data.

Pickerbot Mini (Figure 7-16 left): The Pickerbot Mini, designed with a robotic arm, can be programmed using AI and computer vision to interact with objects on the factory floor, such as picking up an SSD and placing it into a server. Similar to the Mecabot Pro, it features a 3D depth-sensing camera and a LIDAR unit for precise navigation and object interaction. It also uses Nvidia AGX Xavier boards equipped with PCIe ports connected to SFP28 NICs for THz link communication.

Both robots will feature additional depth-sensing cameras positioned on the rear, left, and right sides to provide 360-degree coverage, enhancing their ability to navigate and operate autonomously. Additional LIDAR units may also be incorporated if necessary to further augment the sensing capabilities. The sensor data collected by the Mecabot Pro and Pickerbot Mini will be transmitted via THz links to Dell PowerEdge XR4000 servers for real-time analysis. The AI algorithms running on these servers will process the data, enabling advanced functionalities such as predictive maintenance, real-time quality control, and autonomous navigation adjustments. This integration and testing will be conducted at a Dell facility, specifically within a lab environment emulating a miniature factory floor, as depicted in Figure 5-4. This setup will allow us to rigorously evaluate the performance and reliability of the THz communication links and the overall system integration, ensuring that the solutions are robust and effective for real-world factory applications.

8. <u>Use Case Simulation Environments</u>

TUBS is providing the Simulator for Mobile Networks (SiMoNe) for evaluating the use cases of indoor and outdoor scenarios by simulation means. SiMoNe was developed to predict the characteristics of a realistic mobile network for a given scenario. The simulator consists of different prediction models that enable channel predictions, link-level, and system-level simulations.

One of the functions of SiMoNe enables 3D ray tracing predictions for 3D models. The ray tracer is not limited to LoS channel predictions, it is also able to calculate the possible rays between a set of antennas for different reflection orders. The required input data for the ray tracing algorithm are the 3D building data for either indoor- or outdoor scenarios, the material parameters for the calculation of the effects of the interaction of the wave on the matter and the antenna characteristics. The characteristics for TX and RX antennas contain the antenna location, the frequency, the antenna diagrams, as well as the direction and the tilt of the antennas.

After determining the interaction points of the rays, SiMoNe calculates the attenuation of each individual ray. This involves considering the free space path loss, the reflection loss, and the atmospheric attenuation. Additionally, the antenna patterns of both the TX and the RX antenna are factored into the attenuation calculation. For this project, the ray tracer needs to be expanded by the option of adding a RIS object to the simulation parameters. A RIS object has a similar behaviour in the simulation as an antenna; it contains a location, a frequency, an antenna diagram, a direction, and a tilt. To accurately combine the attenuation of the paths that run from TX to RX via the RIS, it is insufficient to merely add these attenuations logarithmically.

Since the path loss is calculated for each path individually in SiMoNe, a way must be found to combine the FSPL attenuations of two paths using the radar equations. Unlike a wall, the RIS spans a relatively small area, which leads to a necessary additional compensation factor, resulting from the radar equation. Eq. 1 and 2 show the attenuation caused by the FSPL and the radar equation with λ being the wavelength, d_1 the distance between TX and RIS, d_2 the distance between RIS and RX and the radar-cross-section.

$$\text{FSPL}_{\text{dB}} = 40\log(\lambda) - 40\log(4\pi) - 20\log(d_1) - 20\log(d_2)$$

(Eq. 1)

$$\text{Radar}_{\text{dB}} = 20\log(\lambda) + 10\log(\sigma) - 30\log(4\pi) - 20\log(d_1) - 20\log(d_2)$$

(Eq. 2)

To get the compensation factor, it is necessary to subtract these two attenuations from each other:

$$\alpha_{\text{dB}} = \text{Radar}_{\text{dB}} - \text{FSPL}_{\text{dB}} = -20\log(\lambda) + 10\log(4\pi) + 10\log(\sigma)$$

(Eq. 3)

To add the attenuations of a TX-RIS ray and a RIS-RX ray together, additionally this compensation factor is added. The radar-cross-section corresponds to the RIS diagram.

A RIS antenna diagram is dependent of the incident angle of the wave hitting the surface. Because of this, it is necessary to have one RIS diagram for each ray hitting the RIS with a different incident angle.

8.1. RIS Example Scenarios:

This chapter presents some example simulations including RIS diagrams. The used RIS diagrams are shown in Figure 8-1 and Figure 8-2. In this study, two passive metasurfaces were designed and simulated in EM simulator and the corresponding radiation patterns were exported to SiMoNe. To reduce the simulation time, the size of the metasurface was chosen to be 4.8λ × 4.8λ with 100 elements, where λ is the wavelength of the operating frequency. Figure 8-1 shows the configuration of the passive metasurface. The RIS element is a square patch backed by a ground plane, and to generate different reflection patterns or provide different phase distributions of the aperture, the sizes of the patches were varied from 0.19 λ to 0.28 λ, which can provide reflection phases in the range of 0 to 360 degrees.
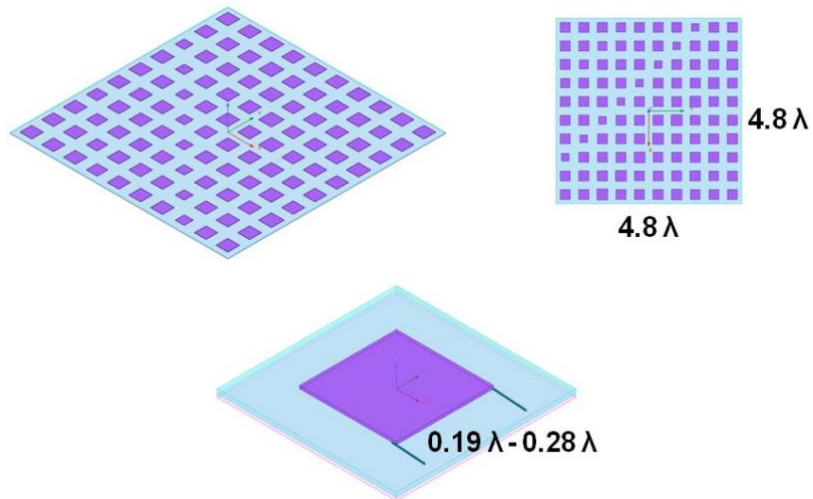
Figure 8-1: Configuration of the 10x10 metasurface that was used to generate reflection patterns.
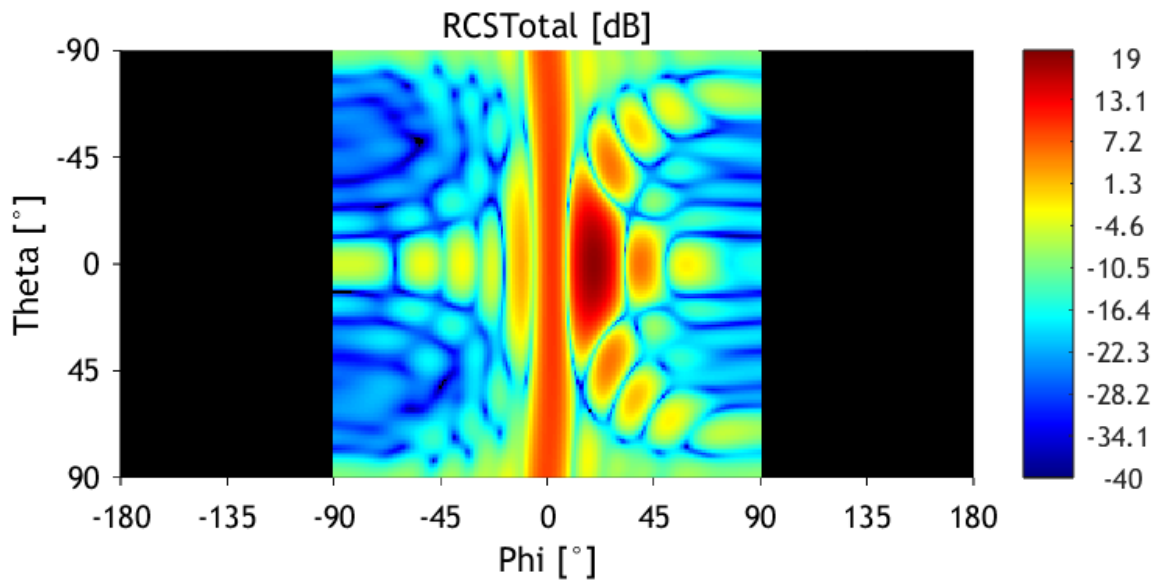
Figure 8-2: Type 1 RIS with a reflection beam at Theta = 0° and Phi = 20°
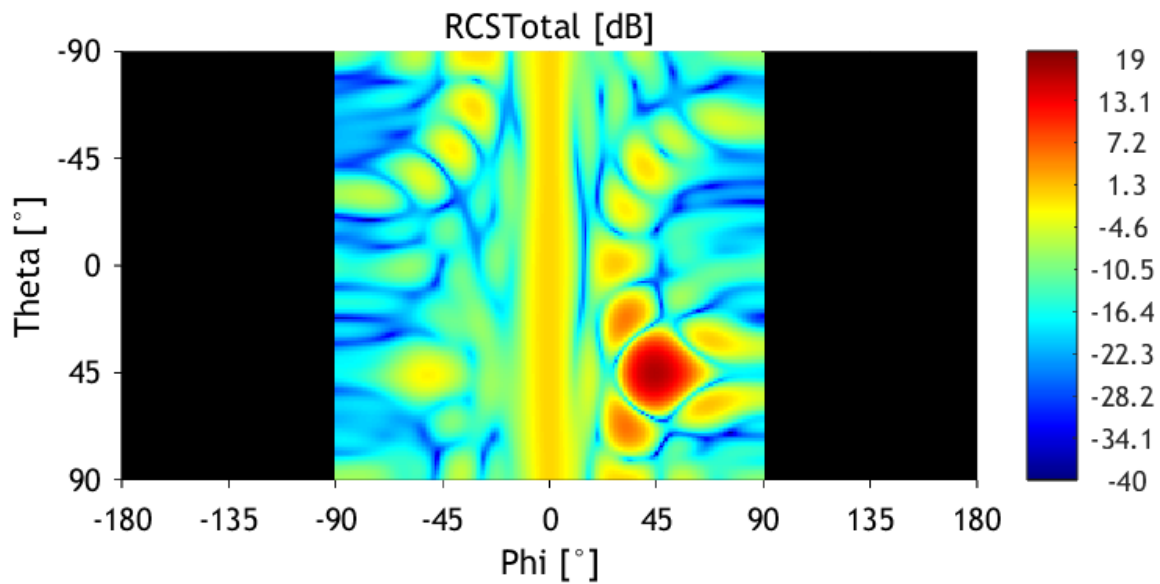
Figure 8-3: Type 2 RIS with a reflection beam at Theta = 45° and Phi = 45°

Theta is the elevation angle of the RIS diagram and Phi is the azimuth angle. The radar-cross-section of the RIS is applied in colour. Because the used RIS is a reflective surface, only the range of Phi = -90° to Phi = 90° has a reflective gain, the back of the RIS is not considered here.

The RIS diagrams have two different beam orientations. Both RIS diagrams have an incident angle of Theta = 0° and Phi = 0°, so they are only valid for rays that hit the surface at a 90° angle. The Type 1 RIS in Figure 8-1 has a main reflection angle of Theta = 0° and Phi = 20°. The Type 2 RIS in Figure 8-2 has a main reflection angle of Theta = 45° and Phi = 45°.

For the following simulations, the factory scenario presented in section 5 is used. The building materials for all surfaces were set to concrete, the reflection order was set to 1. The attenuations were calculated for a frequency of 300 GHz. The RX and TX antennas were considered as omnidirectional antennas with a gain of 0 dB in every direction.

8.1.1. NLoS Case with Type 1 RIS

This case covers the NLoS case considering the RX and TX antenna, which therefore are separated by a pillar. The room of the scenario is the factory building presented in chapter 5. The RIS is mounted 0.1 m in front of the wall. All elements, the TX, RX and RIS are mounted on 3.2 m above the ground, since this is the realistic height for the practical use of RIS in an industrial environment. In Figure 8-3 the positions of the antennas and the RIS as well as the paths resulting out of a raytracing simulation can be seen.
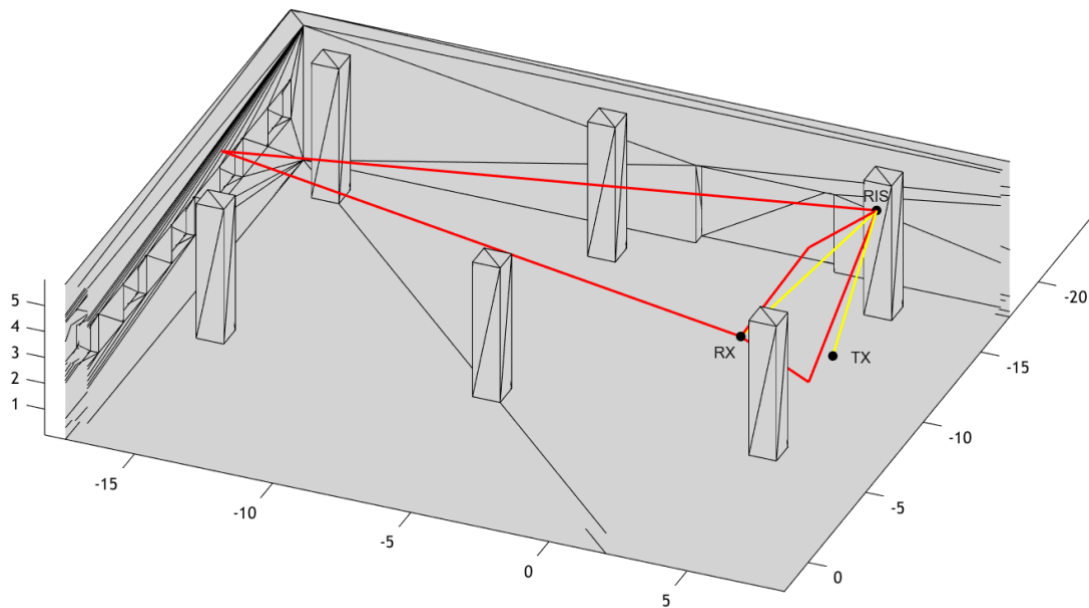
Figure 8-4: Rays of the NLoS case considering TX and RX with RIS in the factory environment. The yellow ray is the direct TX-RIS-RX path, the red rays are containing an additional specular reflection.

The position of the TX and RX antennas and the RIS were chosen so that the angle of the direct TX-RIS-RX path at the interaction point of the RIS is 20°. Because of that, the RIS diagram from Figure 8-1 can be applied, so that the main reflection beam of the RIS points directly at the direction of the RX (after the normal vector of the RIS is aimed at the TX antenna).

This simulation was once performed with the RIS diagram from Figure 8-1 and once with an omnidirectional diagram (with a gain of 0dB).

Figure 8-4 shows the CIR of the scenario with the applied RIS diagram (from Figure 8-1), belonging to the found rays in Figure 8-3. Figure 8-5 shows the CIR of the scenario with an omnidirectional RIS diagram.
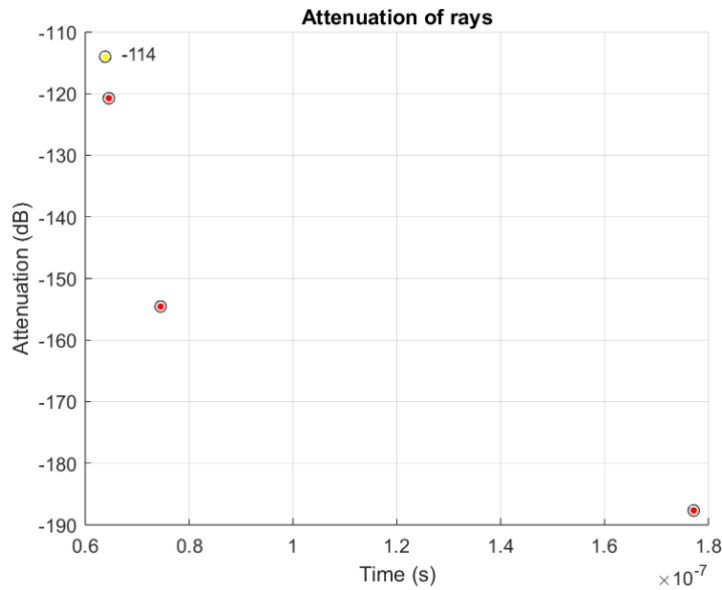
Figure 8-5: CIR corresponding to fig. 8-3 with applied RIS diagram from fig 8-1. The yellow impulse corresponds to the ray only reflected on the RIS, the red impulse to the rays that are containing additional specular reflections.

The red impulses are the impulses of the rays that have a spectral reflection after they got reflected by the RIS. The yellow impulse is the direct TX-RIS-RX path. When comparing the two CIRs from Figure 8-4 and Figure 8-5, the antenna diagram from Figure 8-1 is recognizable.

The CIR from Figure 8-5 contains one more path in comparison to the CIR from Figure 8-4; the reason for this is the fact, that the applied omnidirectional RIS diagram reflects in every direction, also the back with a gain of 0 dB.
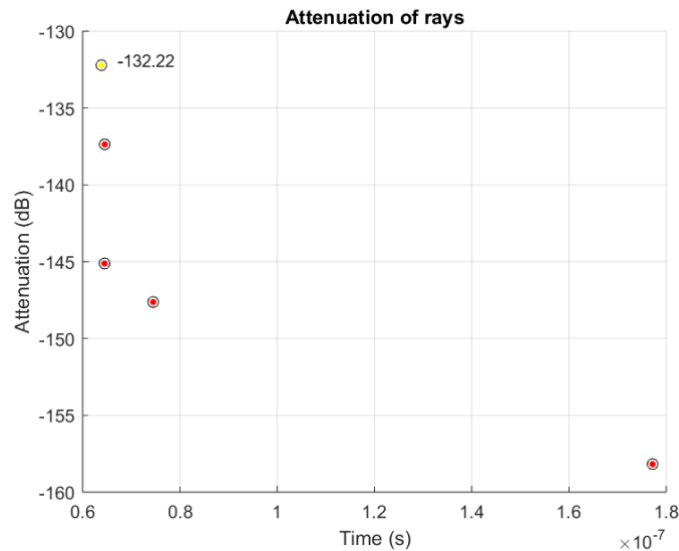
Figure 8-6: CIR corresponding to Figure 8-3 with applied omnidirectional diagram as a RIS diagram. The yellow impulse corresponds to the ray only reflected on the RIS, the red impulse to the ray that contains an additional specular reflection. This CIR contains one ray more than fig. 8-3 and 8-4, because of the used RIS diagram.

8.1.2. *Investigation of different RX positions with Type 1 RIS*

To show the effect of a RIS diagram, which is not pointing directly at the RX antenna with its main reflection beam, the scenario in this subsection will show the CIR's for five different positions of the RX antenna. For this scenario, the main reflection beam of the RIS diagram from Figure 8-1 was rotated to the ground as seen, as in Figure 8-7.
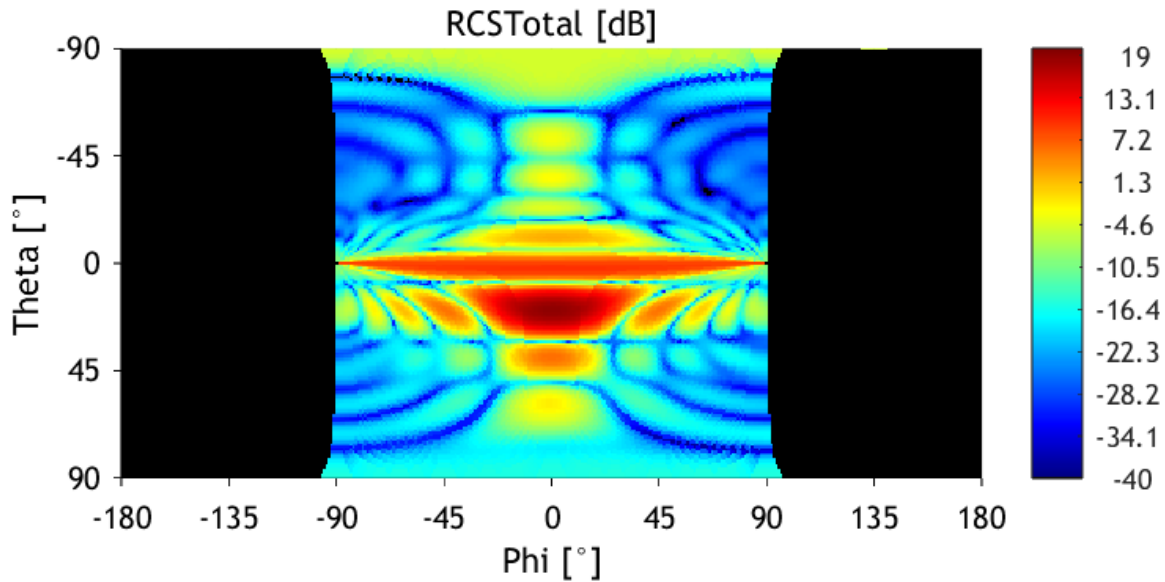
Figure 8-7: Rotated type 1 RIS with a reflection beam at Theta = 20° and Phi = 0° from fig. 8-1 rotated to the ground

The RIS was placed 3.2 m above the ground and 0.1 m in front of the wall. TX was positioned 3 m in front of the RIS at the same height, directly below the ceiling. For the RX antenna five different positions were chosen, as seen in Figure 8-8, all of these positions have a height of 1 m. RX3 is positioned directly in the main beam of the RIS reflection beam. RX2 and RX1 have a difference of 1 m resp. 2 m to RX3, the antennas RX4 and RX5 have a difference of 1 resp. 2 m to RX3 into the other direction.
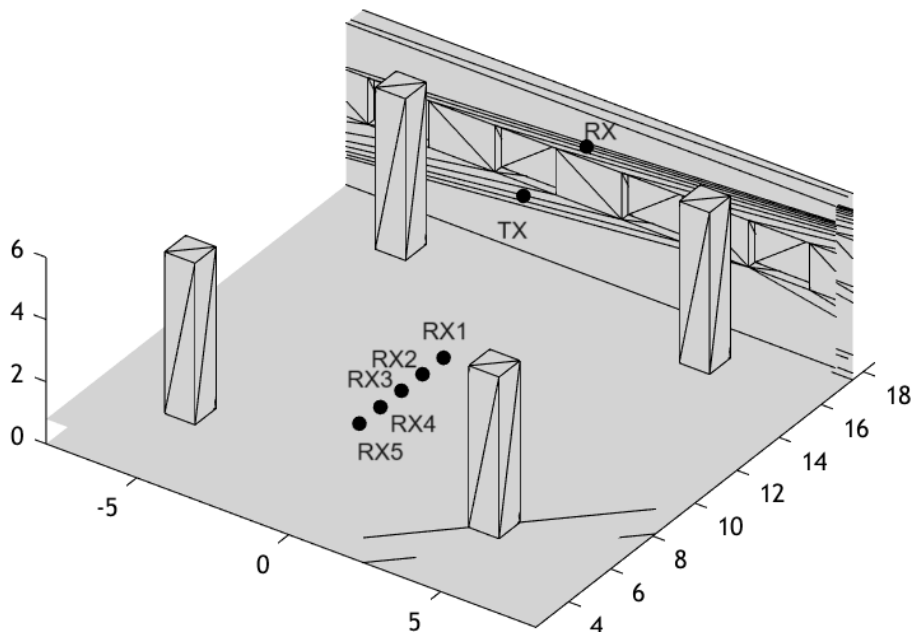
Figure 8-8 Plot of the antenna and RIS positions.

For each of these RX positions, the CIR was calculated as seen in Figure 8-8.
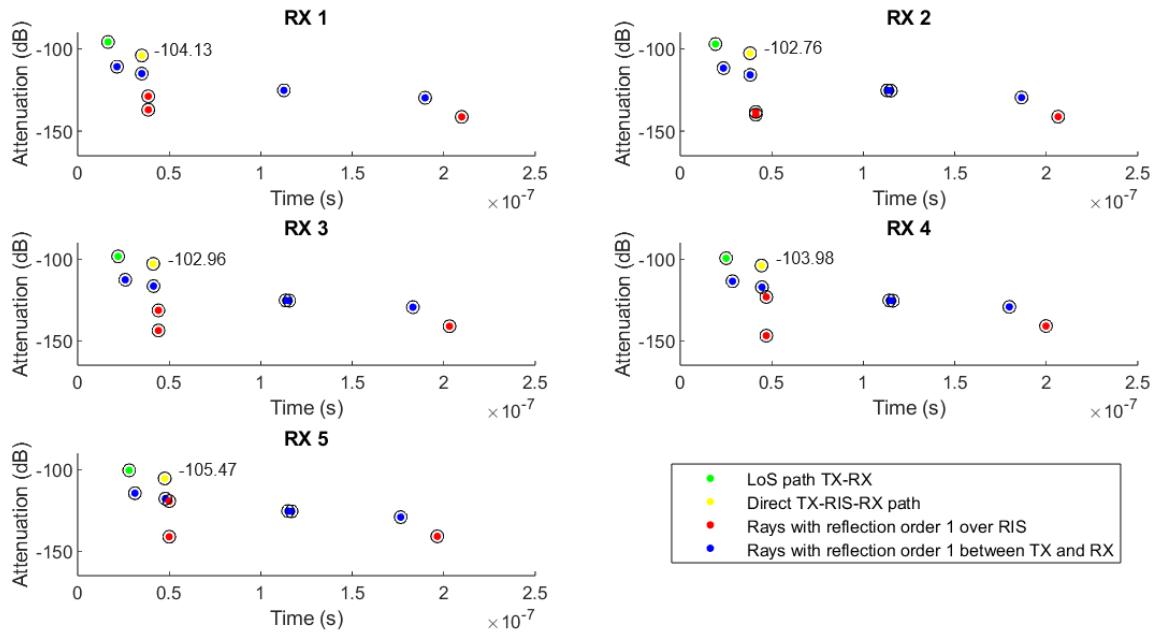
Figure 8-9: Plot of the CIR's at the different RX antenna positions as shown in Figure 8-7, with reflection order 1. The attenuations of the direct TX-RIS-RX paths were written to the respective impulse in the CIR.

The green dots show the direct LoS paths between TX and RX, the blue dots the rays from TX to RX, with one specular reflection. The yellow dots are the direct TX-RIS-RX paths, and the red dots correspond to the paths with one specular reflection after the RIS reflection.

The attenuations of the direct TX-RIS-RX paths were written to the respective impulse in the CIR (Figure 8-9). The 3D scenario with antenna position RX3 is shown in Figure 8-10 with the same colour assignments.
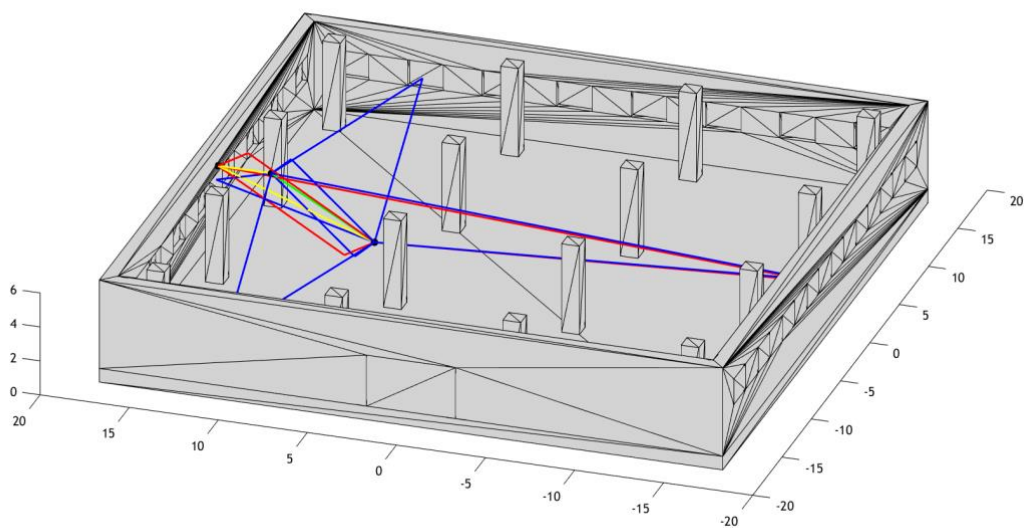
Figure 8-10: 3D plot of the found rays with RX3 from Figure 8-7

Using the link budget tool developed in D2.1 [27], the heatmap of the SNR was calculated, as shown in Figure 8-11. In this calculation, it is assumed that the Tx is located 3 meters away from the RIS, and the Tx has a Tx antenna with a gain of 20 dBi and the Tx power is 20 dBm. For the Rx, the receiver has an Rx antenna with a gain of 10 dBi. In this calculation, the blockage from the pillars of the factory was considered and the LOS signal was not considered.
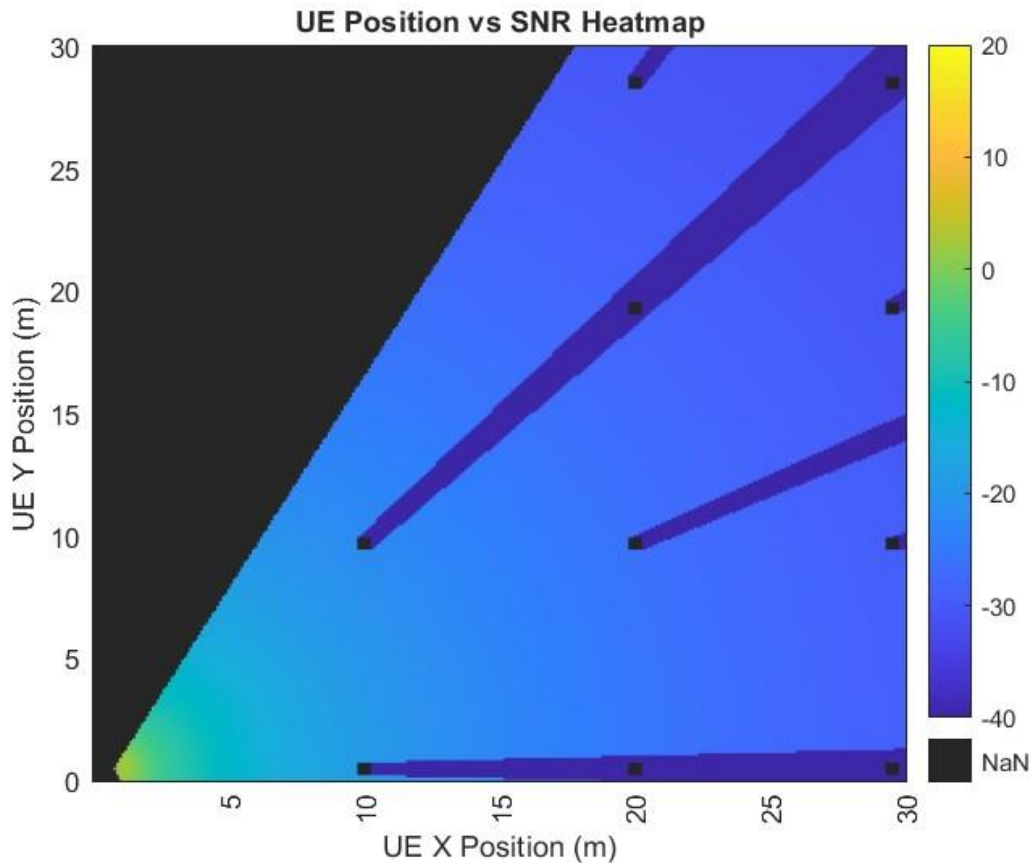
Figure 8-11: Plot of the SNR heatmap in the factory use case. In the calculation, the RIS is placed at (0,0) and its reflection beam was configured to 20-degree. The black square dot represents the pillars of the factory.

8.1.3. Investigation of different Rx positions with Theta = 45°, Phi = 45° RIS diagram

To show the effect of a RIS diagram, for a different RIS diagram and different RX positions as presented in section 8.1.2, the RIS diagram from Figure 8-2 was used in this section.
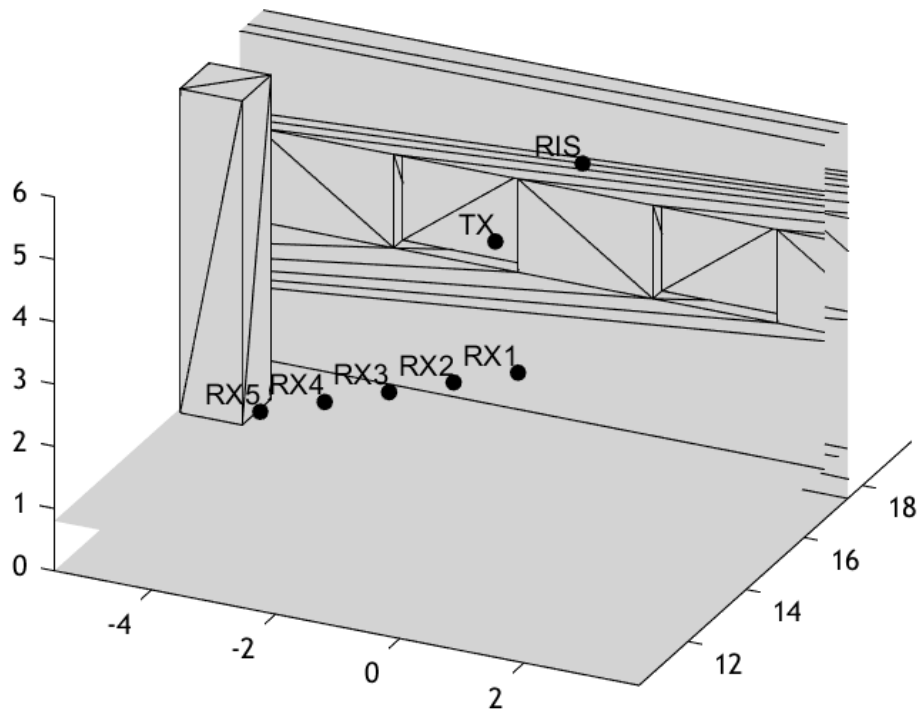
Figure 8-12: Plot of the antenna and RIS positions

The RIS was placed 3.2 m above the ground and 0.1 m in front of the wall. TX was positioned 3 m in front of the RIS at the same height. For the RX antenna five different positions were chosen, as seen in Figure 8-12, all of these positions have a height of 1 m. RX3 is positioned directly in the main beam of the RIS reflection beam. RX2 and RX1 have a difference of 1 m resp. 2 m to RX3, the antennas RX4 and RX5 have a difference of 1 resp. 2m to RX3 into the other direction.

For each of these RX positions, one CIR was calculated as seen in Figure 8-13.
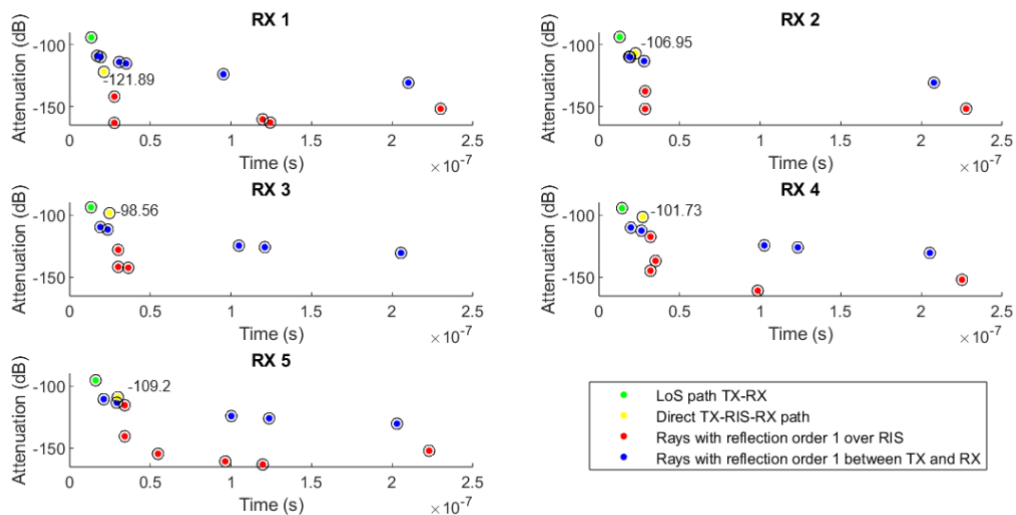
Figure 8-13: Plot of the CIR's at the different RX antenna positions as shown in Figure 8-10, with reflection order 1.

Using the same parameters used in the previous section, the corresponding SNR heatmap was calculated (Figure 8-14).
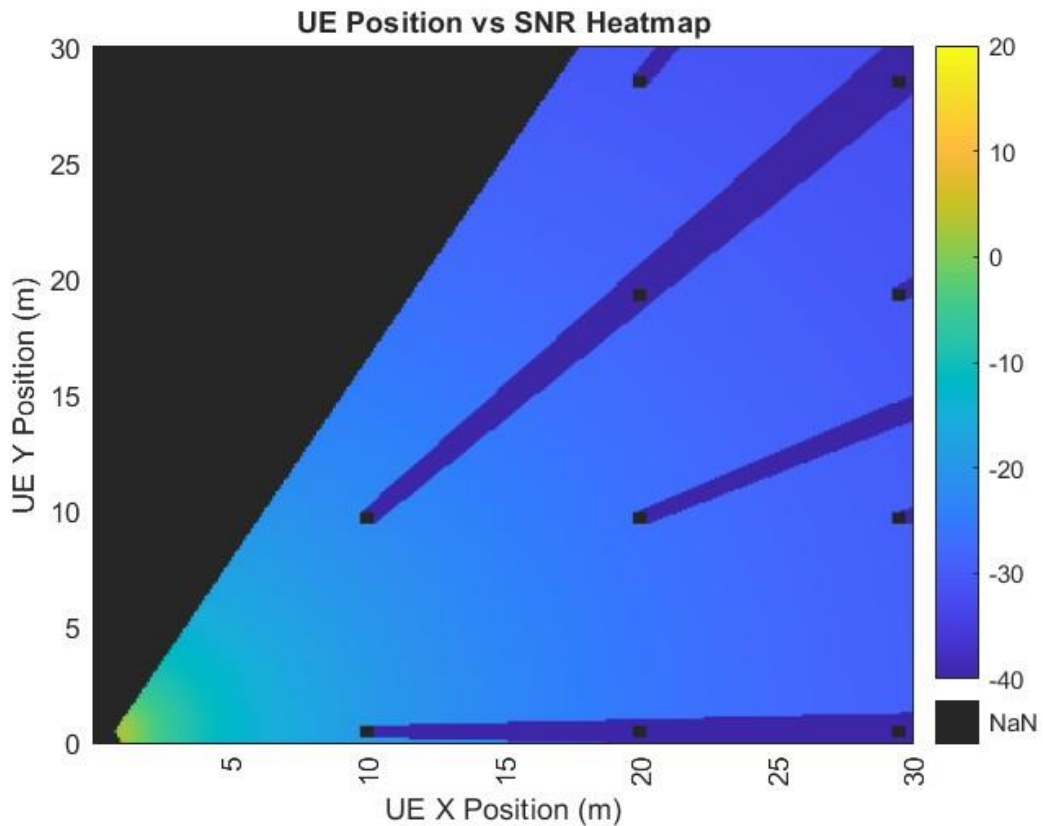
Figure 8-14: Plot of the SNR heatmap in the factory use case. In the calculation, the RIS is placed at (0,0) and its reflection beam was configured to 45-degree. The black square dot represents the pillars of the factory.

8.2. Link Level Simulator

Additionally, SiMoNe comes with a link level simulator (LLS), which is able to simulate the physical layer and signal processing aspects between the transmitter and the receiver. It examines the transmission of data symbols through the channel, considering effects such as noise, interference, and channel impairments. It is possible to use different coding schemes like LDPC and RS.

The LLS uses previously calculated ray tracing results to model the channel. Different tools such as constellation diagrams, eye diagrams and plots of the spectrum of the signal at different parts of the transmission process can be visualised and interpreted.

Figure 8-15 shows, how the simulator realises the different parts of the transmission through the channel. At the transmitter side a sequence of bits is generated. These bits are then passed to the encoder, the interleaver and the modulator. The channel block simulates the noise and the effects caused by the ray tracer. The receiver side demodulates, deinterleaves and decodes the transmitted data back accordingly.
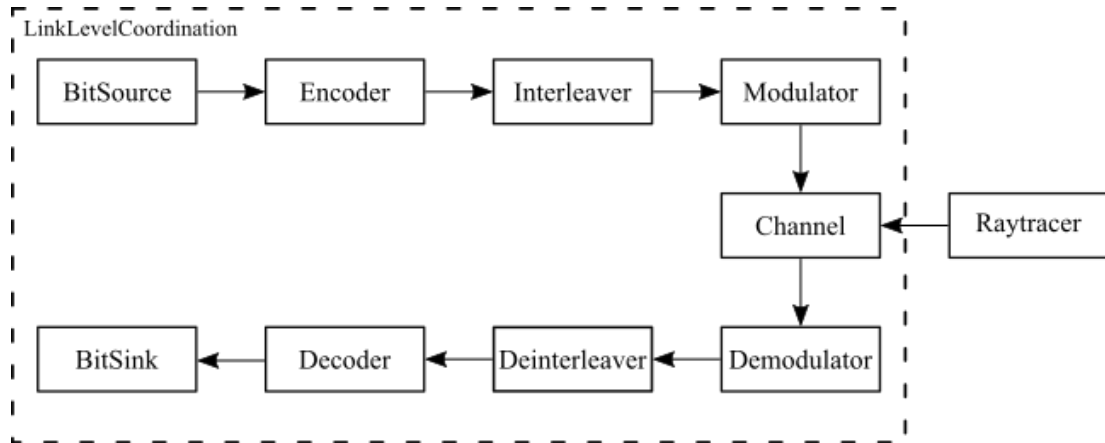
Figure 8-15: Block diagram of the link level simulator

Investigation of NLoS case in the LLS (from section 8.1.1)

As mentioned before, the LLS can be used to further analyse the simulation results from the ray tracer in the form of a CIR on a physical level. To show these analyses, the ray tracing results from chapter 8-11 are passed to the link level simulator. In order to have a realistic environment, the LLS was used with specific properties derived from the 802.15.3d standard for an example simulation. The frequency is set to 300 GHz, utilising the QPSK modulation technique and a bandwidth of 2.16 GHz. The coding type employed is LDPC 11/15. The system operates with a noise figure of 10 dB and at a temperature of 290K. Pilot signals and interleaving were not considered here; the signal power was set to 0 dBm. Figure 8-16 to Figure 8-18 present some of the different analysis tools of the LLS that can be used.
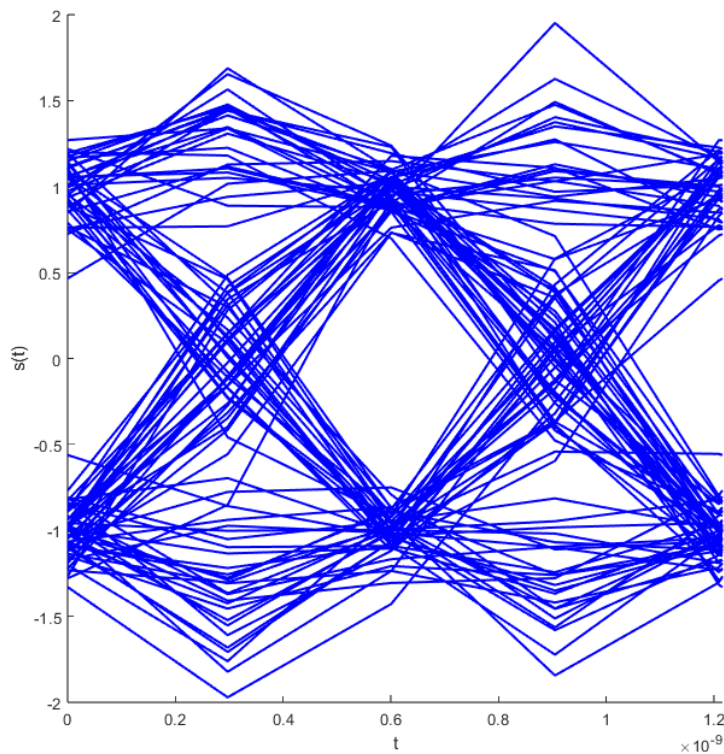
Figure 8-16: Eye diagram of the scenario described in chapter 8-11 in the previously described 802.15.3d channel.
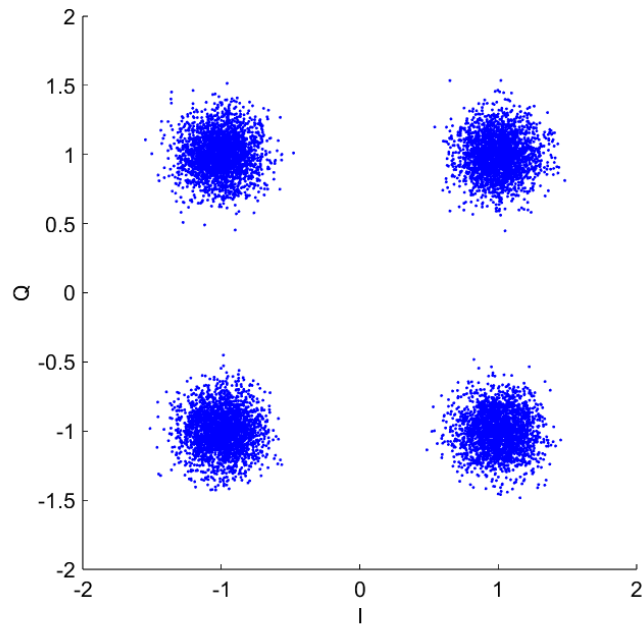
Figure 8-17: Constellation diagram of the scenario described in chapter 8-11 in the previously described 802.15.3d channel.
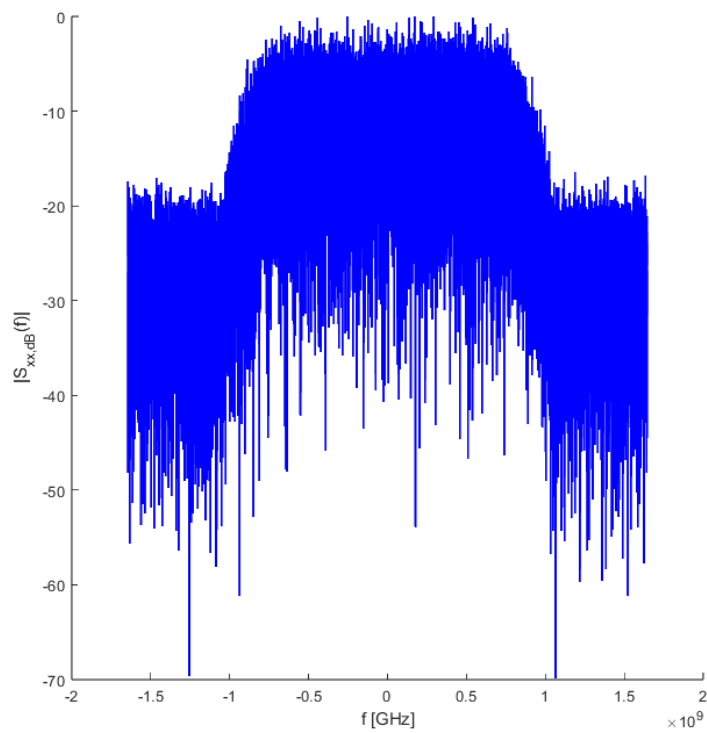
Figure 8-18: Spectral density diagram of the scenario described in chapter 8-11 in the previously described 802.15.3d channel

9. <u>Updated KPI Definitions and Requirements for THz</u>

To evaluate the performance and usability of the use cases and scenarios envisioned in this deliverable, as well as the results that will be delivered throughout the TERRAMETA project, it is important to define the Key Performance Indicators (KPIs) as well as the intended requirements that are expected to be covered. This section provides a slight revision of the KPI requirements from D2.1, incorporating additional information discovered and investigated in the meantime. KPI definitions remain unchanged and can be found in D2.1.

9.1. 6G Requirements

To realise the benefits brought under the 6G vision (see also Section 5.3), the community has set to establish realistic yet ambitious target values for the considered KPIs that go beyond of what it currently technologically plausible. This effort is still ongoing (with the TERRAMETA Consortium being an active participant via its dissemination and standardisation efforts), therefore target KPI values are not yet final. Nevertheless, some indicative proposed requirement values that concern general 6G networks are presented in Table 2 below.

9.1.1. <u>Generic Requirements</u>

Table 2: - 6G Requirements [26]

KPI	6G requirement
Peak data rate	1 Tbps
User experienced data rate	1 Gbps
Peak spectral efficiency	60 b/s/Hz
User experienced spectral efficiency	3 b/s/Hz
End-to-End latency	1 ms
Radio-only latency	100 microseconds
Block Error Rate (BLER)	10e^-9
Connection density	10e^7 devices/km^2
Network energy efficiency	1 pJ/b
Position accuracy	0.1 m
Maximum frequency	10 THz
Maximum bandwidth	100 GHz

It should be noted that the values provided in Table 2 *are only speculative as the 6G requirements have not been agreed upon via standardisation bodies. Additionally, some KPIs may not be relevant in some WPs.*

9.1.2.Requirements and KPIs for Manufacturing Use-Cases

An investigation was performed to determine the bitrate required for real-time transmission for each 3D depth-sensing camera. One of these tests can be seen in Figure 9-1, showing a 3D camera looking at a robot for reference testing, with the camera data being sent to a server. The output of the RGB camera feed is visible, and to the left, in a terminal window, is a measure of the real-time bitrate used to transmit this RGB and depth data stream, which is 350 Mbps. A screenshot of the output of the depth stream can be seen in Figure 9-2, looking at the robot. After this screenshot was taken, the resolution and frame rate of the streams were increased, with a peak bitrate of 450 Mbps. Based on the 450 Mbps required for a single camera, it can be assumed with an array of 4 cameras, plus an additional LIDAR unit, the minimum bitrate required would be 2.25 Gbps, with further increases if additional cameras are required for further blind-spot coverage on the robot. As such, the requirements table has been updated accordingly.
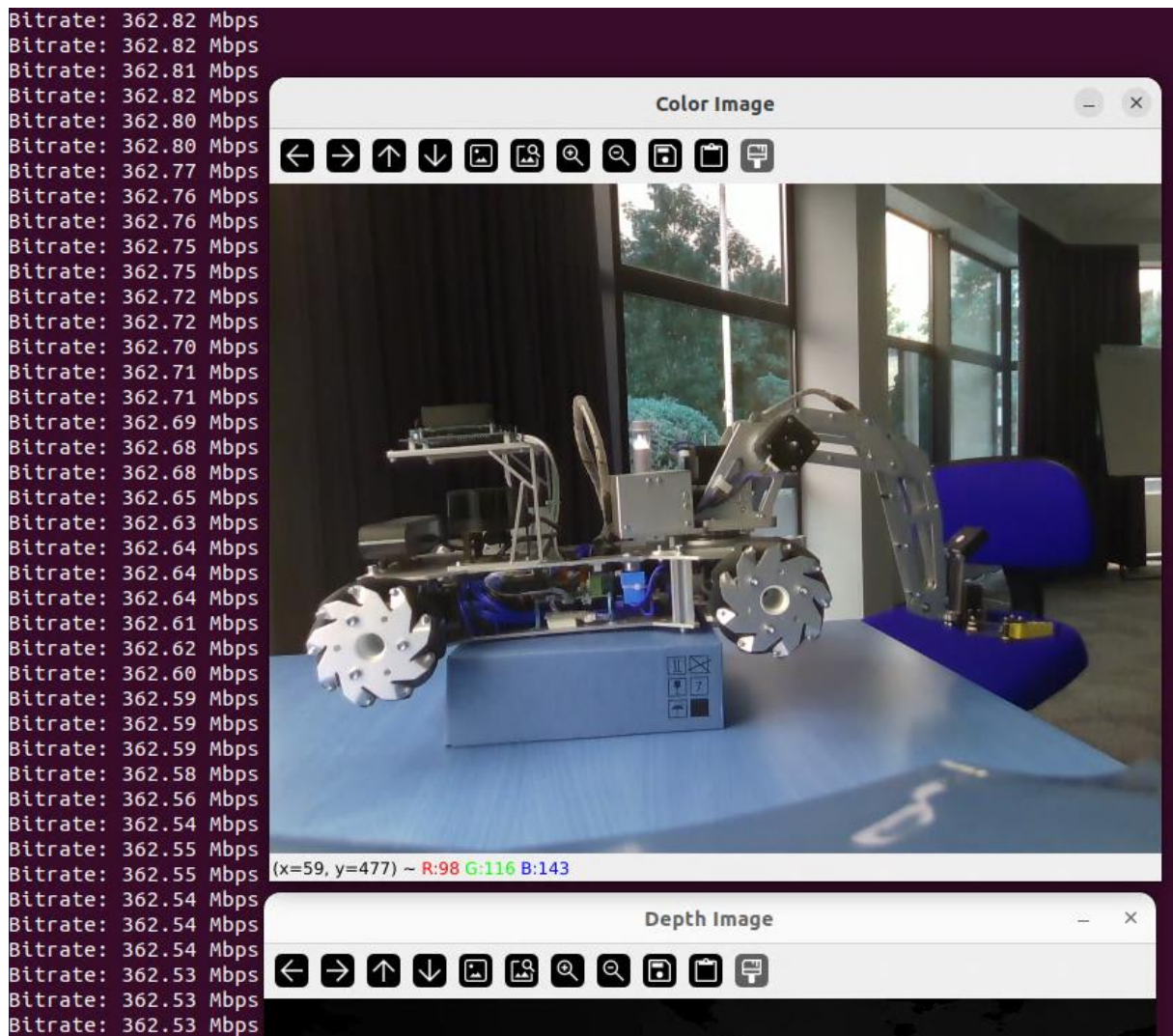
Figure 9-1: Output of robot to server sensor data transmission
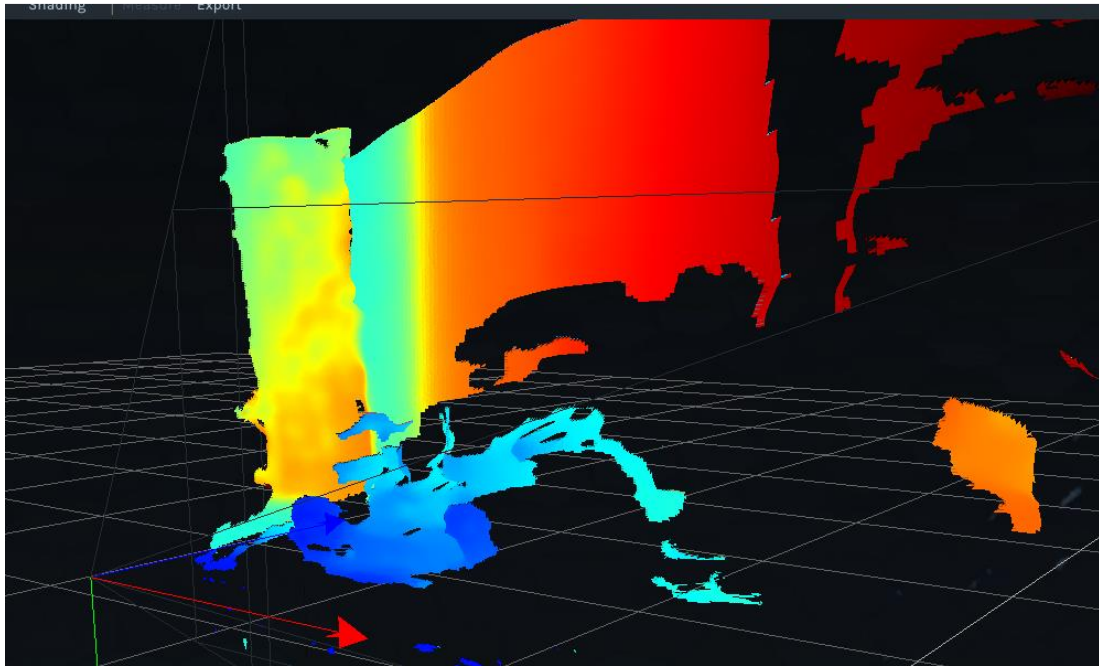
Figure 9-2: Output of the depth camera stream

Table 3: Manufacturing requirements and KPIs

KPIs/Requirements	Description
Minimum Bitrate	2.3 Gbps
Minimum Range	10 m
Signal-to-Noise Ratio (SNR)	5 dB
Bandwidth Utilisation	2 GHz
Frequency Band	140-300 GHz
Modulation & Coding Schemes	Based on IEEE 802.15.3d (300 GHz), OOK, BPSK, QPSK, 8-PSK, 8-APSK, 4-256-QAM, FEC 14/15, 11/15 LDPC
Bit Error Rate	Less than 10e^-4
Packet Loss	Less than 1%
Throughput	2.25 Gbps
Latency	Less than 10 ms end-to-end
Jitter	Less than 2 ms

10. Updated Deployment Scenarios and Use Cases

A set of scenarios and use cases regarding the deployment of THz RIS technology were identified in Deliverable 2.1 [27], with the table summarising them, included in the present document. Therein, the different use cases are logically organised per application type, and some distinctive characteristics of each use case are presented (indoor/outdoor, near-field/far-field, etc.) to identify the systematic setup where they can be considered. Although not all these use cases will be investigated within TERRAMETA, their multitude shows the potential impact of this technology in future networks. In the present document, we provide an updated version of the scenarios and use cases for THz RISs. Specifically, we introduce three new use cases regarding the "High-Resolution Localisation, Sensing and 3D Mapping" scenario. Furthermore, a new scenario is identified, namely "Sustainable and energy autonomous environments" as well as two new use cases for "High-Capacity Connectivity". The updated use cases are briefly described in Table 4 and extensively elaborated in Subsections 10.1, 10.2, and 10.3.

Table 4: Updated taxonomy and characteristics of the TERRAMETA application types and use cases.

Application Type	Use case	Indoor / Outdoor	Near-Field / Far-Field	RIS Types and Operation Modes	Key use case and network aspects
Coverage Extension	Blind spot coverage	Both	Both	Reflective	Blocked LoS
	Hybrid indoor/outdoor repeater	Indoor-to-Outdoor	Both	Reflective, Transmissive, Reconfigurable	Either static or reconfigurable repeater
Network interoperation	Multi-carrier/multi-RIS operation	Outdoor	Far-Field	Reflective, Reconfigurable	Multiple network operators
	Infrastructure sharing	Outdoor	Far-Field	Reflective, Reconfigurable	Multiple network operators
Backhaul Planning	Backhaul and integrated access	Outdoor	Far-Field	Reflective	Backhaul topologies
High-Capacity connectivity	Direct short-range links	Indoor	Near Field (mainly) / Both	Reflective, Reconfigurable	Multiple user terminals
	Ultra-directive short-haul and mid-haul	Both	Both	Transmissive, Reconfigurable	Even fixed beam antennas may be used
	D2D connectivity	Both	Both	Reflective, Reconfigurable, Static	D2D (BS-free) networks

	RIS-assisted beam management	Both	Both	Reconfigurable, Static, Transmissive, Refractive	RIS is part of the BS infrastructure, reducing costs.
Sustainable and energy autonomous environments	RIS-assisted simultaneous wireless power delivery and communications	Both	Near	Reconfigurable	Facilitation of power delivery without communication disruptions.
Localisation and Sensing	THz RIS-aided backhaul link sensing and localisation	Outdoor	Both	Reflective, Reconfigurable, Receiving	Inter-base station, NLoS
	THz RIS-aided multi-access sensing	Both	Both	Reflective, Reconfigurable, Receiving	Multiple targets
	THz RIS-aided outdoor-to-indoor Sensing	Outdoor-to-Indoor	Both	Reflective, Reconfigurable, Receiving, STAR RIS	Can be integrated to existing WLAN infrastructure
	RIS-enabled localisation and mapping without access points	Outdoor	Far-field	Reflective, Reconfigurable	RIS's control unit communicates with the UE
	Hybrid RIS-enabled joint self and UE localisation	Outdoor	Far-field	Hybrid (simultaneously receiving and reflecting),	H-RIS's control unit communicates with the UE

				Reconfigurable	
	Multiple RIS-enabled localisation	Outdoor	Far-field	Reflective, Reconfigurable	Deployment of at least two RISs.
RF sensing	ISAC with Dynamic Metasurface Antennas (DMAs)	Both	Near Field	Receiving, DMA	Can serve multiple users
	Environmental mapping and imaging (RF mapping)	Both	Near Field	Receiving, DMA	3D reconstruction of targets
	Large-scale distributed sensing in factory	Indoor	Near Field	Receiving	Detection of passive objects
	Enhancing throughput, localisation, and mapping in factory settings	Indoor	Near Field	Reflective, Reconfigurable, Receiving, Transmissive	Mobility and blockage scenarios
Network resilience / Multiple Access	Software-defined networking enhancement in data centres	Indoor	Both	Reflective, Reconfigurable, Transmissive	Dynamic management of multiple server nodes

10.1. High-Capacity Connectivity

Device-to-Device connectivity enabled by RIS
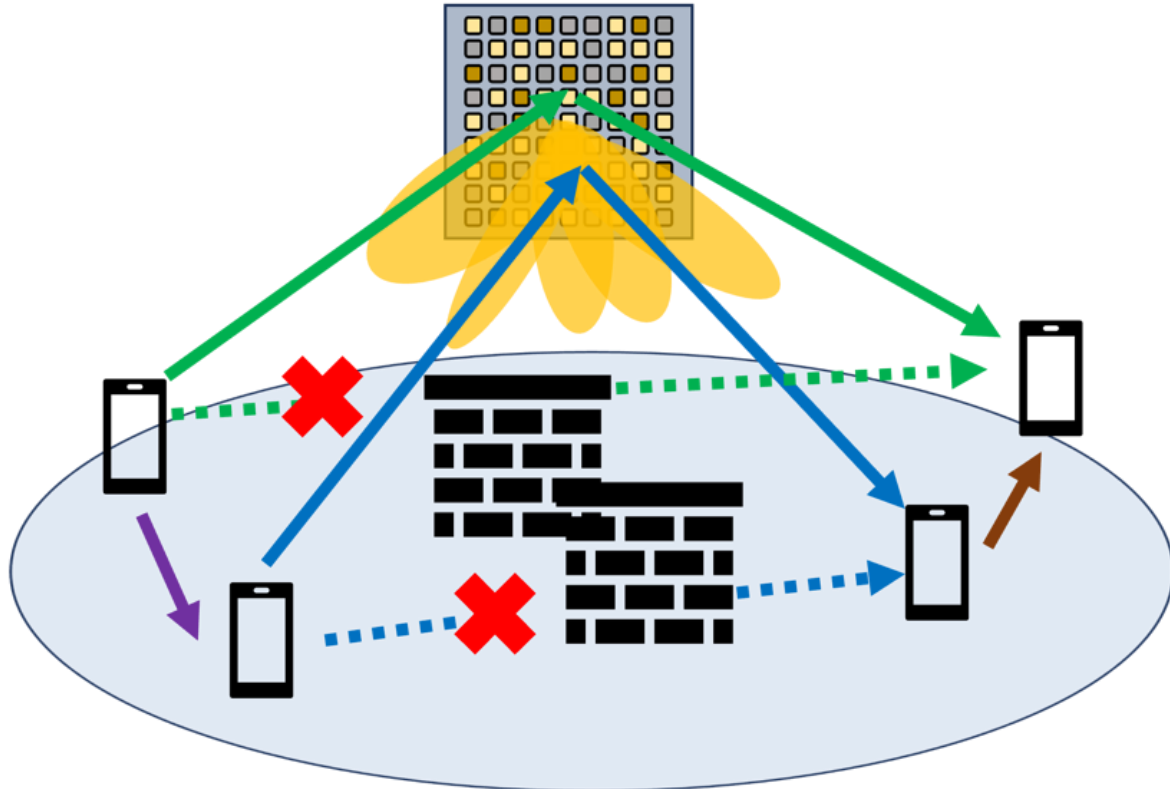
Figure 10-1: RIS-assisted D2D communications.

One of the core goals of 6G networks is the support of the interconnectivity of large amounts of UEs, either via the networks' endpoints or, predominately, through direct device-to-device (D2D) connections. THz networks are poised as one of the key enablers of D2D networks since devices are placed in shorter distances (where the effects of the increased THz attenuation are less severe) and typically require extreme bandwidth levels. D2D communications, however, face characteristic shortcomings. Mainly, UE devices are rarely equipped with proper hardware capabilities (e.g., MIMO antennas) to support key technologies of 6G/THz networks like spatial multiplexing and precise beamforming. Crucially, UE devices typically exhibit unpredictable mobility patterns, making characteristics of the D2D links (blocked line of sight, multipath, interference) difficult to anticipate, and thus optimise.

The inclusion of RISs specifically for the purpose of assisting D2D communications is a potential solution to both of the above challenges, as shown in Figure 10-1. Capitalising on its large number of elements, the RIS is able to perform high-precision beamforming to and from target devices, alleviating the need for multi-antenna equipment on the UEs. Additionally, with proper RIS placement, virtual line-of-sight links can be established among the participating users. Another benefit of RISs in this scenario is their capabilities for "shared multi-tenancy": Different physical parts of the surface may be utilised to serve different D2D connections simultaneously, which is an extra degree of freedom over standard time/frequency/spatial multiplexing for multiple access. Such considerations are extremely important since the number of D2D connections in specific scenarios is expected to far outnumber the UE-BS connections in the future.

RIS-assisted beam management
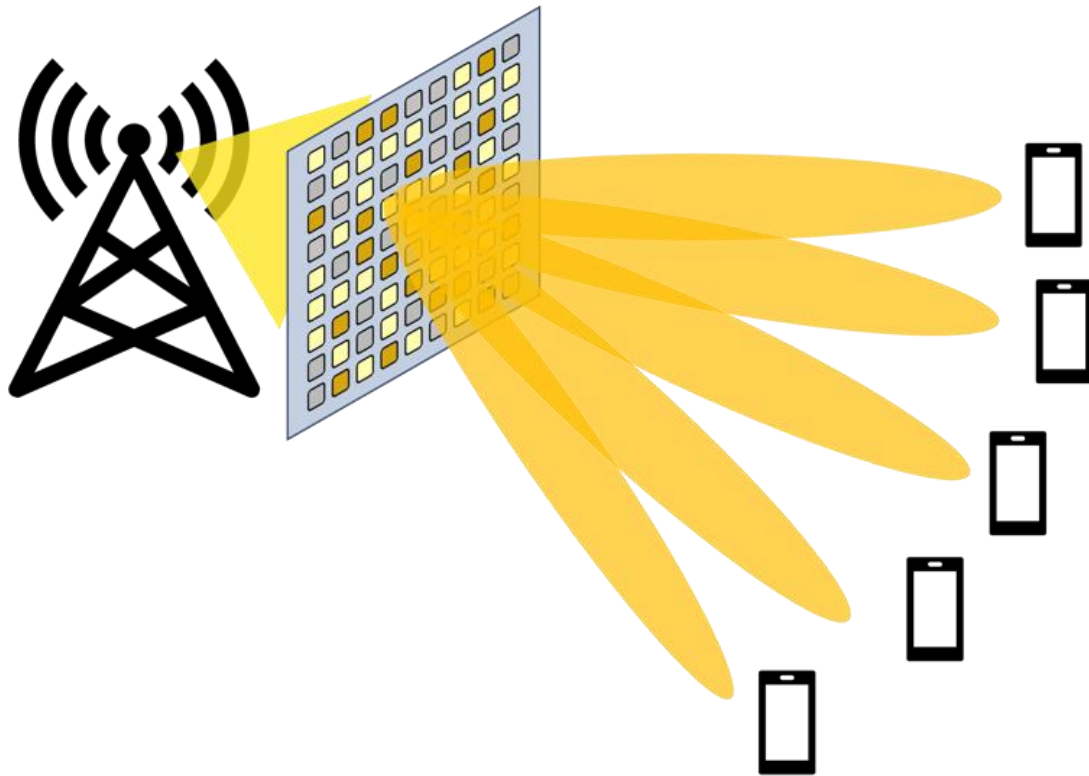
Figure 10-2: Beam management at the BS via RIS diffraction.

The key benefit of RISs is their inclusion of very large numbers (in the orders of thousands) of unit elements with miniscule manufacturing cost and power consumption. Such benefits are directly exploited under the common practice in placing RISs at key environment locations to boost specific areas (of either blocked signal, high UE concentration, or demanding communication and sensing requirements). However, another use case for metasurfaces that can act as lenses is their adoption as analogue beamforming devices onto the BSs. In fact, as the network requirements increase, BSs adopted by the standards are expected to contain many antenna elements to support paradigms such as massive MIMO. The complexity, cost, and power consumption for the typical hybrid (digital and analogue) beamformers may soon prove to be a limiting factor when scaling up the next-generation infrastructure.

To that end, it is envisioned that transmissive or lens RISs will play the role of analogue beamformers, even at the BS's side, as shown in Figure 10-2. The proposed architecture would include lower complexity Radio Frequency Chains (RFCs) that emit a signal from the BS's antenna (or small number of antennas). Low complexity digital or hybrid beamformers may be used to give an initial beam shape. Alternatively, a horn antenna may be in place to provide directivity. Regardless of those choices, the transmitted signal is treated as a feed to the back side of an RIS, closely placed to the antennas. Assuming diffraction capabilities by the metasurface elements, the desirable beamforming patterns can be created by the induced phase shifts so that high spatial multiplexing can be achieved with lower hardware costs. The limitations of phase quantisation and lack of amplitude control from the RIS hardware are offset by the large number of its unit elements, allowing fine grained control over the generated beams.

10.2. Sustainable and energy autonomous environments

RIS-assisted Simultaneous Power Delivery and Communication
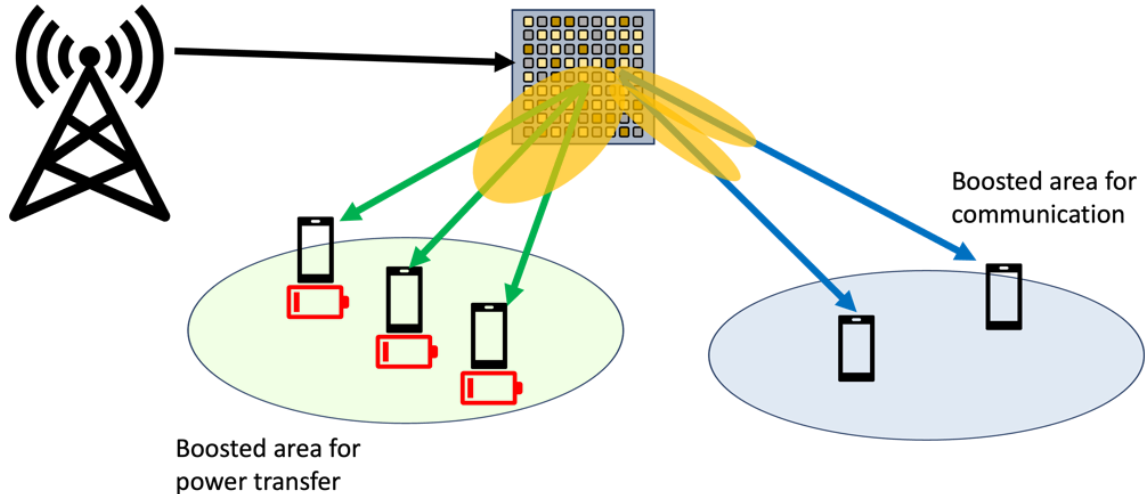
Figure 10-3: - Simultaneous wireless power delivery and communication via RIS multi-beamforming.

Notwithstanding the important benefits of unprecedented bandwidth, one of the challenges under THz communications is the need for increased power consumption to transmit the high frequency carrier signals. While this effect can be mitigated via multiple network and hardware design advancements, at least some types of mobile devices may likely need to be sensitive to their power consumption. One of the promising technologies in resolving the power issue is that of wireless power delivery, under which, devices with specifically designed RFCs are able to absorb impinging electromagnetic (EM) waves and harness their power to charge or operate their own electronic circuitry. While the envisioned technology is still at its early stages of development, two of the most important challenges include (a) the disruption of the rest of telecommunication operations by absorbing data-bearing signals, and (b) the exponential power attenuation over the travelled distance exhibited by EM waves.

THz networks endowed by RISs are potentially capable of circumventing both of the above challenges. Firstly, THz networks are designed in ways to overcome the already severe THz attenuation, e.g., by operating over shorter distances and by making use of view dominant reflection surfaces or by creating virtual lines of sight via the inclusion of RISs. As a second point, the inclusion of RIS allows for precise beamforming towards desired locations. This effect can be exploited for power delivery under the following points: (a) RISs may concentrate the signal strength to the devices requiring power delivery via precise beamforming. (b) By constructing multi-beam reflection patterns, both communication and power-requesting users can be facilitated at the same time, enabling simultaneous wireless power delivery and communication (Figure 10-3).

10.3. High-Resolution Localisation, Sensing, and 3D Mapping

The large-scale antennas required at THz frequencies generate highly directional beams, which are effective in overcoming path loss and provide precise angular resolution. Additionally, the extensive bandwidth available at THz frequencies facilitates high data rates and enables superior range resolution via Time of Arrival (ToA) estimation, making it ideal for both communication and radar sensing applications. Consequently, THz and RIS-THz systems can leverage these attributes to achieve exceptional accuracy in localisation tasks.

RIS-enabled localisation and mapping without access points

RISs are capable of offering new deployment paradigms for self-localisation without the need for widely scaled infrastructure. Concretely, when the positions of multiple RISs are known to the UE at the time of operation, beacon signals may be transmitted toward their surfaces, whose reflected components may be collected back at the device to determine information such as Angle of Arrival (AoA) and Doppler shifts [28]. This methodology concurrently offers increased privacy levels, as the pilot signals are not received by any other entities, apart from the participating user. This setup can effectively be seen as a monostatic setup with the static object being the RIS. Similar to radar operations, the UE may transmit signals toward the RIS and listen to the echoed signal to compute its position with respect to the (known) position of the surface. For enhanced performance, the reflecting patterns of the RIS may be dynamically shifted thus offering new degrees of freedom and achieving high-resolution localisation.

This use case is illustrated in Figure 10-4; the UE transmits pilot signals and from the echoes, it is able to estimate its own position, while the RIS beamforms towards the UE. Moreover, from the echoed signal the UE is able to estimate over time the position and sizes of its surrounding objects, categorising those as static reflection points and moving scattering points, thus enabling mapping of the environment.
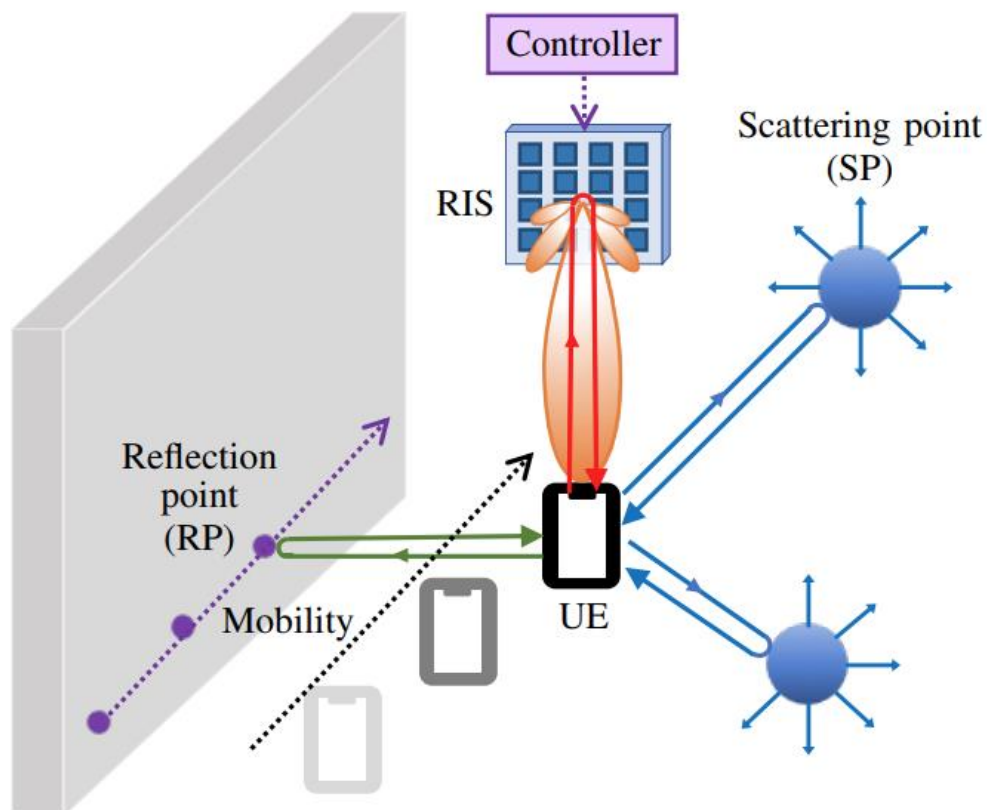
Figure 10-4: System setup of [28]. A mobile UE transmits signals that are reflected from the static environment and the RIS. By processing the reflected signals, the UE is able to simultaneously localise itself and map objects in the environment.

Hybrid RIS joint self and UE localisation

In most RIS-related localisation use cases, the RIS state (i.e., its position and rotation angles) is considered known a-priori. While lack of knowledge of the RIS position and orientation generally does not affect RIS-aided communication, it prevents RIS-aided UE localisation. Furthermore, one cannot separately estimate the AoA and Angle of Departure (AoD) at the passive RIS, thus, adding sensing capabilities to the RIS can be a promising solution to overcome this challenge. Motivated by the latter we introduce a new use case capitalising on the sensing capabilities of the H-RIS architecture. According to this RIS hardware architecture, waveguides feed the incident signals at each hybrid meta-atom to RX RF chains, which are connected to a baseband unit, while it can simultaneously reflect a portion of the incident wave [27].

In this use case, we envision a BS-UE downlink operation assisted by an H-RIS as depicted in Figure 10-5. During the process of pilot signalling from the BS, both the UE and H-RIS stack their observations and separately estimate their AoAs and ToAs. Subsequently, we assume that the HRIS and the UE, share their observations via a reliable link with a fusion centre. The fusion centre then processes their cumulative observations and is able to simultaneously estimate the UE's 3D position as well as the 3D rotation matrix of the H-RIS and its 3D position. It should be noted that, for this use case to be carried out, the H-RIS needs to follow a protocol for its beampattern as described in [29].
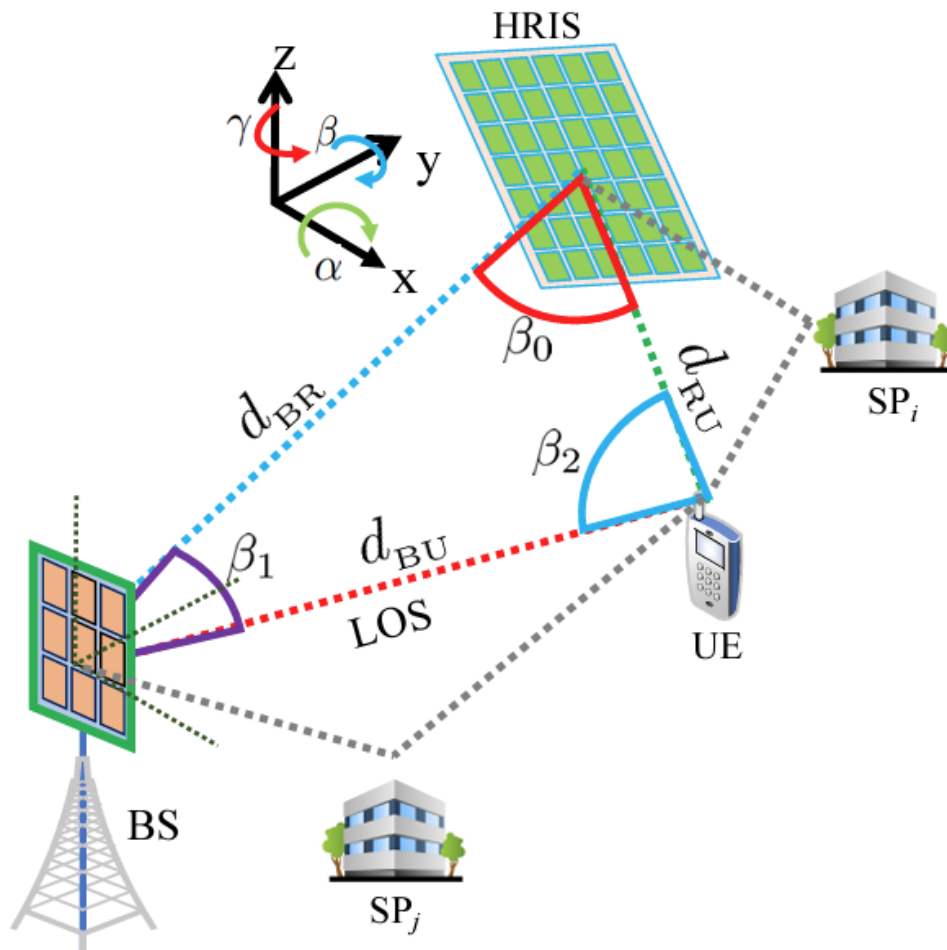
Figure 10-5: The considered wireless system of [29] comprising a multi-antenna BS, a single-antenna UE, and an H-RIS. The 3D location of the UE and the 6D state of the H-RIS are unknown.

Multiple RIS-enabled localisation via beam sweeping

A single RIS has been considered in most use cases for simplicity, but the incorporation of multiple metasurfaces could be a key factor in potential applications that require extreme KPI levels (e.g., coverage and accuracy). In this use case we envision a downlink scenario where a BS communicates with a UE with the aid of at least two RISs. We assume that the position of the RISs is considered known and that they have LoS link with the UE. During the localisation process, both RISs perform beam sweeping in consecutive order (one remains fixed while the other beam sweeps and so on). The UE estimates its received SNR for each beam and determines which beams from both RISs resulted in the best SNR. Since a LoS link is assumed between the RISs and the UE, the preferred beams are the ones pointing towards the UE's position. In that manner, localisation can take place even in far-field scenarios, via geometric trilateration as shown in Figure 10-6. This use case is especially intriguing for real-world deployment since it has already been experimentally demonstrated in a train station from Société nationale des chemins de fer français (SNCF), at Rennes, in France, as a genuine effort of the RISE-6G EU Horizon project [30].

In this use case more RISs can be considered to enhance the localisation resolution. In that case, multiple lines will be drawn from each RIS towards the UE and the estimated UE's position will be the one that minimises the distance from all the lines.
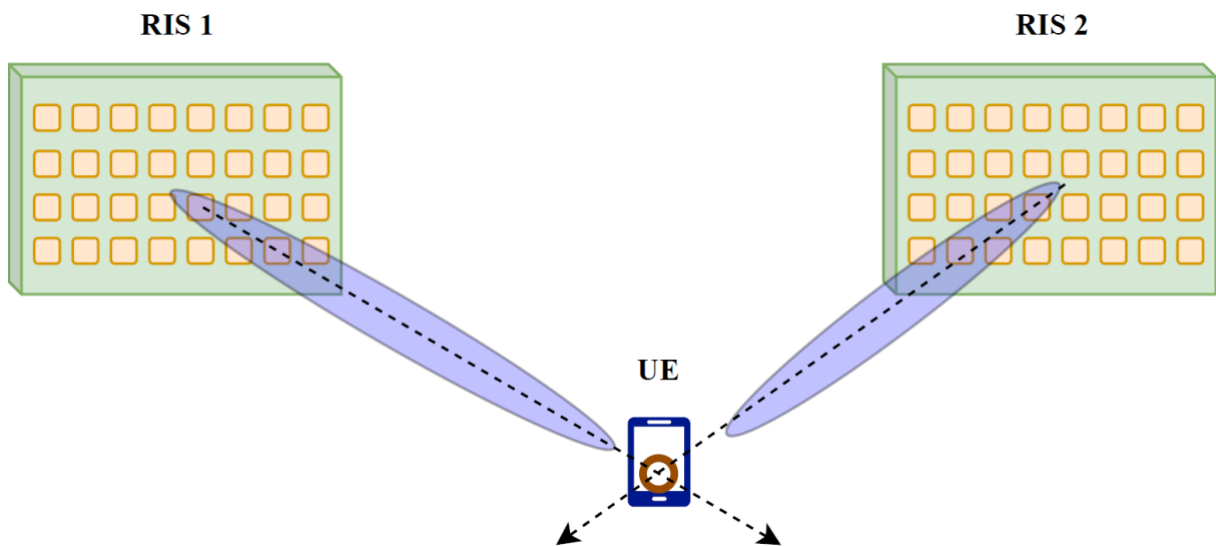
Figure 10-6: Two RIS-enabled localisation via finding the intersection point of the selected beams.

11. <u>Conclusion</u>

D2.2 has outlined the comprehensive approach of the TERRAMETA project in advancing THz communications and RIS technologies. Throughout this document, we have detailed the updated network architecture, requirements, and use case scenarios that leverage the capabilities of THz frequencies and RIS to address the demands of future communication networks.

The integration of THz and RIS technologies presents significant potential for enhancing wireless communication systems. By incorporating these technologies into factory and Telco environments, we aim to showcase their ability to improve coverage, reliability, and data throughput for many applications. The deployment strategies discussed, such as optimising RIS placement on factory layout pillars and the use of mobile RIS platforms, highlight the necessary adaptability and efficiency of these solutions in dynamic and challenging environments.

The hardware integration architecture section provided detailed insights into the design and implementation of the necessary hardware components, ensuring seamless operation and high performance. The collaboration between various project partners in developing sub-THz components, RF front-ends, and baseband units underscores the project's commitment to achieving practical, real-world applications for THz and RIS technologies.

Simulations played a crucial role in validating and optimising the proposed network architectures. By creating realistic simulation environments, we were able to test and refine our solutions, ensuring they meet the high demands of future communication networks. These simulations not only highlighted potential challenges but also provided valuable insights into the optimal configurations and parameters for THz and RIS technologies.

Additionally, the importance of extending existing standards, such as IEEE 802.11 and 3GPP, to better support THz and RIS communications was discussed. The directional nature of THz links and the real-time control required for RIS, present new challenges that need to be addressed. By proposing enhancements to these standards, we aim to ensure the network architectures are robust, flexible, and capable of supporting the advanced capabilities needed in future communication networks.

In conclusion, WP2 and D2.2 have made significant strides in developing the potential of THz and RIS technologies through architecting future use cases and network frameworks in which, such high frequency communications are vital for demanding use cases. It has not only designed this but also shown how these communication technologies can be integrated into existing network standards, built simulation environments to validate that the use cases are viable, and shown how the final real-word hardware systems can be integrated for real device testing. This deliverable serves as a comprehensive guide to the network architecture, additional use case scenarios, hardware integration, and simulation environments, providing a solid foundation for TERRAMETA's other technical WPs, and future deployment and standardisation of THz and RIS technologies.

12. **References**

[1] Thames, Lane, and Dirk Schaefer. "Software-defined cloud manufacturing for industry 4.0." Procedia cirp 52 (2016): 12-17.

[2] Wang, Jue, Abdullah Al-Khalidi, Sean Ahearne, and Edward Wasige. "22Gbps/80cm Low-cost THz wireless system." In 2021 51st European Microwave Conference (EuMC), pp. 209-212. IEEE, 2022.

[3] Stachniss, Cyrill, John J. Leonard, and Sebastian Thrun. "Simultaneous localization and mapping." Springer Handbook of Robotics (2016): 1153-1176.

[4] Lu, Yuqian, et al. "Digital Twin-driven smart manufacturing: Connotation, reference model, applications and research issues." Robotics and computer-integrated manufacturing 61 (2020): 101837.

[5] Alexandropoulos, George C., Antonio Clemente, Sérgio Matos, Ryan Husbands, Sean Ahearne, Qi Luo, Verónica Lain-Rubio, Thomas Kürner, and Luís M. Pessoa. "Reconfigurable Intelligent Surfaces for THz: Hardware Design and Signal Processing Challenges." In 2024 18th European Conference on Antennas and Propagation (EuCAP), pp. 1-5. IEEE, 2024.

[6] Sönmez, Şafak, et al. "Handover management for next-generation wireless networks: A brief overview." 2020 IEEE Microwave Theory and Techniques in Wireless Communications (MTTW) 1 (2020): 35-40.

[7] Charan, Gouranga, Muhammad Alrabeiah, and Ahmed Alkhateeb. "Vision-aided 6G wireless communications: Blockage prediction and proactive handoff." IEEE Transactions on Vehicular Technology 70.10 (2021): 10193-10208.

[8] Al Emam, Fatma A., Mohamed E. Nasr, and Sherif E. Kishk. "Context-aware parallel handover optimization in heterogeneous wireless networks." Annals of Telecommunications 75 (2020): 43-57.

[9] Fu, Xiaojian, et al. "Terahertz beam steering technologies: from phased arrays to field-programmable metasurfaces." Advanced optical materials 8.3 (2020): 1900628.

[10] Huang, Chongwen, Zhaohui Yang, George C. Alexandropoulos, Kai Xiong, Li Wei, Chau Yuen, Zhaoyang Zhang, and Mérouane Debbah. "Multi-hop RIS-empowered terahertz communications: A DRL-based hybrid beamforming design." IEEE Journal on Selected Areas in Communications 39, no. 6 (2021): 1663-1677.

[11] Yan, Wencai, et al. "Beamforming analysis and design for wideband THz reconfigurable intelligent surface communications." IEEE Journal on Selected Areas in Communications (2023).

[12] Shafie, Akram, et al. "Spectrum allocation with adaptive sub-band bandwidth for terahertz communication systems." IEEE Transactions on Communications 70.2 (2021): 1407-1422.

[13] Barazideh, Reza, et al. "Reinforcement learning for mitigating intermittent interference in terahertz communication networks." 2020 IEEE International Conference on Communications Workshops (ICC Workshops). IEEE, 2020.

[14] Wang, Chaoyang. "QoS-Aware Subchannel and Power Allocation Algorithm in Terahertz Communication System." 2021 13th International Conference on Communication Software and Networks (ICCSN). IEEE, 2021.

[15] Liu, Yan, et al. "Machine learning for 6G enhanced ultra-reliable and low-latency services." IEEE Wireless Communications 30.2 (2023): 48-54.

[16] Petrov, Vitaly, Thomas Kurner, and Iwao Hosako. "IEEE 802.15. 3d: First standardization efforts for sub-terahertz band communications toward 6G." IEEE Communications Magazine 58.11 (2020): 28-33.

[17] El Jbari, Mohamed, Mohamed Moussaoui, and Noha Chahboun. "Coding and modulation for terahertz." Terahertz Wireless Communication Components and System Technologies. Singapore:

Springer Singapore, 2022. 59-79.

[18] Morales, Daniel, and Josep M. Jornet. "ADAPT: An Adaptive Directional Antenna Protocol for medium access control in Terahertz communication networks." Ad Hoc Networks 119 (2021): 102540.

[19] Ghafoor, Saim, et al. "MAC protocols for terahertz communication: A comprehensive survey." IEEE Communications Surveys & Tutorials 22.4 (2020): 2236-2282.

[20] Kanagarathinam, Madhan Raj, and Krishna M. Sivalingam. "Challenges in Transport Layer Design for Terahertz Communication-Based 6G Networks." 6G Mobile Wireless Networks. Cham: Springer International Publishing, 2021. 123-136.

[21] 3GPP, TSG RAN WG3 R3-161813, Transport requirement for CU and DU functional splits options, 2016.

[22] ETSI mWT ISG, Evolution of Fixed Services for Wireless Backhaul of IMT 2020 / 5G, 2019. [Online]. Available:

https://www.itu.int/en/ITU-R/study-groups/workshops/fsimt2020/Pages/default.aspx

[23] RISE-6G Deliverable D2.5, "RISE network architectures and deployment strategies analysis: First results," July 2022.

[24] J. L. Gonzalez-Jimenez et al., "A 57.6 Gb/s wireless link based on a 26.4 dBm EIRP D-band transmitter module and a channel aggregation chipset on CMOS 45 nm," in Proc. IEEE Radio Freq. Integr. Circuits Symp. (RFIC), Jun. 2023, pp. 97–100.

[25] TERRAMETA Deliverable D3.2, " Report on THz components design (first)" January 2024.

[26] H. Tataria, M. Shafi, A. F. Molisch, M. Dohler, H. Sjöland and F. Tufvesson, "6G Wireless Systems: Vision, Requirements, Challenges, Insights, and Opportunities," in Proceedings of the IEEE, vol. 109, no. 7, pp. 1166-1199, July 2021, doi: 10.1109/JPROC.2021.3061701.

[27] TERRAMETA Deliverable D2.1, "Requirements, use cases, and scenario specifications," June 2023.

[28] H. Kim, H. Chen, M. Furkan, Y. Ge, K. Keykhosravi, G. C. Alexandropoulos, S. Kim, and H. Wymeersch, "RIS-Enabled and Access-Point-Free Simultaneous Radio Localization and Mapping," in IEEE Transactions on Wireless Communications, 2023.

[29] R. Ghazalian, G. C. Alexandropoulos, G. Seco-Granados, H. Wymeersch, and R. Jäntti, "Joint 3D user and 6D hybrid reconfigurable intelligent surface localization," IEEE Transactions on Vehicular Technology, to appear, 2024.

[30] RISE-6G Deliverable D7.3, "Final results of PoCs and trials," December 2023.